



**US Army Corps
of Engineers®**
Engineer Research and
Development Center

Environmental Quality Technology Program

Unexploded Ordnance (UXO) Data Analysis System (DAS)

Ricky A. Goodson, John Cliff Morgan, Dwain K. Butler,
Morris P. Fields, Hollis H. Bennett, Jr., and Tere A. DeMoss

September 2009

Unexploded Ordnance (UXO) Data Analysis System (DAS)

Ricky A. Goodson, John Cliff Morgan, Dwain K. Butler, Morris P. Fields, Hollis H. Bennett, Jr., and Tere A. DeMoss

*Environmental Laboratory
U.S. Army Engineer Research and Development Center
3909 Halls Ferry Road
Vicksburg, MS 39180-6199*

Final report

Approved for public release; distribution is unlimited

Prepared for Environmental Quality Technology Program
Washington, DC

and Headquarters, U.S. Army Corps of Engineers
Washington, DC 20314-1000

Under Restoration Requirement A (1.6a) UXO Screening, Detection, and Discrimination

Abstract: This report documents efforts to develop a common processing and interpretation platform for UXO survey data, hereinafter referred to as the UXODAS. Development of the common software platform assumes (1) that the data will be accessible in readable formats, and (2) that the data result from the most commonly used geophysical sensor types, specifically total field magnetometers (TFM), frequency-domain electromagnetic induction (FDEM) systems, and time-domain electromagnetic induction (TDEM) systems. The common platform will enable interoperability and incorporate in a readily available software package the capability and tools to import, process, interpret, and visualize the results of UXO geophysical surveys. The software platform will be a continuing work in progress, with the capability to easily incorporate new processing and interpretation tools (modules) as they become available. The immediate goal is to make available to the user community the processing and interpretation tools developed under the Army Environmental Quality Technology UXO Research and Development Program by the US Army Engineer Research and Development Center (ERDC).

DISCLAIMER: The contents of this report are not to be used for advertising, publication, or promotional purposes. Citation of trade names does not constitute an official endorsement or approval of the use of such commercial products. All product names and trademarks cited are the property of their respective owners. The findings of this report are not to be construed as an official Department of the Army position unless so designated by other authorized documents.

DESTROY THIS REPORT WHEN NO LONGER NEEDED. DO NOT RETURN IT TO THE ORIGINATOR.

Contents

Figures and Tables	v
Preface	viii
Unit Conversion Factors.....	ix
1 Introduction.....	1
Background	1
Data processing overview and requirements	3
Selection of the ERDC UXODAS base platform	6
Scope of report.....	6
2 Sensor Systems	8
Sensor systems	8
Time domain electromagnetic induction (EMI) systems	8
<i>EM61-MK2 EMI system</i>	8
<i>High power (HP) modification</i>	9
<i>Geonics EM-63 EMI system</i>	10
Frequency domain EMI systems.....	11
<i>GEM-3-E EMI system</i>	11
<i>System configuration GEM-3-E</i>	12
Passive systems	13
<i>Geometrics 823A cesium vapor total field magnetometer (TFM) description</i>	13
Other systems.....	14
<i>Geonics EM-61HH hand-held EMI sensor</i>	14
<i>The ERDC Hand-held Dual TFM/EMI Sensor</i>	16
<i>ArcSecond LASER positioning system</i>	17
G-tek SAM system	18
Magnetometer array.....	19
<i>Data processing description</i>	20
3 Data Import and Processing Procedures	22
Import into Oasis Montaj	22
Area coverage.....	23
Time synch.....	26
Drift correction	28
4 Anomaly Selection	31
UX-Detect	31
<i>Histogram-based algorithm</i>	34
Extraction of anomaly data.....	37

5 Discrimination.....	39
Modeling/Inversion	39
GEM-3	43
EM-63	45
Cooperative inversion.....	47
Parameter classification	50
Signature matching.....	52
6 Results/Performance	55
Test site description	55
Standardized test site scoring procedure	57
TM-4 magnetometer.....	59
EM-63 EMI system	59
GEM-3-E EMI system	60
UXO-DAS and UXO lab workshops	61
7 Conclusions & Recommendations.....	64
Conclusions	64
Recommendations	65
References.....	67
Appendix A.....	69
Appendix B.....	74

Report Documentation Page

Figures and Tables

Figures

Figure 1. Key steps in the UXO environmental remediation process.....	3
Figure 2. Example: Fort Ord, CA, ODDS UXO Test Sites—Illustrating the ubiquitous increase in number of targets with decreasing target declaration threshold—TDEM survey data.....	4
Figure 3. The ERDC UXODAS concept of operations.....	7
Figure 4. The EM61-MK2	9
Figure 5. Geonics EM-63 on the the ERDC UXO/CM test stand.....	10
Figure 6. The GEM-3-E during survey.....	12
Figure 7. G-823A magnetometer	13
Figure 8. The Geonics EM-61HH on data collection pass.....	15
Figure 9. The ERDC Hand-held Dual TFM/EMI with ArcSecond positioning system.....	16
Figure 10. Components of the ERDC Hand-Held Dual TFM/EMI	17
Figure 11. Setup and calibration using light bar for the ArcSecond LASER position system.....	18
Figure 12. SAM System fielded in Yuma, Arizona	19
Figure 13. UXO-DAS import menu	23
Figure 14. GEM-3 import dialog box.....	23
Figure 15. GEM-3 database.....	24
Figure 16. Dialog box for extracting a single channel from an array channel.....	24
Figure 17. EM-63 import dialog box.....	24
Figure 18. EM-63 database.....	25
Figure 19. Line path plot.....	25
Figure 20. Coverage map.....	26
Figure 21. Dialog for latency correction.....	27
Figure 22. Gridded image of an anomaly before lag correction.....	27
Figure 23. Gridded image of the same anomaly after lag correction.....	28
Figure 24. Gridded image of EM-63 data showing instrument drift.....	29
Figure 25. Gridded image of EM-63 data after drift correction.....	29
Figure 26. Dialog box for drift correction of GEM-3 In-phase channel.....	30
Figure 27. Dialog box for drift correction of GEM-3 Quadrature channel.....	30
Figure 28. Target anomaly map created with UX-Detect.....	32
Figure 29. Gridded magnetometer data (units = nT).....	33
Figure 30. Analytic signal grid calculated from the magnetometer data shown in Figure 29.....	33
Figure 31. Grid and histogram (at bottom) of GEM-3 in-phase anomaly data for frequency = 1 (90Hz).....	35
Figure 32. Grid and histogram (at bottom) of GEM-3 in-phase anomaly data for frequency = 3 (390Hz).....	35

Figure 33. Grid and histogram (at bottom) of GEM-3 in-phase anomaly data for frequency = 5 (1290Hz).....	36
Figure 34. Grid and log histogram (at bottom) of GEM-3 in-phase anomaly data for frequency = 5 (1290Hz) with background peak excluded.....	36
Figure 35. Extraction of GEM-3 anomaly data dialog box.....	37
Figure 36. Extraction of EM-63 anomaly data dialog box.....	38
Figure 37. Extraction of magnetometer anomaly data dialog box.....	38
Figure 38. MATLAB® inversion of magnetometer data.....	40
Figure 39. Magnetometer inversion dialog box.....	40
Figure 40. Measured (left) and modeled (right) / magnetometer data (units = nT).	41
Figure 41. Magnetometer anomaly for which inversion failed due to the presence of another anomaly nearby (units = nT).	41
Figure 42. Magnetometer inversion dialog box for a single target	42
Figure 43. Measured (left) and modeled (right) magnetometer data after re-inversion with polygon mask (units = nT).	42
Figure 44. MATLAB® inversion of EM-61 data.....	43
Figure 45. Gridded map of measured anomaly and model fit for GEM-3 (units = PPM).....	44
Figure 46. Measured and model frequency curves.....	44
Figure 47. Gridded map of measured anomaly and model fit produced by MATLAB® inversion code for EM-63 data (units = mV).....	45
Figure 48. UX-Analyze target-fitting dialog box.....	46
Figure 49. EM-63 inversion parameters dialog box.....	46
Figure 50. UX-Analyze Add/Review window.....	48
Figure 51. UX-Analyze complete anomaly map.....	49
Figure 52. Fitted results dialog.....	49
Figure 53. Gridded map of measured anomaly and model fit for EM-63	50
Figure 54. Cooperative inversion flowchart.....	50
Figure 55. SVM concept in MATLAB®.....	51
Figure 56. Signature-matching module.....	52
Figure 57. Aerial views with layout of the APG Standardized UXO Technology Demonstration Site	56
Figure 58. Overlay map of Standardized UXO Technology Demonstration Site.....	57

Tables

Table 1. Specifications for the EM61-MK2	9
Table 2. Geonics EM-63 Specifications	11
Table 3. Specifications for the GEM-3-E.....	12
Table 4. Specifications for the G-823A.....	14
Table 5. Specifications for the EM-61HH	15
Table 6. Specifications for the G-tek SAM System	20
Table 7. Advanced parameters that control the EM-63 inversion.....	46
Table 8. Summary of YPG Blind Grid Results (Full Ground Truth).....	59

Table 9. Summary of YPG Blind Grid Results (Ferrous Only).....	60
Table 10. Summary of YPG Blind Grid Results (for EM63).....	60
Table 11. Summary of APG Blind Grid Results Using Signature Matching (All Frequencies)	62
Table 12. Summary of APG Blind Grid Results Using Signature Matching (Excluding 90-Hz Data)	62
Table 13. Summary of APG Blind Grid Results Using Signature Matching (Excluding 90-Hz and 150-Hz Data)	63

Preface

This report describes efforts conducted under the sponsorship of the Environmental Quality Technology (EQT) Program A (1.6.a), Unexploded Ordnance (UXO) Screening, Detection, and Discrimination Management Plan. Work was conducted under BA2/3 Major Thrust Area III, "Sensor Design and Enhancement" and BA4 Major Thrust Area III, "Hardware/Software Integration." The work documented in this report was performed during the period 01 October 2002 through 30 September 2006. Dr. M. John Cullinane, U.S. Army Engineer Research and Development Center (ERDC), was Technical Director, Military Environmental Engineering and Sciences, Environmental Laboratory (EL).

John H. Ballard, ERDC, was the program manager for research and development of the Environmental Quality Technology (EQT) Program A (1.6.a) UXO Screening, Detection, and Discrimination Management Plan during the execution of this project. George Robitaille, U.S. Army Environmental Center (USAEC), was program manager for technology demonstrations of EQT UXO program technologies. Ricky A. Goodson was principal investigator for this work. Software development and testing were performed by Goodson and John Cliff Morgan. Data analysis was performed by Goodson, Morgan, Morris P. Fields, Hollis "Jay" Bennett, and Tere A. DeMoss.

This project was performed under the general supervision of Dr. Ed Russo, ERDC, Chief, Ecosystems Evaluation and Engineering Division.

At the time of publication of this report, EL Director was Dr. Elizabeth C. Fleming, ERDC Director was Dr. James R. Houston, and ERDC Commander was COL Gary E. Johnston.

Unit Conversion Factors

Multiply	By	To Obtain
acres	4,046.873	square meters
feet	0.3048	meters
gallons (U.S. liquid)	3.785412 E-03	cubic meters
inches	0.0254	meters
miles (U.S. statute)	1,609.347	meters
pounds (mass)	0.45359237	kilograms

1 Introduction

This report documents the Unexploded Ordnance (UXO) Data Analysis System (DAS). The development effort was conducted under the Department of Army Research and Development DOE4 (BA4) Technology Demonstration Program. Data analysis was conducted under the Department of Army Research and Development DOE3 (BA3) Program. Post-demonstration analysis focused on the functionality of sensor systems, the evaluation of the noise level of the data collected, ability of the systems to detect and discriminate, and positioning accuracy of the systems. The stability of the system was evaluated through histograms and statistical measurements of data collected during the technology demonstration. Based on the characteristics and initial analysis of the collected data, target detection/discrimination (Miller et al. 2001) techniques were applied and evaluated.

This project addressed the Environmental Quality Technology (EQT) Program thrust area entitled “UXO Technology Demonstration, Work Unit “UXO Detection Design Demonstration and Validation.” The immediate goal is to make available to the user community the processing and interpretation tools developed under the Army EQT UXO Research and Development Program.

Background

UXO cleanup (environmental remediation) requires location of surface and buried ordnance items. Location of subsurface UXO requires surveys with geophysical sensor systems. At a minimum, the data acquired with the geophysical systems are analyzed to give horizontal positions of potential UXO (detection). The data can also be interpreted to establish depth estimates for the targets. Further interpretation of the data was done to classify the targets. The simplest level of classification would be a UXO or non-UXO designation (discrimination) with the highest level being a designation of a specific type of UXO (identification). Clearly, target detection is important, because of the serious consequences of missing potentially live UXO's. The targets detected in geophysical surveys include both UXO and non-UXO. The discrimination step is critical for reducing environmental remediation costs. Approximately 75 percent of overall UXO site cleanup costs are expended excavating and disposing of

non-UXO. The components required for UXO geophysical surveys and interpretation include the geophysical sensor system, survey navigation and measurement positioning capability, data storage capability, and data processing/interpretation software.

Historically, considerable effort has been expended in developing data formatting standards for geophysical survey systems (e.g., the Society of Exploration Geophysicists data formats for seismic, gravity, magnetic, electromagnetic induction, and ground penetrating radar data), with the objective of allowing data sharing and interoperability of processing algorithms. Efforts to establish data standards have continued in UXO applications of geophysical systems, such as the DARPA UXO Backgrounds Program (e.g., George et al. 1998) and through technology workshops conducted by the Joint UXO Coordinating Office (e.g., Office of the Under Secretary of Defense (Acquisition and Technology) 1997).

Unfortunately, recent efforts have not always exploited the considerable prior investment in data file format specification. Fortunately, however, modern geophysical systems manufacturers either (1) store data files in formats readily “readable” by most software programs (e.g., ASCII), or (2) provide translation software to convert the data from the stored data format (e.g., binary) to a “higher level” format (e.g., ASCII); data file headers are generally flexible enough to specify requisite survey details and instrument settings. Also, most geophysical survey systems currently in use and contemplated for use for UXO survey application have positioning/navigation recording capabilities, such as integrated time- or distance-cued measurements or GPS data stream input.

This report documents a common processing and interpretation platform for UXO survey data, hereinafter referred to as the UXODAS. Development of the common software platform assumes (1) that the data would be accessible in readable formats, and (2) the data were collected using the most commonly used geophysical sensor types, specifically total field magnetometers (TFM), frequency-domain electromagnetic induction (FDEM) systems, and time-domain electromagnetic induction (TDEM) systems. The common platform enables interoperability and data incorporation into a single software package, providing the capability and tools to import, process, interpret, and visualize the results of UXO geophysical surveys from a variety of sensors. Developmental plans include adding new processing and interpretation tools (modules) to the UXODAS as they become available. An immediate goal is to make

available to the user community the processing and interpretation tools developed under the Army EQT UXO Research and Development Program by ERDC.

Data processing overview and requirements

The basic steps in UXO environmental remediation are illustrated in Figure 1. The ERDC UXODAS plays a role in all aspects of the process shown in Figure 1, except the excavation and disposal steps.

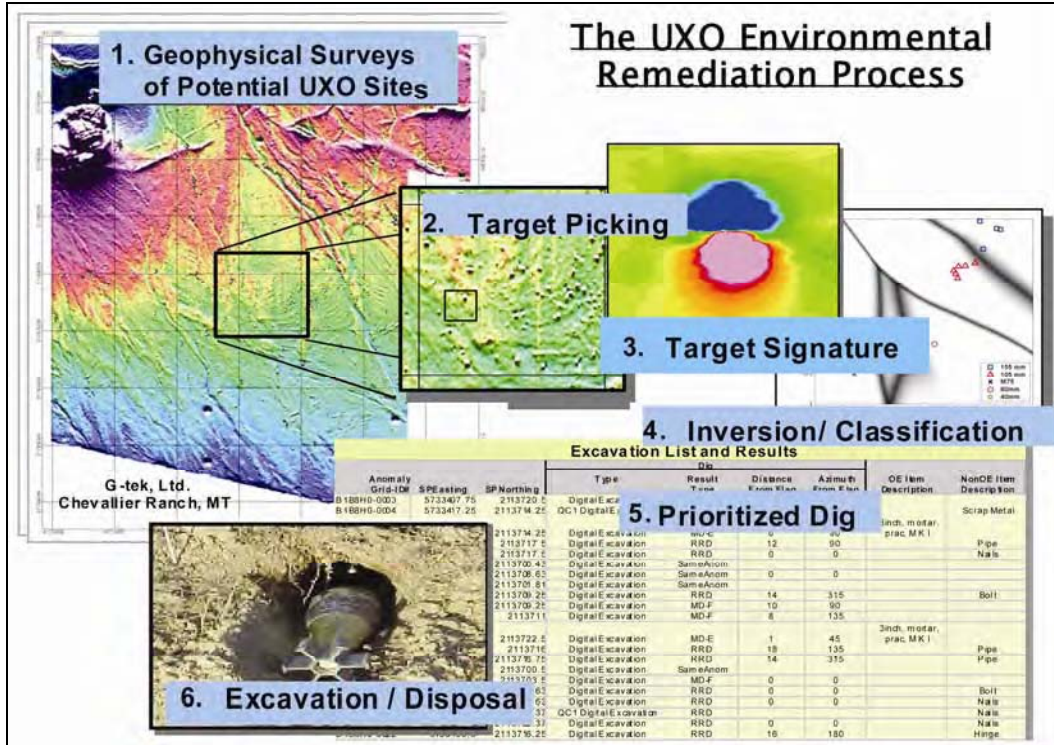


Figure 1. Key steps in the UXO environmental remediation process.

The preliminary step in the process involves identification of potentially UXO-contaminated sites, through research activities such as archival search, footprint reduction, and/or wide area assessment. For the acquisition of geophysical survey data over sites of interest associated with Step 1, the role of UXODAS is limited in its ability to read, display, and import surveys for recognizable data formats, and to check the quality of the data to assure the UXODAS algorithms will be able to process the survey data.

The primary functions of UXODAS in Step 1 are for data corrections and visualization in quality analysis/quality control (QA/QC). Target picking

(Step 2) is a non-trivial step in the process, since detection of a target in the presence of noise involves empirical judgment, even for approaches that involve automated target picking algorithms. For example, using a target-picking threshold that is too low, relative to background/noise, will result in an untenable number of targets for analysis; this concept is illustrated by Figure 2, which illustrates the ubiquitous “exponential” increase in number of targets with decreasing threshold. Target analysis, in most cases, requires “extraction” or specification of the target signature (Step 3), which includes an area of data surrounding the target location. The size of the extracted data area depends on the sensor type and the processing algorithm to be utilized. Once targets have been identified and the target signatures extracted, the signatures are analyzed. The formal process of analyzing target signatures to match to a library of signatures or to fit to a geometrical/parametrical model (geophysical inversion, Step 4) results in information or parameters that can be used in a formal discrimination/classification process (e.g., Butler et al. 2003). Finally, the process must result in a dig list (Step 5). Optimally, the dig list should be prioritized, based on a goodness-of-fit or -classification criterion. One approach suggested by Billings (Billings et al. 2002a) produces a prioritized dig list based on a discriminant value. In the Billings et al. approach, digging continues until (1) no UXO’s are found in the last 50 holes, or (2) a predefined discriminant value is reached, and (3) until all the seeded items have been found.

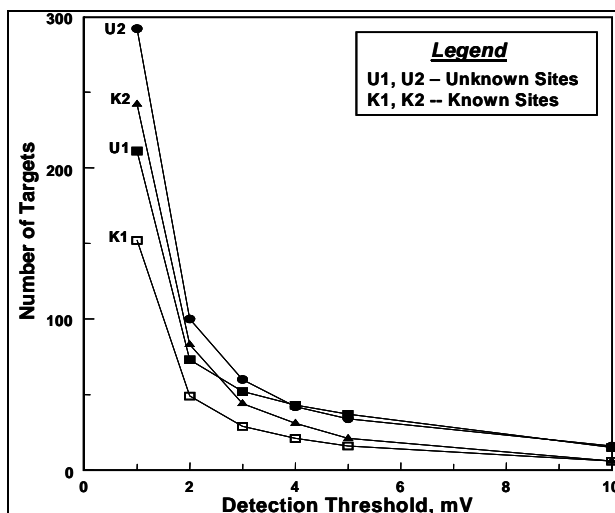


Figure 2. Example: Fort Ord, CA, ODDS UXO Test Sites—Illustrating the ubiquitous increase in number of targets with decreasing target declaration threshold—TDEM survey data.

There are special and general-purpose software programs and platforms that can be used for geophysical data processing and analysis. Special-purpose programs are generally directed to visualization and interpretation of data from a specific class of geophysical systems/methods (e.g., electrical resistivity or time-domain electromagnetic induction). These special-purpose programs are developed and distributed by both the equipment manufacturers themselves and by companies whose sole business is geophysical software development (e.g., Interpex Ltd.¹). General-purpose programs/platforms include two- and three-dimensional data visualization programs (solely for data plotting and display), geographic information systems (GIS; map-based and relational database manaGEMent, map layer queries, and map display products), general-purpose geophysical data processing and analysis platforms (with relational database capabilities; e.g., Geosoft's Oasis Montaj²), high-level mathematical/technical programming platforms (e.g., MATLAB®³), and general-purpose high-level programming languages (e.g., C++ or Visual Basic⁴).

MATLAB® and Oasis Montaj (Geosoft) are the platforms used extensively by the ERDC in the EQT UXO Program. MATLAB® has been used as the development platform for the forward and inverse modeling and algorithm development for TFM, FDEM, and TDEM applications. While MATLAB® can handle large datasets, it is not efficient for production data processing and analysis; the software's strengths lie in sophisticated mathematical programming and matrix-based operations capability. Also, MATLAB® has extremely easy and versatile graphical output capabilities that can expedite the development process. Geosoft, however, was specifically designed to import, process, and analyze the large datasets produced during geophysical surveys. Many routine geophysical data processing functions are built into Geosoft. Oasis Montaj is built around a versatile relational database structure, and it is simple to add processing functionality with GX's (Geosoft executables) and DLL's (dynamic linked libraries). Geosoft has become, virtually, the de facto data processing and analysis platform for geophysical data associated with UXO environmental restoration efforts; many requests for proposals and resulting contracts for

¹ Interpex Ltd., Golden, Colorado 80402 8040280402P.O. Box 839 • Golden • ado • 80402 • USA

² Geosoft Inc., Toronto, Ontario, Canada M5H 2C9

³ The MathWorks, Inc., Natick, MA 01760-2098

⁴ Microsoft Corporation, Redmond, WA 98052-6399

UXO geophysical surveys include specifications for use of the Geosoft software.

Selection of the ERDC UXODAS base platform

One of the prime developers of forward and inverse modeling capability for the ERDC is the Geophysical Inversion Facility of the University of British Columbia (UBC). Like in-house development efforts at the ERDC and other collaborators, UBC uses MATLAB® as the primary development platform. UBC has packaged their developments into a user-friendly MATLAB®-based program called UXOLAB that they will distribute and maintain. Due the wide usage and production processing capability, the ERDC selected Geosoft as the platform for incorporation of in-house and collaborator-developed (primarily UBC, Duke University, and AETC Inc.) processing and analysis tools. The ERDC UXODAS will have import capability for data from a variety of geophysical systems, pre-processing capability, anomaly (target) selection, signature analysis, signature matching, parameter extraction, including forward and inverse modeling, cooperative inversion of multi-sensor datasets, discrimination and classification algorithms, prioritized target list output capability, and visualization tools. Initially, the ERDC will maintain UXODAS, until potential commercialization by collaborators.

Scope of report

The concept of UXODAS is illustrated in Figure 3. Many of the concepts and modules that form UXODAS are previously documented (e.g., Billings et al. 2002b; Butler et al. 1998; Pasion and Oldenburg 2001; Goodson et al. 2002; Simms et al. 2004). Chapter 2 presents the data acquisition capabilities and requirements, including brief descriptions of the geophysical systems. Pre-processing steps and capabilities are discussed in Chapter 3, and anomaly (target) selection approaches are presented in Chapter 4. The important discrimination and classification capabilities and approaches are discussed in Chapter 5, including forward and inverse modeling, cooperative inversion algorithms, signature matching, and dig sheet preparation and output. System performance is discussed in Chapter 6. Finally, a summary and conclusions are contained in Chapter 7.

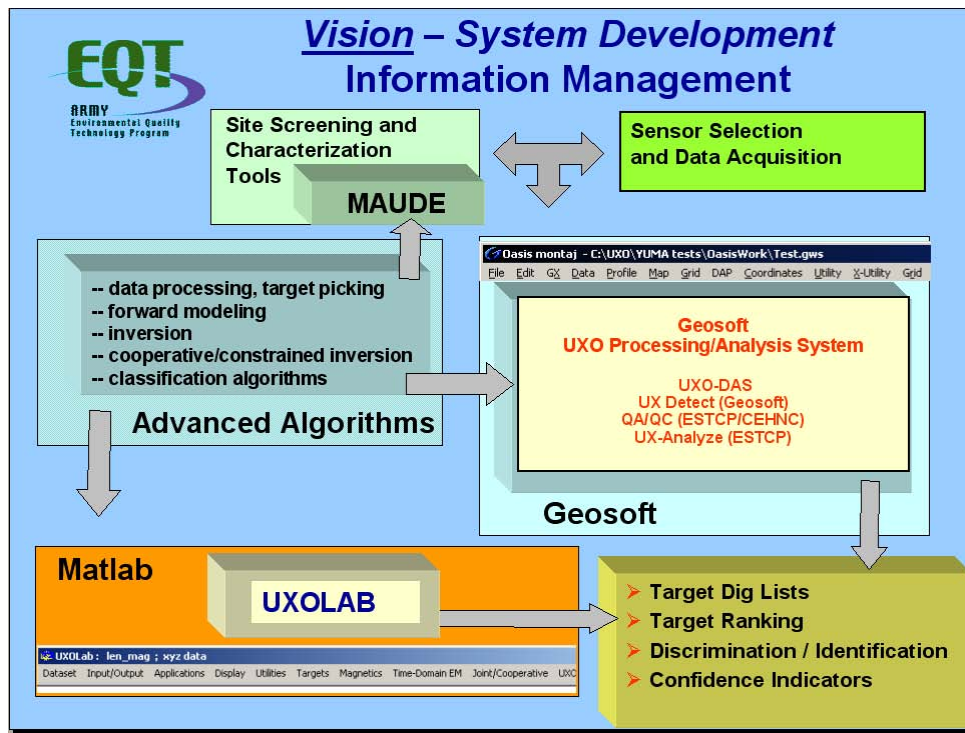


Figure 3. The ERDC UXODAS concept of operations.

2 Sensor Systems

Sensor systems

This section gives a brief overview of the types of sensors used for data collection. The sensors are grouped into the following system types: time domain, frequency domain, passive, and other sensors. Each section includes a general description of the sensor, the data collected, and how the data are reformatted for import into DAQ/DAS.

Time domain electromagnetic induction (EMI) systems

EM61-MK2 EMI system

The EM61-MK2, an enhanced version of the patented EM61, is a time domain metal detector, which detects both ferrous and non-ferrous objects with excellent spatial resolution (Figure 4). Target response is a single, sharply defined peak, facilitating quick and accurate location. A single 200-L (55-gal) drum can be detected at depths greater than 3 m.

Data from multiple time gates (three or four, user-selectable) are recorded to provide a more complete measurement of the response decay rate for improved target characterization (and discrimination). Early time gates increase the maximum depth of detection for all targets; a mid-range time gate, equivalent in position to the original EM61, offers comparison with, and continuation of, original EM61 data sets.

The Allegro CX field computer supports the acquisition of data. Important features include real-time graphic display of data for review and quality control; high-capacity data storage (min. 330,000 data points) for extended survey time; increased rate of data collection; and additional input connections for simultaneous collection of both EM and GPS data.

The EM61-MK2 is GPS compatible; a fully integrated Trimble Ag132 - with no requirement for a separate GPS receiver console. The system can be pulled as a trailer, in single or multiple unit configurations, or carried by an operator with a belt harness. Table 1 lists system specifications.

High power (HP) modification

To increase the depth at which any target is detectable, the high power (HP) modification provides an eight-fold increase in the amount of signal received from a standard transmitter coil resulting in significant improvements in the signal-to-noise ratio. Relative to the standard EM61-MK2 (or EM61), the depth of detection for any target will increase between 45 percent and 80 percent, depending on target characteristics.



Figure 4. The EM61-MK2

Table 1. Specifications for the EM61-MK2

MEASURED QUANTITIES	Four time gates of secondary response in mV
EM SOURCE	Air-cored coil, 1- x 0.5-m size
CURRENT WAVEFORM	Unipolar rectangular current with 25% duty cycle
EM SENSORS	1. Main: Air-cored coil, 1- x 0.5-m in size, coincident with EM source 2. Focusing: Air-cored coil, 1- x 0.5-m in size, 30 cm above main coil
MEASURING RANGES	10,000 mV
DYNAMIC RANGE	18 bits
OUTPUT MONITORS	Color TFT active matrix LCD 320x240 pixels, and audio tone
DATA STORAGE	Over 1,000,000 data sets
POWER SUPPLY	12 V rechargeable battery (approx. 4 hr continuous)
OPERATING WEIGHTS & DIMENSIONS	Backpack: 60 x 30 x 20 cm; 8 kg Coil Assembly: 100 x 50 x 5 cm (bottom), 100 x 50 x 2 cm (top); 14 kg (23 kg in trailer mode)
POSITIONING	Wheel triggered and GPS

Geonics EM-63 EMI system

The EM63 Metal Detector advances the application of time domain electromagnetic (TDEM) methods to the detection of unexploded ordnance (see Figure 5). Measurement of the full transient electromagnetic response with the EM63 offers improved detection capability and information on target characteristics.



Figure 5. Geonics EM-63 on the ERDC UXO/CM test stand.

Comparable to the EM-61 MK2, the EM-63 generates a pulsed primary magnetic field that induces eddy currents in nearby metallic objects. The decay rate of these eddy currents with time generates a secondary magnetic field with a specific rate of decay that is intrinsic to the size, shape, orientation, and metal composition of the object itself. Measurement of the secondary magnetic field decay (the transient response), therefore, will provide important information toward: a more complete characterization and classification of the target; identification and rejection of the characteristic response from certain geologic materials

(e.g. magnetite); and consequently, a reduction in target selection error (the "false-positive rate").

The EM-63 accurately measures the complete transient response over a wide dynamic range of time: measurements are recorded at 26-time spaced gates, covering a time range from 180 μ s to 25 ms. Data acquisition is supported by the PRO4000 field computer, with 16 MB data storage capacity, which is able to simultaneously receive GPS data for location control. Table 2 lists system specifications.

Table 2. Geonics EM-63 Specifications

Measured Quantities	26 time gates of secondary response in mV covering range from 180 μ s to 25 ms
EM Source	Air-cored coil, 1- x 1-m size
Current Waveform	Bipolar rectangular current
EM Sensors	a) Main: Air-cored coil, 0.5 x 0.5 m in size, coincident with EM source b) Focusing: Air-cored coil, 0.5 x 0.5 m in size, 60 cm above main coil
Measuring Ranges	10,000 mV
Dynamic Range	18 bits
Output Monitors	16-line graphic LCD with 24 characters per line
Power Supply	12-V rechargeable battery for 8 hr continuous use
Data Output	RS232 serial port
Data Storage	Solid state memory with capacity of 31,000 data sets
Operating Weight & Dimensions	Sensor: 100 x 100 x 60 cm : 32 kg Console: 38 x 19 x 6 cm : 4.5 kg Battery: 23 x 21 x 14 cm : 10 kg
Shipping Weight & Dimensions	104 x 104 x 22 cm (box 1): 60 kg 58 x 48 x 47 cm (box 2): 46 kg
POSITIONING	Wheel triggered & GPS post-processed

Frequency domain EMI systems

GEM-3-E EMI system

The GEM-3-E is a broadband, programmable EMI System (Figure 6). The GEM-3-E consists of a circular sensor head assembly, a three-button user interface or Personal Data Assistant graphical interface, the electronics

console, and the WinGEM software. The sensor head is available in three different sizes. The 40- and 64-cm sensor heads come mounted on a boom for handheld operation; whereas the 96-cm sensor head is usually mounted on a cart. The sensor head assembly consists of (1) the primary transmitter (Tx) coil, (2) a bucking Tx coil, and (3) a receiver (Rx) coil. The bucking Tx creates a magnetic cavity (null-field region), where the Rx coil is placed. Table 3 lists system specifications.



Figure 6. The GEM-3-E during survey.

Table 3. Specifications for the GEM-3-E

Multiple-frequency operation	Up to 15 frequencies
Frequency band	30 to 47970 Hz
Coil configurations	Horizontal coplanar; 40-, 60-, 96-cm diameter sensor heads
Battery	Standard 12-V notebook computer battery (B905S)
Battery life	~4 hrs
Weight	9 lb (4 kg)
Basic output	Inphase and quadrature response in parts per million (ppm)
PC software	WinGEM2k
Positioning	Utilizing GPS data

System configuration GEM-3-E

The GEM-3-E, used at the ERDC, consisted of the 96-cm head with the data acquisition box, a laptop computer for the controller unit, and a NavCom GPS rover. The GPS rover was secured to the mast of the GPS antenna and the controller was in the data acquisition box. The controller

for the GEM-3-E generates a digital composite current waveform, consisting of a user-selectable number of frequencies, to the primary and bucking Tx coils. The frequencies chosen for the ERDC data acquisition were 90, 210, 390, 750, 1470, 2910, 5850, 11430, 21690, and 41010 Hz.

Passive systems

Geometrics 823A cesium vapor total field magnetometer (TFM) description

The Geometrics 823A cesium vapor TFM (see Figure 7) is designed for mobile or base station applications, where high sensitivity and rapid sampling and recording of the earth's magnetic field are required. The system consists of a cesium sensor, with associated cables and driver electronic package, and a separate high-resolution counter. The G-823A operates on 24-32 VDC power. Tuning through the earth's magnetic field range is fully automatic, including automatic hemisphere switching. The sensor/electronics package is watertight and temperature controlled. The G-823A was set to collect at 10 samples per second. The G-823A system specifications are shown in Table 4.



Figure 7. G-823A magnetometer

Table 4. Specifications for the G-823A

Operating Principle	Self-oscillating split-beam Cesium Vapor (non-radioactive Cs-133)
Operating Zones	The earth's field should be at an angle greater than 10° from the sensor's equator and at 10° away from the sensor's long axis. Automatic hemisphere switching.
Operating Range	20,000nT to 100,00nT
Power	24 to 32 VDC, 0.75 amp at turn-on and 0.5 amp thereafter
Heading Error	+/- 0.15 nT throughout polar and equatorial spins, 360°.
Absolute Accuracy	>5nT throughout range.
Sensitivity	Typically 0.003nT P-P at a 0.1-sec sample rate (90% of all readings falling within the P-P envelope).
Data Output	One cycle of Lamour frequency = 3.49nT, 2 V P-P coupled through the sensor power input.
Altitude	Up to 300,00 ft (9,000 m).
Water Tight	Sealed for up to 2 ft (0.9 m).
Sample Interval	0.01, 0.02, 0.05, 0.1, 0.2, 0.5, 1, 2, 5, and 10 seconds, or by external cycle command.
Positioning	Post Processing

Other systems

Geonics EM-61HH hand-held EMI sensor

The EM61HH (Figure 8) is a "hand-held" complement to the EM-61 MK2 (Figure 4), providing greater sensitivity to smaller targets at shallow depths. A single 20-mm projectile can be detected to a depth of greater than 0.5 m. Comparatively, a single 200-l (55-gal.) drum can be detected to depths of greater than 2 m.

Data are collected from a single receiver at four time gates after transmitter turn-off. Information from four gates provides for the discrimination of targets based on the response decay rate; the early time data will detect both small and large targets with short and long decay rates respectively, while the late time data will detect only larger targets with relatively long response discrimination.

With a narrower spatial focus than the standard EM-61 MK2, the EM-61HH Mk2 is a relatively less sensitive footprint to sources of potential interference. As a result, data can be collected in closer proximity to cultural features such as fences and buildings. Additionally, the narrower focus provides enhanced target resolution, and consequently improves discrimination of multiple targets.

The EM-61HH MK2 can be operated either with or without wheels (Figure 8). In either configuration, the smaller, more portable design offers improved access to areas of difficult terrain and dense vegetation. Table 5 lists system specifications.



Figure 8. The Geonics EM-61HH on data collection pass.

Table 5. Specifications for the EM-61HH

Measured Quantities	Four time gates of secondary response in mV
EM Source	Air-cored coil, 17 cm diameter
Current Waveform	Uni-polar rectangular current with 25% duty cycle
EM Sensor	Air-cored coil, 17 cm diameter
Measuring Ranges	10,000 mV
Dynamic Range	18 bits
Output Monitors	16-line graphic LCD with 24 characters per line, and audio tone
Power Supply	12-V rechargeable battery for 4-hr continuous use
Data Output	RS232 serial port
Data Storage	330,000 data sets
Operating Weight & Dimensions	Back pack: 60 x 30 x 20 cm; 8 kg
Sensor Assembly	33 x 20 cm; 2.8 kg (7.5 kg with wheels)
Shipping Weight & Dimensions	50kg, 117 x 50 x 54 cm
Positioning	Wheel logged & GPS post processing

The ERDC Hand-held Dual TFM/EMI Sensor

The ERDC Hand-held Dual TFM/EMI Sensor hardware (Figures 9 and 10) is comprised of an EMI sensor, cesium (Cs) vapor magnetometer, fluxgate magnetometer, hand-held data acquisition computer, integrated power supply, interconnection cables, and deployment hardware (backpack, mounting pole, etc.). The EMI system is the Geophex GEM-3; the magnetic system is the Geometrics model 823A Cs vapor magnetometer. The fluxgate magnetometer is a Bartington model Mag-3MRN60, three-axis fluxgate magnetometer. The system weighs approximately 46 lb, when the ArcSecond positioning system (described next) is attached and is completely man portable (no wheels).



Figure 9. The ERDC hand-held Dual TFM/EMI with ArcSecond positioning system.

During standard usage, the fluxgate magnetometer is used to provide the instrument attitude relative to the Earth's magnetic field. The data from the fluxgate was routed through the secondary pre-amp in the magnetometer and incorporated into the magnetometer data stream. This combined data stream, along with the positioning data stream, is then put into the GEM-3, which was modified to have an extra serial input. All data streams are combined into a single binary data file on the GEM-3. This binary file is decoded into three separate files containing the standard GEM-3 data, "GPS" position file, and magnetometer/fluxgate file.

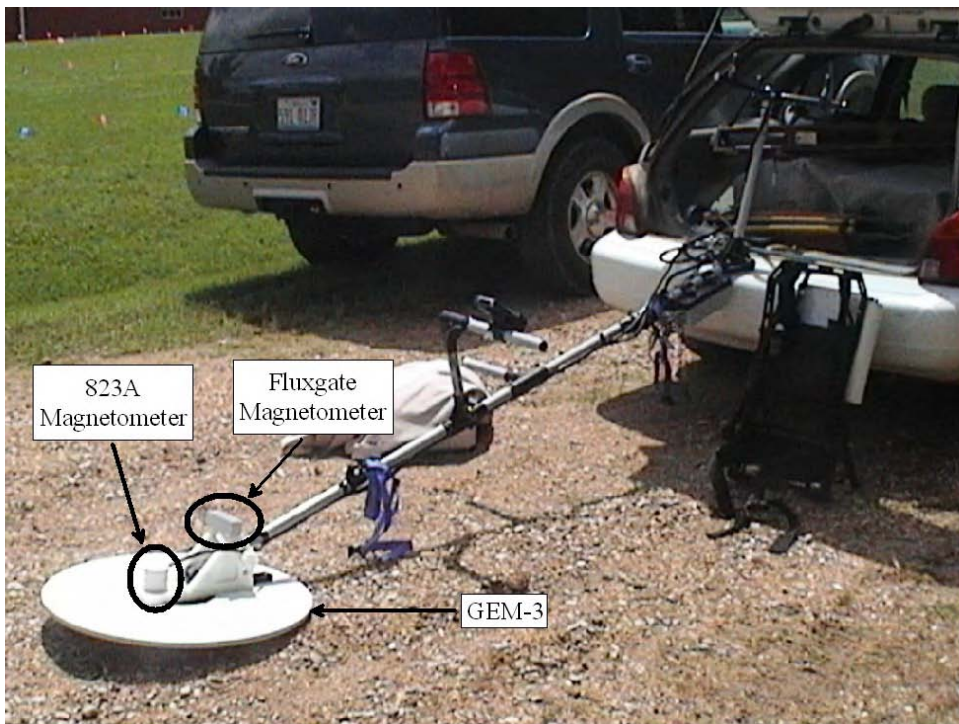


Figure 10. Components of the ERDC hand-held Dual TFM/EMI

ArcSecond LASER positioning system

The positioning system used in tests at the ERDC was the ArcSecond positioning system. The ArcSecond system (Figure 9) configured for this application is comprised of four remote beacons and an array of four sensors that are mounted on the structure that is being positioned. The beacons transmit a timing pulse and two crossed rotating lasers. Upon detection of these lasers, each sensor is provided with a measurement of the vertical and horizontal angle of the sensor position relative to the transmitting beacon. Given precise knowledge of each beacon's position and orientation, these angles are used to triangulate the sensor positions in three dimensions. Given the exact positions of each of the three sensors in the array, the position and orientation of the geophysical sensors can be determined, assuming that the positioning sensor array is fixed rigidly to a non-flexing geophysical sensor carry assembly.

Because the ArcSecond system uses angular measurements from the beacons rather than distance measurements, the setup and calibration of the beacon positions are more complex than other systems. The position and orientation of each beacon must be accurate and stable. Each deployment must be initialized by calibrating the system (Figure 11). A minimum of six measurements are taken so that the beacon locations and

orientations can be determined relative to each other. The sensors are positioned during the course of the geophysical survey relative to the beacon network frame of reference. These positions are then translated to a local or standard coordinate system.

In the integration of the ArcSecond positioning system with the dual sensor, the problem of time latency is corrected by using a time alignment scheme similar to that used for GPS systems. The ArcSecond system was modified to emulate GPS systems by providing a PPS trigger pulse and 'standard' NMEA data strings via an RS232 data link. This provides for ease of integration of the ArcSecond system with any geophysical systems that are currently capable of integration with GPS systems.



Figure 11. Setup and calibration using light bar for the ArcSecond LASER position system (Phasell).

G-tek⁵ SAM system

Sub Audio Magnetics (SAM) is a method by which a total field magnetometer sampling at a very high rate may be used to simultaneously acquire both Total Magnetic Intensity (TMI) and Total Field Electromagnetic Induction (TFEMI) data (Figure 12). The SAM system consists of the following components: (1) single TFM or array of TFM's, (2) a large transmitter loop (EM source), and (3) data acquisition and display (Output Monitors) (see Table 6).

⁵ G-tek Australia Pty Ltd. (now Gap Geophysics Australia Pty Ltd., South Brisbane, Queensland, Australia).



Figure 12. SAM System fielded in Yuma, Arizona

Magnetometer array

The SAM-capable TM-6 magnetometer array was developed and built by G-tek. The TM-6 magnetometer system has been designed to interface with a variety of positioning devices, as different application localities have different characteristics and requirements. When using the magnetometer for SAM applications, GPS time must be accessible at least once every 30 minutes in order to maintain precise clock synchronization. However, this time signal may be unobtainable in conditions such as wooded areas where DGPS positional accuracy is not satisfactory. In such situations, a cotton-thread-based odometer system developed by G-tek and used for over 25 years provides a good alternative. However, emerging new technologies such as the robotic total station (RTS) are also compatible with the magnetometer array. At the Aberdeen Proving Ground site, both the odometer and RTS will be used in the forested area to evaluate their relative performance. System specifications are listed in Table 6.

Table 6. Specifications for the G-tek SAM System

Measured Quantities	Sample Rates 1200, 2400, or 4800 per second
EM Source	Wire Loop (typically 33m x 33m)
Current Waveform	Bipolar rectangular current
EM / TFM Sensor	Cesium Vapor Magnetometer
Output Monitors	Screen of PDA 320x240 pixels
Positioning	GPS real time processing

Additional features of the SAM include:

1. Accepts Larmor signal input from a hand-held array of four optically pumped magnetic sensors;
2. Simultaneously acquires magnetic field measurements from each sensor at selectable rates up to 4,800 per second;
3. Measurements are acquired at precisely equal time intervals that are synchronized to GPS time;
4. The RMS noise floor for each measurement sample rate typically lies between 1 nT at 10,000 per second to 1 pT at 100 per second when plotted on a logarithmic abscissa. (This program proposes sampling at 4,800 per second at which the noise is approximately 0.2 nT, reducible in late-time by the averaging of consecutive samples);
5. Accepts position and time information, including 1 pps strobe from DGPS;
6. Magnetometer, DGPS, and batteries to power a quad-sensor array for typically 2.5 hr are carried in a backpack weighing approximately 8 kg;
7. Graphic user interface implemented on a Pocket PC;
8. Electromagnetic Transmitter: An 8-turn wire loop is laid out along a meandering path surrounding the grid area to be surveyed (typically 33 m × 33 m). A Zonge GGT-10 current transmitter energizes this loop with a bi-polar, 12 – 20 Amp square wave current of typically 50 percent duty cycle and 15 Hz frequency. The transmitter and receiving magnetometer are precisely synchronized using GPS time.

Data processing description

Raw TM-6 data are processed using a proprietary software package referred to as ‘MagPi,’ which performs all preprocessing procedures including separation of the magnetic (TMI) and electromagnetic data (TFEMI) sets, waveform stacking, removal of unwanted frequency

components such as 60-Hz noise, EM decay curve integration, decimation, and merging of DGPS time/position and low-pass filtering. The MagPi output is usually in the form of Excel style (*.csv files) (time decays) or Geosoft XYZ files. The Geosoft Mapping Package is used for data manaGEMent, gridding, map creation and display, and other specialized filtering. Two software products, MagSys (G-tek) and UXOLAB (UBC), are used for additional interpretation of the gridded data, in order to provide automatic anomaly picking, calculation of certain anomaly parameters, forward modeling, and inversion. The SAM method provides two complementary data sets (TMI and TFEMI) that are perfectly geo-referenced because the same sensor is used to acquire both data types simultaneously. For these technology demonstrations, the individual data sets will be processed separately to the point of producing the XYZ files, but the results will be presented as a single joint interpretation, combining selected information from each data set in a logical manner that optimizes target detect/discrimination. In the specific case of small ordnance items such as grenades and submunitions, the TFEMI response is likely to be below the noise floor with the TFEMI, in which case the interpretation will be based on the TMI alone.

3 Data Import and Processing Procedures

As data are acquired in the field, the field team must display the data and check for any serious sensor or other problems that would make the data unsuitable and indicate the need to reacquire data in an area. Several quality control procedures and standard data correction methods are used to ensure the quality of the data collected during the field investigation. These include displaying line path and coverage maps to verify that the area was adequately covered, correcting positioning errors due to time lag between the data acquisition and the reporting of sensor position, and correcting sensor drift.

Import into Oasis Montaj

All of the previously discussed sensor systems have the ability to output data in an ASCII format. Oasis Montaj has a general-purpose import procedure for bringing ASCII data into a database that allows the user to select channels to import and specify names and formats for them. In order to simplify the import procedures, GXs to import data from specific sensors have been developed and placed in the UXO-DAS menu. Links to the Oasis Montaj functions to import ASCII and Geosoft XYZ data are also included on the UXO-DAS menu for convenience. Data in a different format than expected or from an unsupported sensor can still be imported using the built-in Oasis Montaj import procedure.

The UXO-DAS import menu is shown in Figure 13 and selection of the GEM-3 menu item results in the dialog shown in Figure 14. Figure 15 shows the imported GEM-3 data in an Oasis Montaj database. The inphase and quadrature data for all frequencies are stored in the array channels IP and Q, respectively. Array channels provide a quick graphical look at the nature of the inphase and quadrature frequency curves and simplify some processing steps. However, it may also be desirable to look at individual channels. A single channel of data can be extracted from an array channel selecting the Extract Channel item from the UXO-DAS menu. The dialog shown in Figure 16 will be displayed. The user selects the array channel, names the output channel, and specifies the (zero-relative) number of the channel to extract.

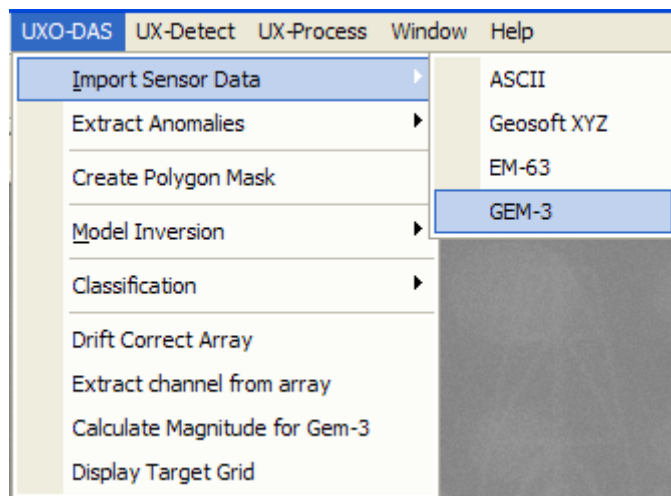


Figure 13. UXO-DAS import menu



Figure 14. GEM-3 import dialog box

The import dialog box for the EM-63 is shown in Figure 17 and the resulting database is shown in Figure 18. The 26 time channels of the EM-63 are stored in the array channel Z1. As for the GEM-3 data, a single channel can be extracted from the array channel using the Extract Channel function.

Area coverage

The first QA/QC task is to examine the spatial distribution of the acquired data to ensure that the survey area is adequately covered. After each data acquisition, a line path plot should be generated. This data visualization tool will verify that no significant gaps are present in the newly acquired data or between the new data and the previously acquired data. It will also show irregularities in the positioning data, such as a temporary loss of GPS signal. If a loss of positioning data is of short duration, the missing positions can be interpolated from known positions without the need to reacquire data. A line path plot is shown in Figure 19. When all the data for an area are collected, a coverage map of the area should be generated using Geosoft's UX-Detect software module. A coverage map, such as that shown in Figure 20, will quickly show any gaps in coverage of an area.

based on a user-defined grid size. Grid cells with a value of zero (0), which is displayed in white, indicate gaps in the area coverage at the resolution being displayed. The percentage of grids that are covered can also be calculated.

L0:0	X	Y	IP	Q	Sample	powerIn	Qsum	marker	stat
0.0	*	*			0	0.000078	-2175.79	*	
1.0	*	*			1	0.000078	-2178.20	*	
2.0	*	*			2	0.000078	-2177.53	*	
3.0	*	*			3	0.000078	-2175.48	*	
4.0	*	*			4	0.000077	-2172.74	*	
5.0	*	*			5	0.000076	-2160.64	*	
6.0	*	*			6	0.000075	-2136.59	*	
7.0	*	*			7	0.000074	-2115.61	*	
8.0	*	*			8	0.000074	-2107.45	*	
9.0	*	*			9	0.000074	-2103.11	*	
10.0	757668.453	3638306.980			10	0.000074	-2100.95	*	
11.0	757668.452	3638306.980			11	0.000074	-2100.17	*	
12.0	757668.452	3638306.980			12	0.000074	-2100.33	*	
13.0	757668.452	3638306.980			13	0.000074	-2099.84	*	
14.0	757668.451	3638306.980			14	0.000074	-2099.05	*	
15.0	757668.451	3638306.980			15	0.000074	-2097.74	*	
16.0	757668.450	3638306.980			16	0.000073	-2098.02	*	
17.0	757668.450	3638306.980			17	0.000073	-2098.53	*	
18.0	757668.450	3638306.980			18	0.000074	-2097.89	*	
19.0	757668.449	3638306.980			19	0.000074	-2097.80	*	
20.0	757668.449	3638306.980			20	0.000073	-2097.92	*	
21.0	757668.447	3638306.980			21	0.000073	-2097.86	*	
22.0	757668.446	3638306.980			22	0.000073	-2097.64	*	

Figure 15. GEM-3 database.

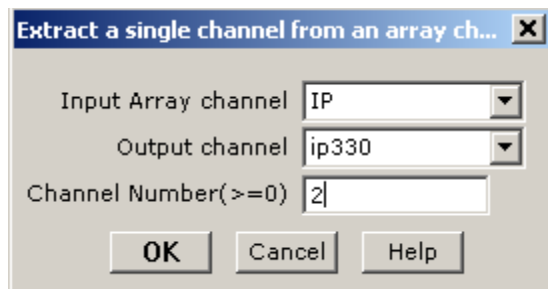


Figure 16. Dialog box for extracting a single channel from an array channel.



Figure 17. EM-63 import dialog box.

D 0:0	X	x	y	z1	ChT	ChB	ChD	ChA	Time
0.0	757670.02	3638307.55			*	*	*	*	
1.0	757670.02	3638307.55			*	*	*	*	
2.0	757670.02	3638307.55			*	*	*	*	
3.0	757670.03	3638307.55			*	*	*	*	
4.0	757670.04	3638307.55			*	*	*	*	
5.0	757670.05	3638307.55			*	*	*	*	
6.0	757670.06	3638307.55			*	*	*	*	
7.0	757670.08	3638307.55			*	*	*	*	
8.0	757670.09	3638307.55			*	*	*	*	
9.0	757670.12	3638307.55			*	*	*	*	
10.0	757670.14	3638307.55			*	*	*	*	
11.0	757670.16	3638307.55			*	*	*	*	
12.0	757670.20	3638307.55			*	*	*	*	
13.0	757670.25	3638307.55			*	*	*	*	
14.0	757670.29	3638307.55			*	*	*	*	
15.0	757670.34	3638307.55			*	*	*	*	
16.0	757670.39	3638307.55			*	*	*	*	
17.0	757670.43	3638307.55			*	*	*	*	
18.0	757670.53	3638307.55			*	*	*	*	
19.0	757670.64	3638307.55			*	*	*	*	
20.0	757670.73	3638307.55			*	*	*	*	
21.0	757670.84	3638307.55			*	*	*	*	
22.0	757670.90	3638307.55			*	*	*	*	

Figure 18. EM-63 database.

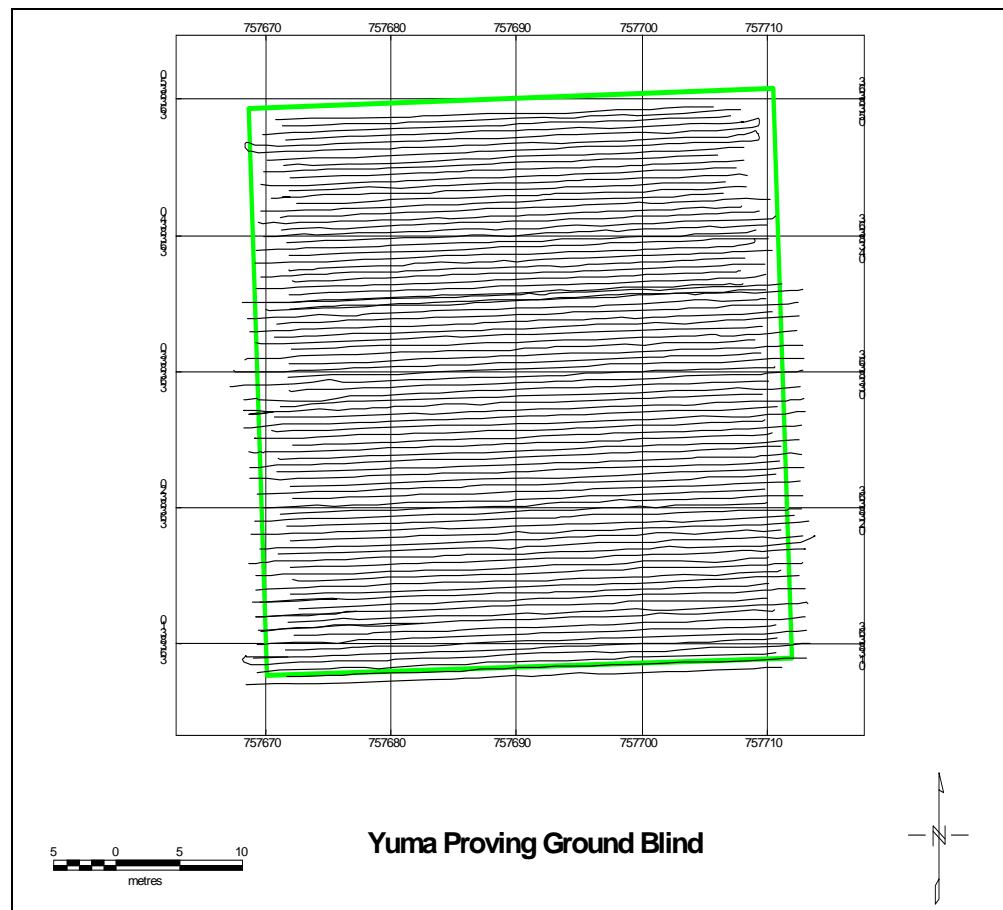


Figure 19. Line path plot.

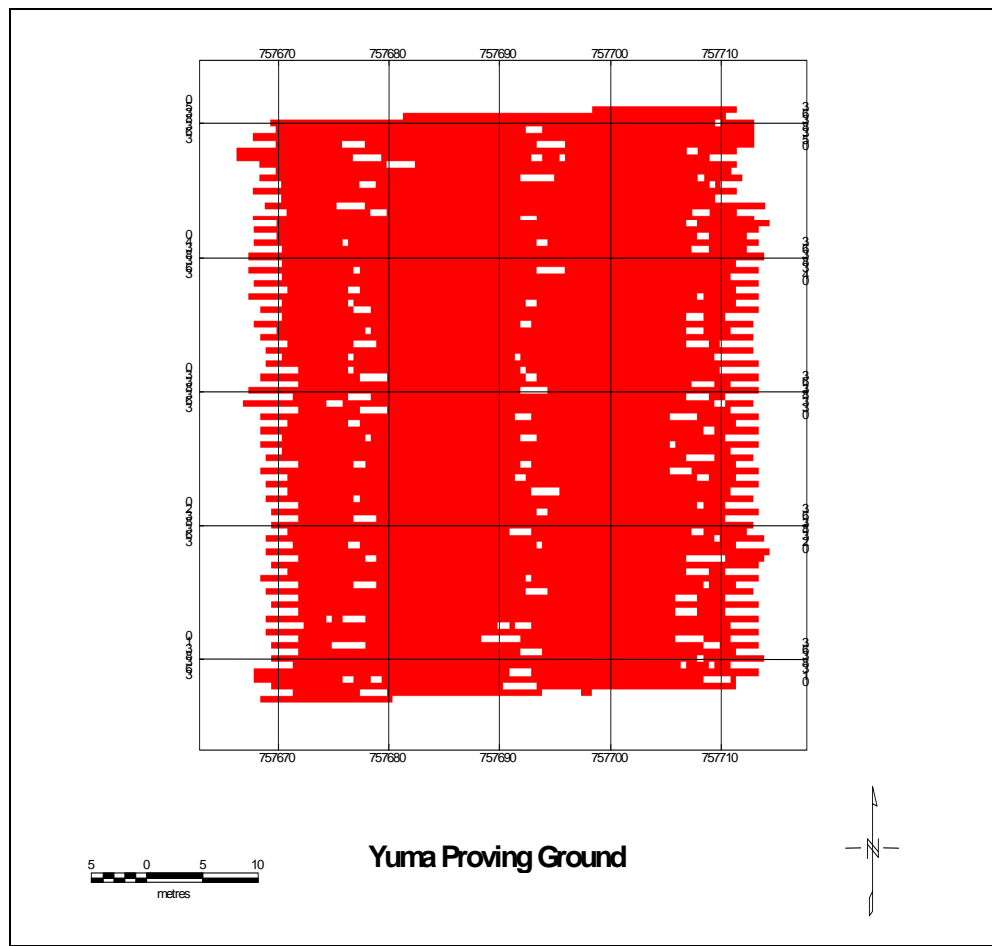


Figure 20. Coverage map.

Time synch

Another common data collection issue is time lag between the collection of sensor data and the reporting of sensor position from GPS or other positioning system. To determine the amount of time lag, a calibration procedure is performed which consists of passing over a target multiple times in opposite directions. From this data, the amount of shift to locate the peak sensor response in both directions at the same xy location can be calculated. The data can then be shifted to correct the time lag using the UX-Process latency correction function as shown in Figure 21. Here, the fiducial channel is used as a reference to shift the data an integral number of data collection points relative to the position data. The sign of the delay indicates the direction of the shift. Using the fiducial channel as reference makes sense as long as the data are collected at regular intervals. However, if the rate of data collection varies, a time channel should be used. Also, the delay that is specified does not have to be an integer. If a decimal delay

is specified, the new positions will be linearly interpolated from the original positions.

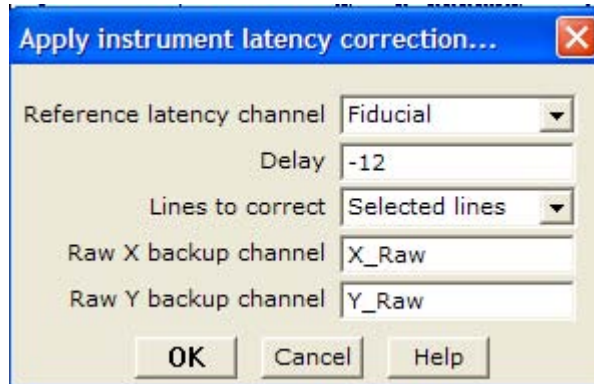


Figure 21. Dialog for latency correction.

Figure 22 dramatically illustrates the effect of time lag on the gridded image of an anomaly. The anomaly in the lower middle section of the image shows up as three separate anomalies corresponding to the three passes of the sensor near it. After the correction, the seemingly multiple targets converge to a single anomaly as shown in Figure 23. Plotting the data in this manner allows the user to verify the accuracy of the time lag correction.

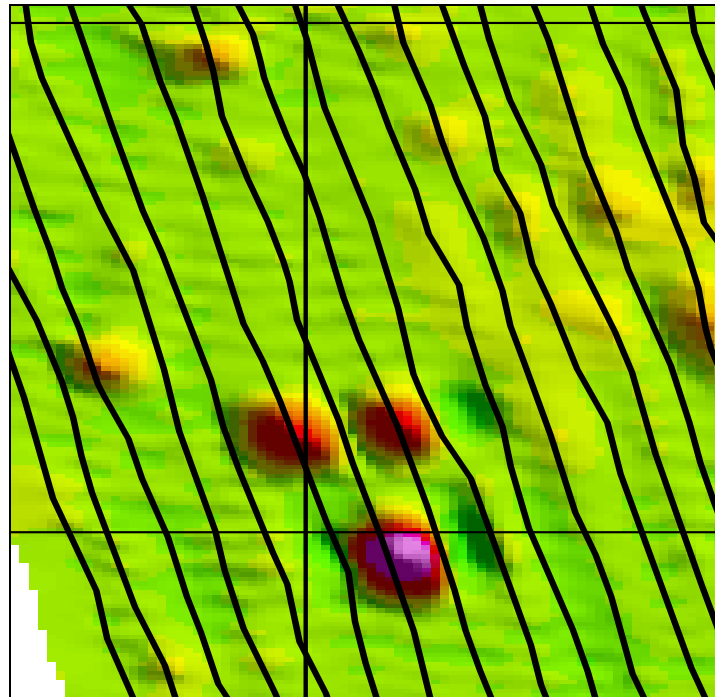


Figure 22. Gridded image of an anomaly before lag correction.

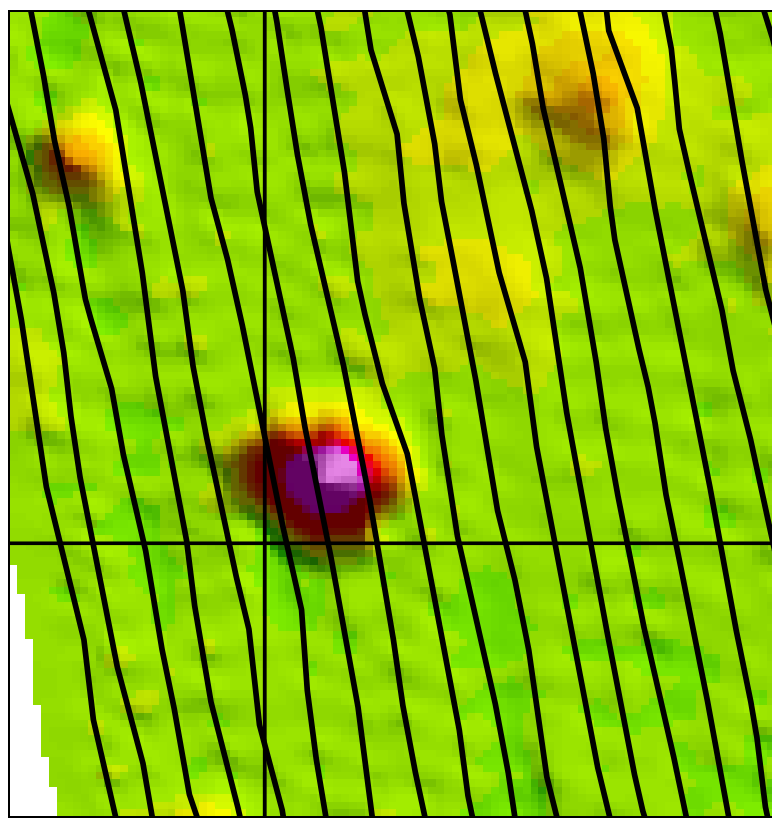


Figure 23. Gridded image of the same anomaly after lag correction.

Drift correction

Another common problem encountered when collecting geophysical data is instrument drift (Figure 24). Sensor signal level varies with time during a data collection due to factors such as changes in temperature and power output from the batteries. Sensor drift can be seen in the color gradations from top to bottom in the gridded image in Figure 24. Figure 25 shows the same data after application of the Geosoft UX-Detect drift correction algorithm. This algorithm calculates the average value for each block of data of a user-specified size and subtracts the average from all the points in the block. A user-specified percentage of points at the high and/or low end of the range of values are excluded from the calculation of the average so that the presence of targets in the data block does not skew the average. Ideally, only background points will be included in the average calculation; however, this can be difficult to achieve in areas of dense target population. The overlapping nature of high frequency target signal responses obscures signals of “pure” background points, making localized averaging more difficult.

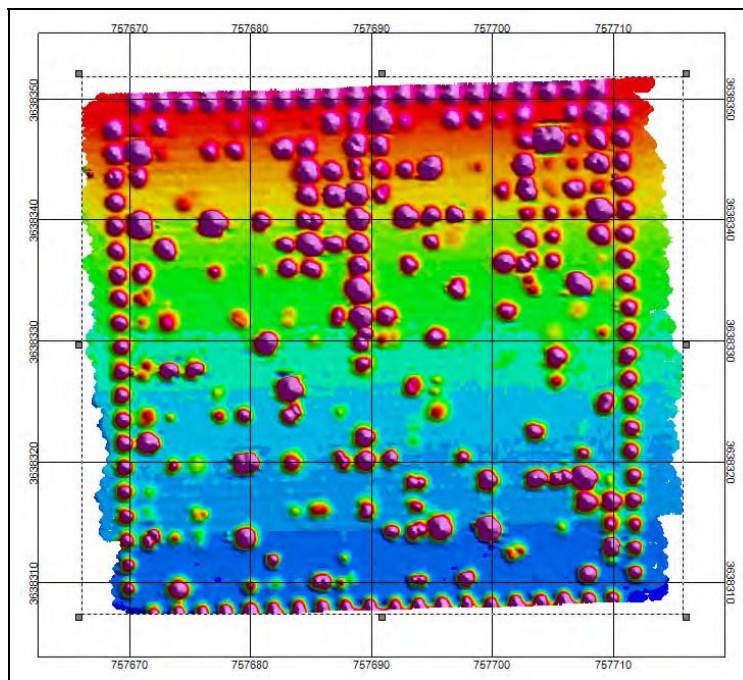


Figure 24. Gridded image of EM-63 data showing instrument drift.

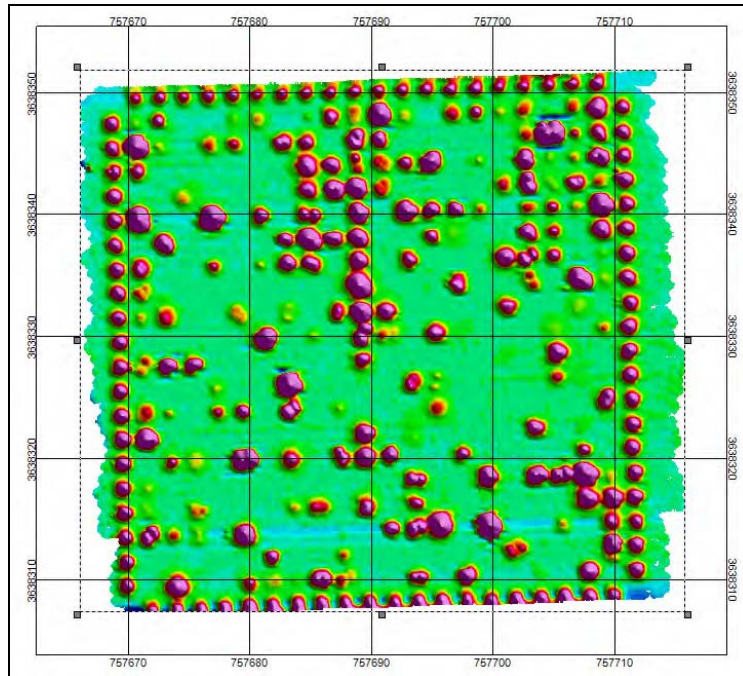


Figure 25. Gridded image of EM-63 data after drift correction.

Drift correction is performed on each data channel independently. For data from sensors, such as the EM-63 and GEM-3, that are stored as array channels, a function is provided in the UXO-DAS menu to perform drift corrections for all the channels in an array. The dialog box for this function is shown in Figure 26. In this example, the maximum number of values

per block is left unspecified, which results in the correction being applied to an entire survey line at a time. The percentage of lowest values to ignore is set much higher than the percentage of highest values to ignore in this case, because the sensor responses of targets are typically negative for the GEM-3 in-phase channel which is being corrected here. Figure 27 shows the percentage to ignore parameters reversed for the quadrature channels because sensor response to targets is typically higher than the background for this channel.

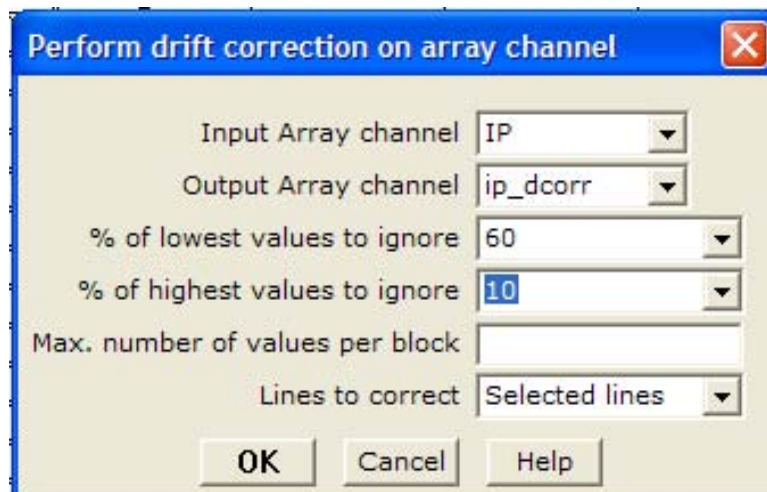


Figure 26. Dialog box for drift correction of GEM-3 In-phase channel.

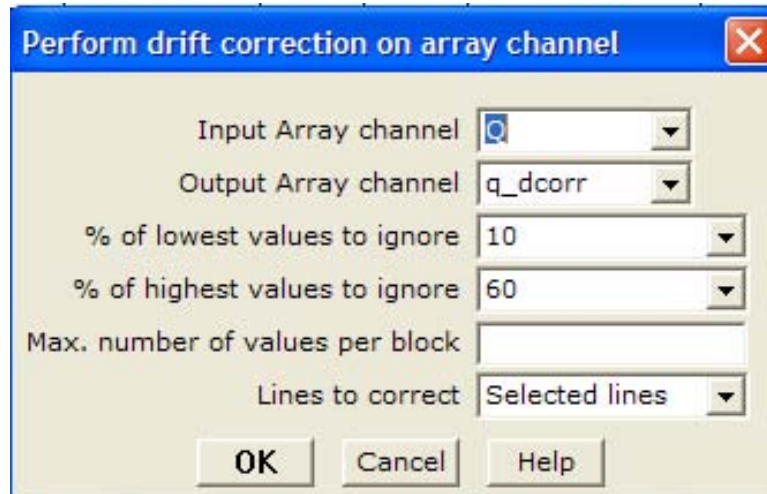


Figure 27. Dialog box for drift correction of GEM-3 Quadrature channel.

4 Anomaly Selection

UX-Detect

Once sensor corrections have been performed and measurement locations have been determined as accurately as possible, the next major step is to select possible target locations. The UX-Detect menu in Oasis Montaj provides the capability to select anomalies in an automated fashion for single-channel sensors or for a single channel of data from a multi-channel sensor. The UX-Detect anomaly-picking algorithms work with regularly gridded data, not the original sensor data. Oasis Montaj provides a number of gridding techniques, but the ones that seem most useful for UXO data are Minimum Curvature and Bi-directional gridding. UX-Detect provides two methods to locate anomalies in a data set: Blakely Test and Peakedness Test. These two algorithms are somewhat similar methods for finding local peaks in regularly spaced gridded data. They tend to produce similar results in most cases, but may vary significantly for some data sets.

As stated earlier, the Blakely or Peakedness Test must be run on gridded data produced from a single data channel. In the case of the EM-63, a logical channel to use is the first time channel since it should have the strongest signal. However, any individual channel or the sum of all the channels can be used. Figure 28 shows a target anomaly map created from a single channel of EM-63 data using the Blakely test. For the GEM-3, selecting targets from a single frequency channel is not a good choice because the strength of response for a given frequency will vary greatly depending on the size and construction material of the targets. Using one frequency would likely result in missing targets that are clearly visible in other frequency channels. Normally, a summary channel is used to locate targets in GEM-3 data. The sensor outputs a Qsum channel, which is the sum of the quadrature responses for all frequencies. As an alternative, a function is provided in UXO-DAS to calculate the sum of the magnitudes of all the frequencies. The magnitude of each frequency is the square root of the sum of the squares of the quadrature and inphase responses at that frequency. The next section describes a different method for selecting anomalies in multi-channel data sets such as the GEM-3 and EM-63.

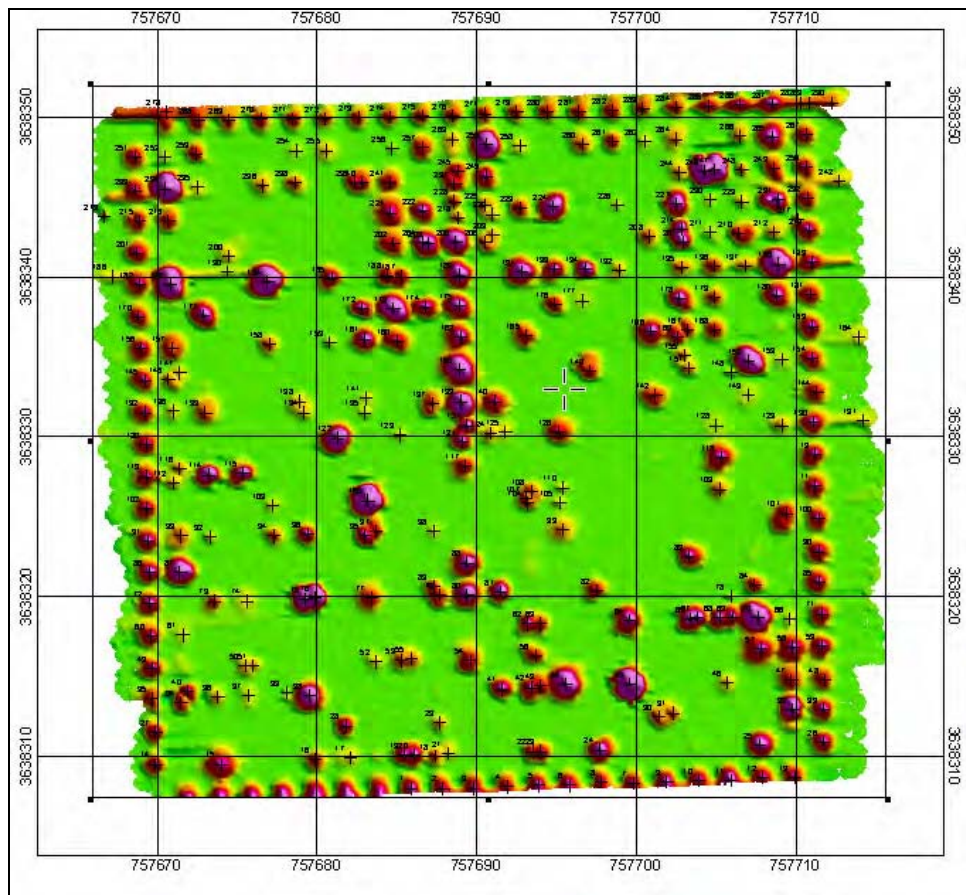


Figure 28. Target anomaly map created with UX-Detect

Selecting anomalies from a single raw channel or summary channel grid works well for EM data. However, anomalies in magnetometer data typically have a bipolar response with a positive peak and a negative peak, as can be seen in Figure 29. For magnetometer data, anomalies are selected in UX-Detect using an analytic signal grid. The analytic signal is the square root of the sum of the squares of the derivatives in the x, y, and z directions. The local peaks in the analytic signal grid should correspond approximately to the centers of magnetic target anomalies. The analytic signal grid can be created from the magnetometer data in UX-Detect using either a step-by-step or an automated procedure. Figure 30 shows the analytic signal grid calculated from the magnetometer data shown in Figure 29. Figure 30 also shows the targets selected from the analytic signal grid using UX-Detect.

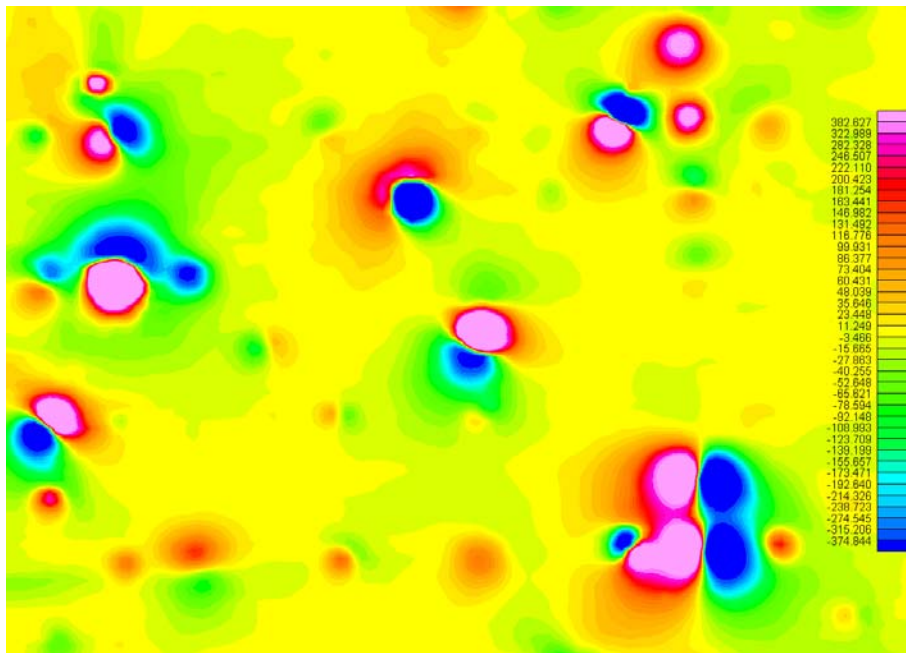


Figure 29. Gridded magnetometer data (units = nT).

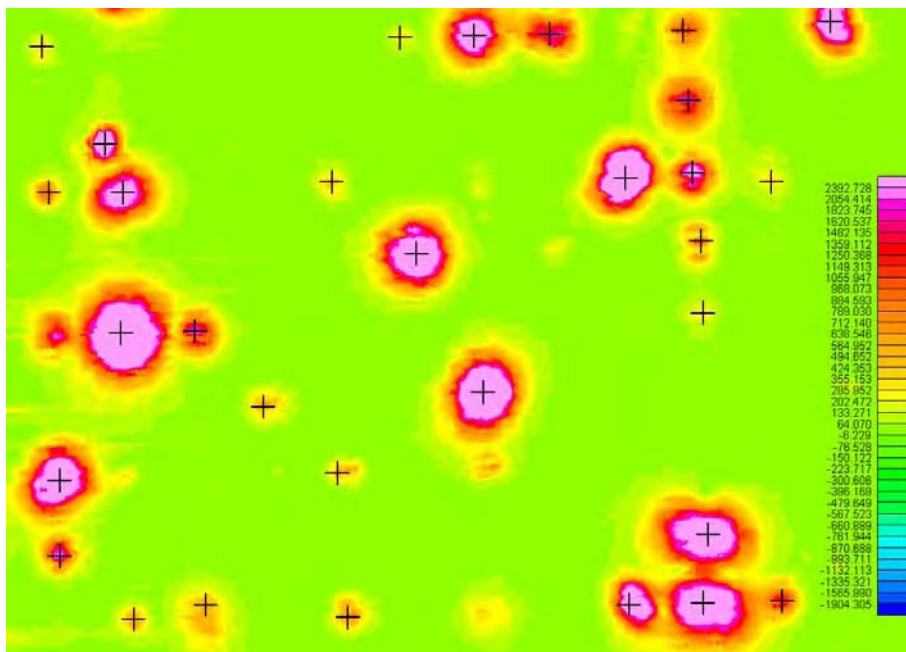


Figure 30. Analytic signal grid calculated from the magnetometer data shown in Figure 29. Anomalies selected by UX-Detect are marked with + (units = nT).

Histogram-based algorithm

The histogram-based anomaly-picking algorithm has not yet been added to the UXODAS package. It is presented here as a new processing and interpretation tool. This algorithm works across all the dimensions of data unlike the Blakely or Peakedness Test, which works only on gridded data produced from a single data channel. The histogram-based method produces background-leveled target selections from multidimensional data.

Figures 31-33 show data taken at the Yuma standardized test area with the GEM-3. The bottom of each figure shows the logarithmic histogram generated for each of three frequencies. At a given frequency, the histogram is a plot of in-phase amplitude versus the number of occurrences in the survey area. The code searches each dimension of the histogram to determine the P_n , which is the peak of the distribution for the n^{th} dimension of this data. The histograms at the bottoms of Figures 31-32 are different, because the variation in the background is different for each frequency.

Visual inspection of Figures 31-32 shows the anomalies in this track data, but may not be immediately obvious to casual inspection. The area represented by background far exceeds the area designated for the anomalies (“targets”); therefore, it is easier to identify background. Previously, this was done by iterating different threshold levels for the background values until a value was found to represent the background noise. Figure 34 is the result of processing the data in Figure 33 by selecting the “Redraw map with peak exclusion” option. This operation excludes the peak histogram bin and a number of other bins on either side of the peak (Valentine and Rana 1996). The algorithm removes the number of bins (entered in the text box) around the peak until the operator determines that most of the background is removed. The exact number of bins excluded is entered in a text box located directly below the “redraw” option button on the screen (Figure 34). Now, the peak of the histogram has been removed from the display color palette. Therefore, when the background surface is subtracted from the original data, the targets or other anomalies are displayed.

A broader implementation of the histogram-based method would characterize the properties of the background distribution. A bimodal peak would indicate the presence of two separate background distributions. In this

case, the operator would subdivide the area until each area showed a single peak. This algorithm determines groups of anomalous points and their centers, and compares the results across all dimensions of the data.

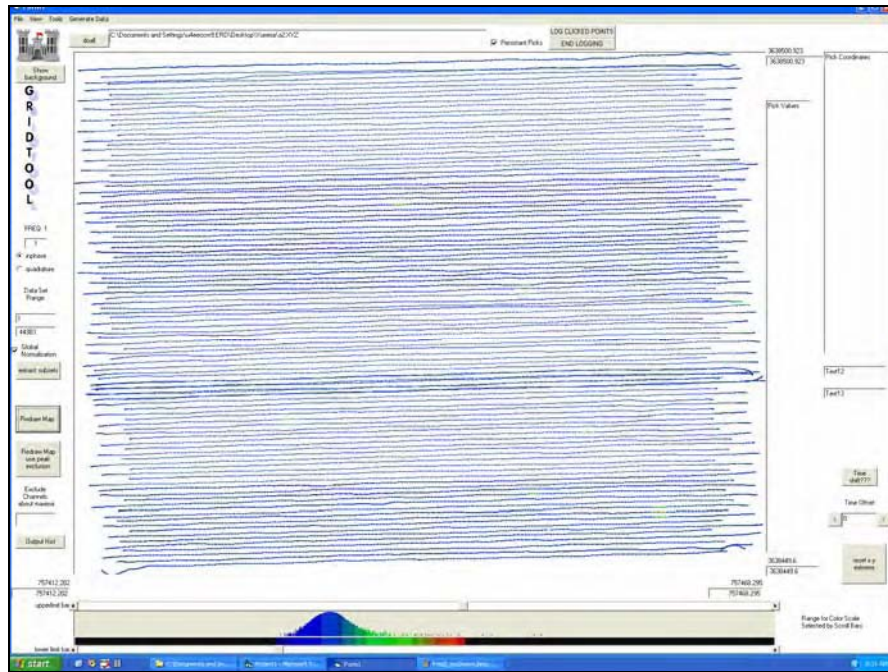


Figure 31. Grid and histogram (at bottom) of GEM-3 in-phase anomaly data for frequency = 1 (90Hz).

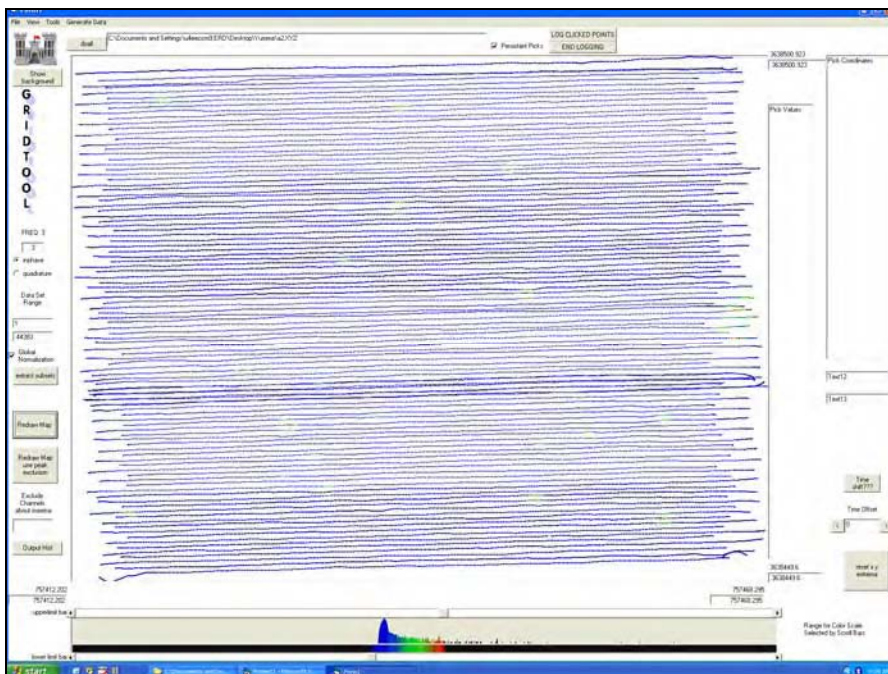


Figure 32. Grid and histogram (at bottom) of GEM-3 in-phase anomaly data for frequency = 3 (390Hz).

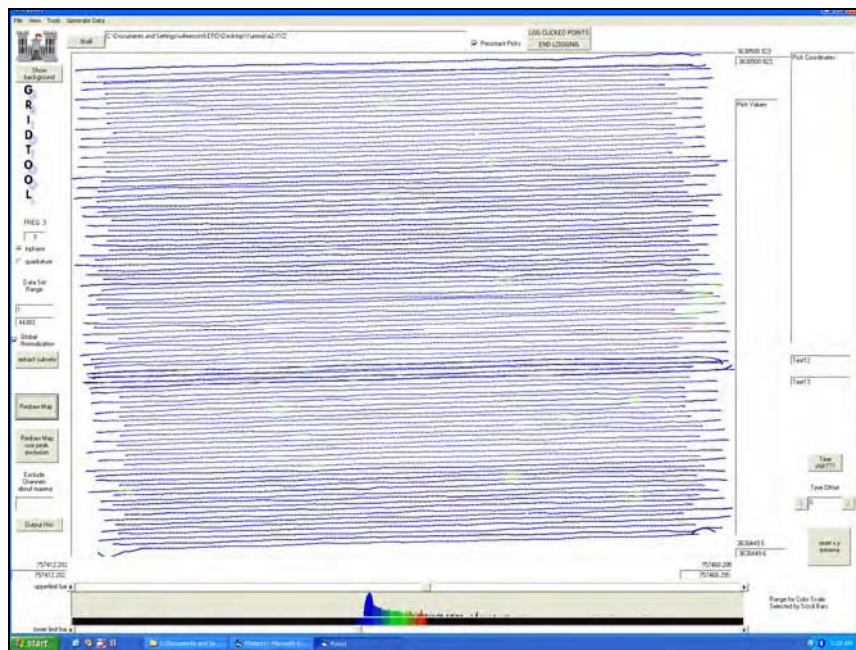


Figure 33. Grid and histogram (at bottom) of GEM-3 in-phase anomaly data for frequency = 5 (1290Hz).

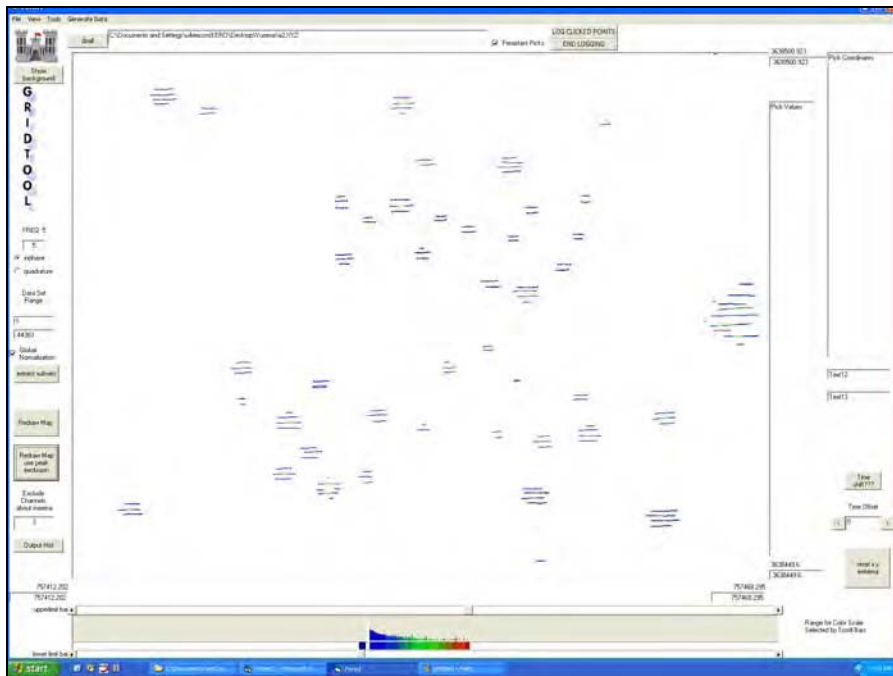


Figure 34. Grid and log histogram (at bottom) of GEM-3 in-phase anomaly data for frequency = 5 (1290Hz) with background peak excluded.

Extraction of anomaly data

Once potential target locations are identified, data are extracted around each anomaly for further analysis. Figure 35 shows the dialog box for extraction of GEM-3 anomaly data. This function extracts all the data points within a square window centered on each anomaly and places them in a single line in a new database. The input target list is the line in the target database containing the list of targets for which to extract data. The in-phase and quadrature channels must be array channels. The summary data channel, which will be used for display purposes when analyzing the data later, will usually be either the qsum or total magnitude channel. The size of the target window is specified in the dialog box. The distance channel is used internally and will be calculated if it does not already exist.

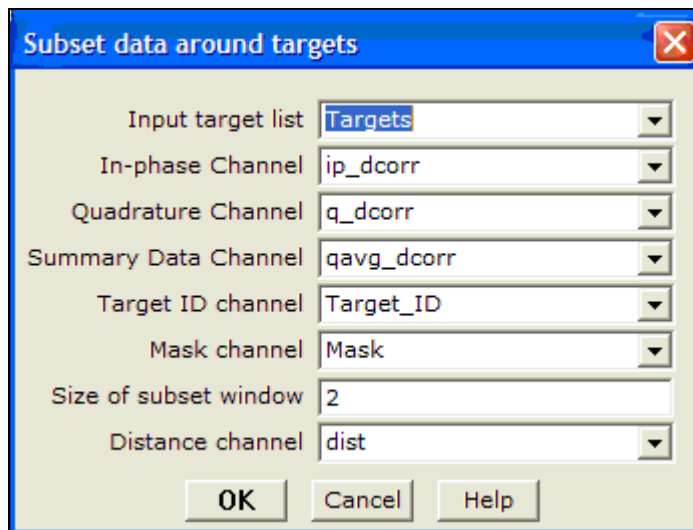


Figure 35. Extraction of GEM-3 anomaly data dialog box.

Similarly, Figure 36 shows the dialog box for extraction of EM-63 anomaly data, and Figure 37 shows the dialog box for extraction of magnetometer anomaly data.

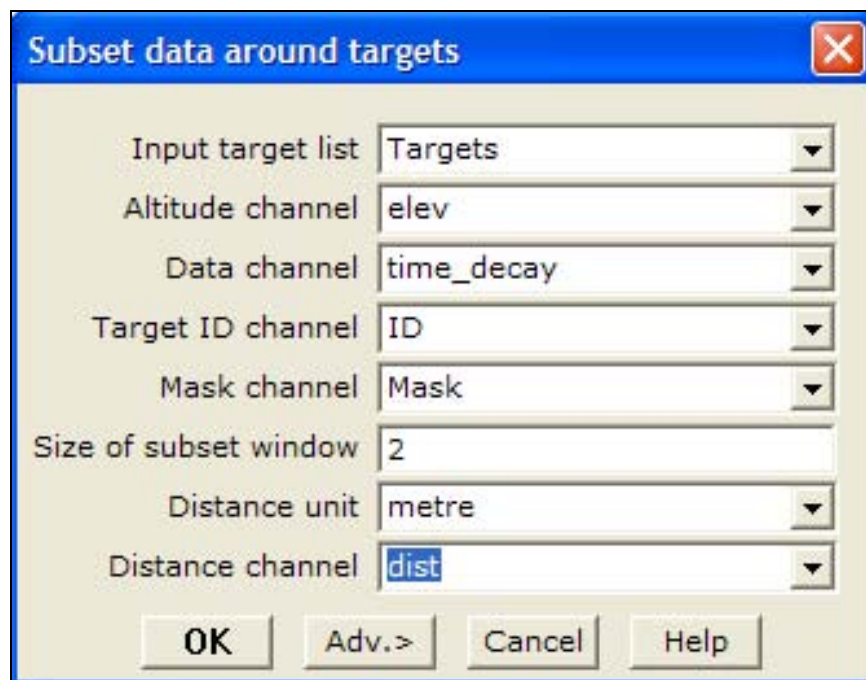


Figure 36. Extraction of EM-63 anomaly data dialog box.

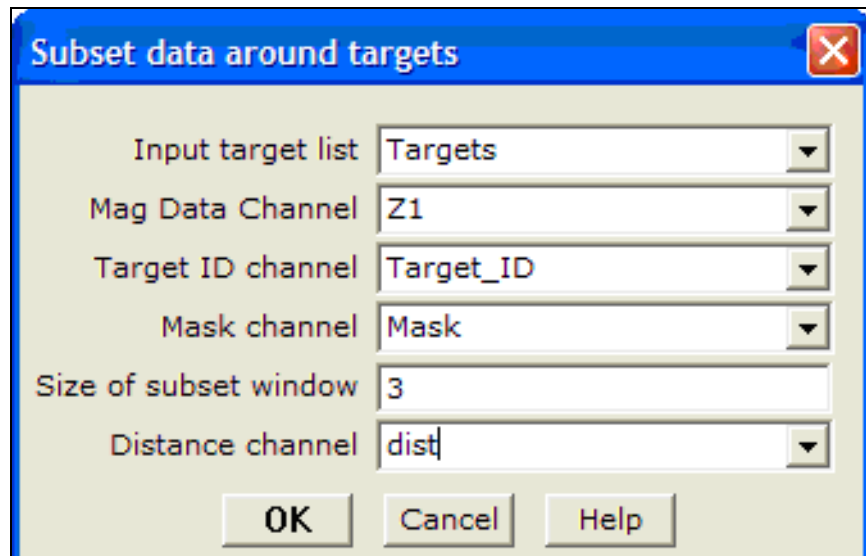


Figure 37. Extraction of magnetometer anomaly data dialog box.

5 Discrimination

Discrimination is the process of separating geophysical anomalies into UXO and non-UXO. If this can be successfully accomplished, then the cost of removal of the UXO can be greatly reduced because only the UXO items need to be excavated for removal. One method of discrimination is to fit measured magnetic, TDEM, or FDEM data to a parametric model and then use the recovered model parameters to classify the anomaly as UXO or non-UXO. Another method of discrimination is to match measured data to signatures of known UXO items and possibly clutter items as well.

Modeling/Inversion

Magnetic dipole model and inversion. Magnetic dipole models and inversion methodologies have been developed and implemented in MATLAB® (Zhang et al. 2003, Billings et al. 2002b). Figure 38 shows a measured anomaly and the model fit to the data by the MATLAB® inversion code. The MATLAB® inversion code can be executed from the UXO-DAS menu in Oasis Montaj and results saved into the Oasis Montaj database. Figure 39 shows the dialog box used to perform inversion on all anomalies in the current database at once. After the inversions are completed, the results for each anomaly can be viewed as shown in Figure 40 to assess the fit quality. In some cases, either the inversion fails or the results are unsatisfactory when reviewed. A common reason for this is the inclusion of data from multiple anomalies in the rectangular area extracted for inversion. An example of an anomaly for which inversion failed is shown in Figure 41. When this occurs, a polygon mask can be drawn around the part of the rectangular region that is considered to be the primary anomaly. The inversion can then be repeated using only the points inside the polygon mask. Figures 42 and 43 show the dialog box to perform inversion on a single anomaly and the results of the inversion of the anomaly using the polygon mask, respectively. Magnetic dipole inversion is also included as part of UX-Analyze, a Geosoft-based software module being developed under ESTCP funding, that will be included in the commercial version of Oasis Monaj.

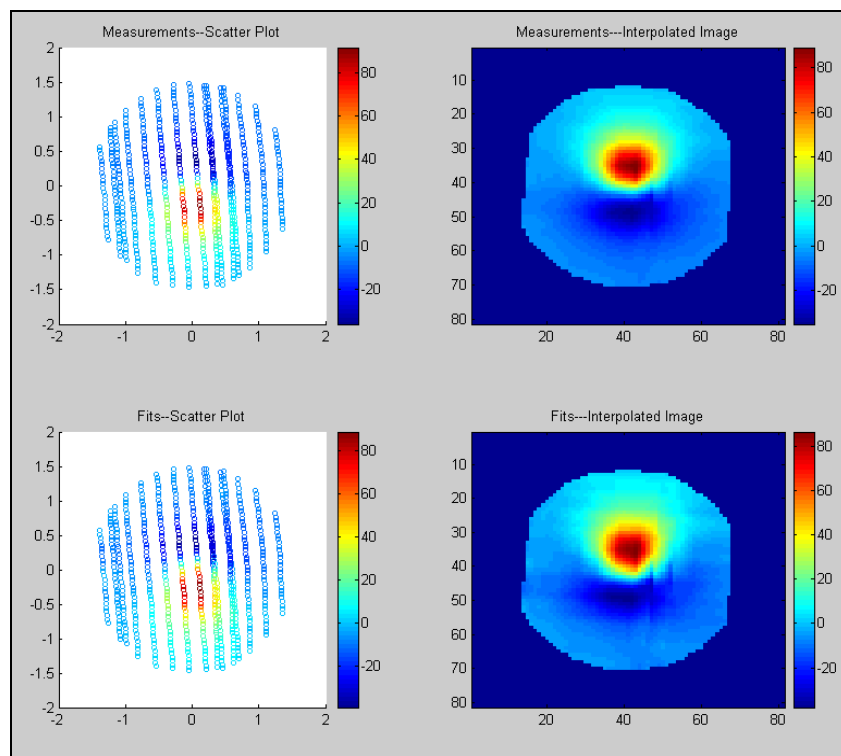


Figure 38. MATLAB® inversion of magnetometer data. Top shows a scatter plot and gridded plot of measured data. Bottom shows corresponding plots of model data. (Units = nT).

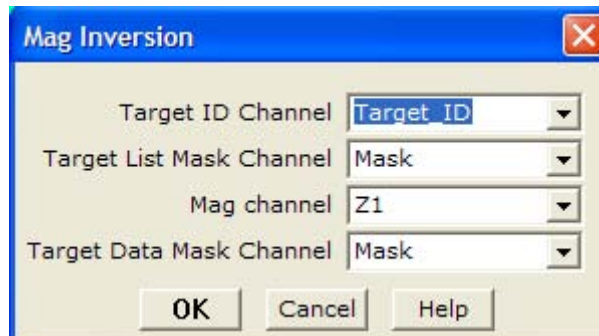


Figure 39. Magnetometer inversion dialog box.

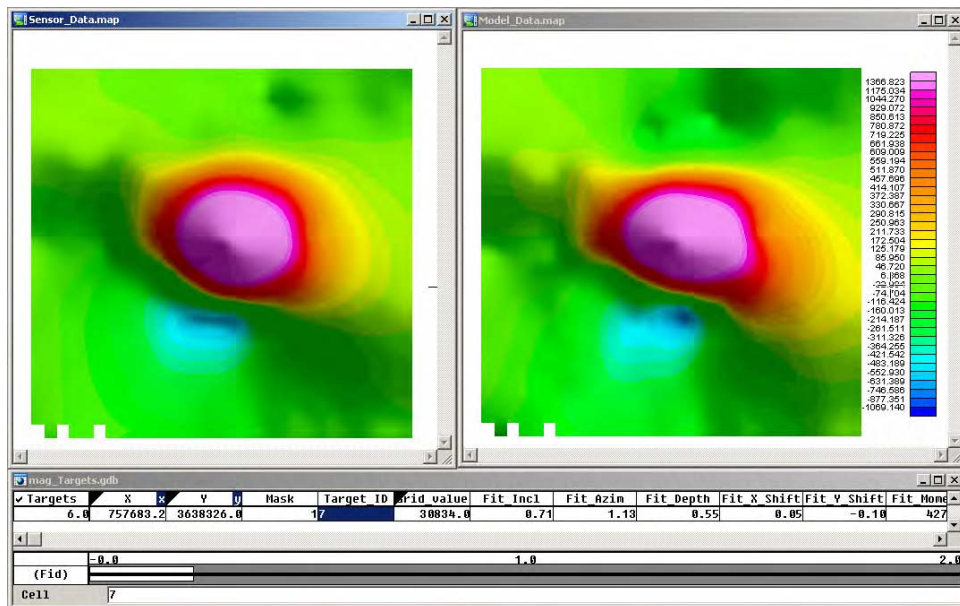


Figure 40. Measured (left) and modeled (right) / magnetometer data (units = nT).

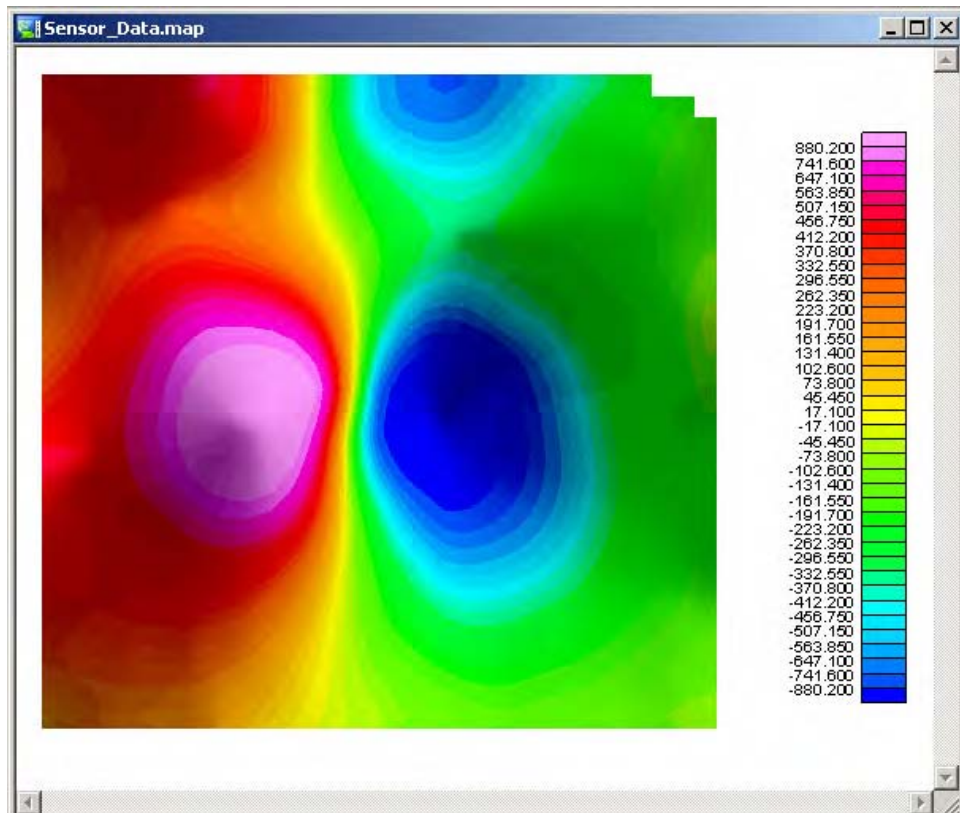


Figure 41. Magnetometer anomaly for which inversion failed due to the presence of another anomaly nearby (units = nT).

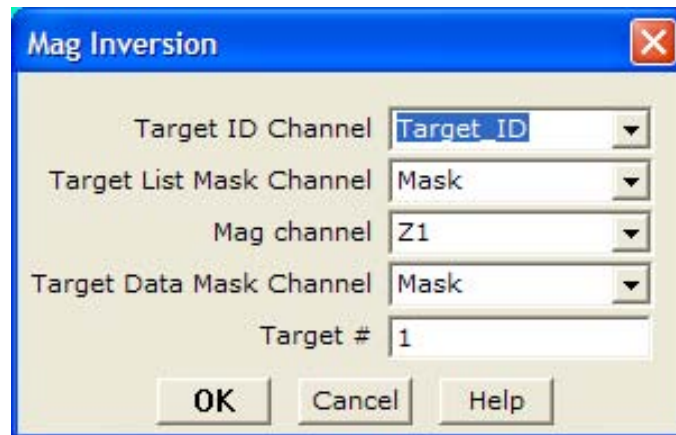


Figure 42. Magnetometer inversion dialog box for a single target.

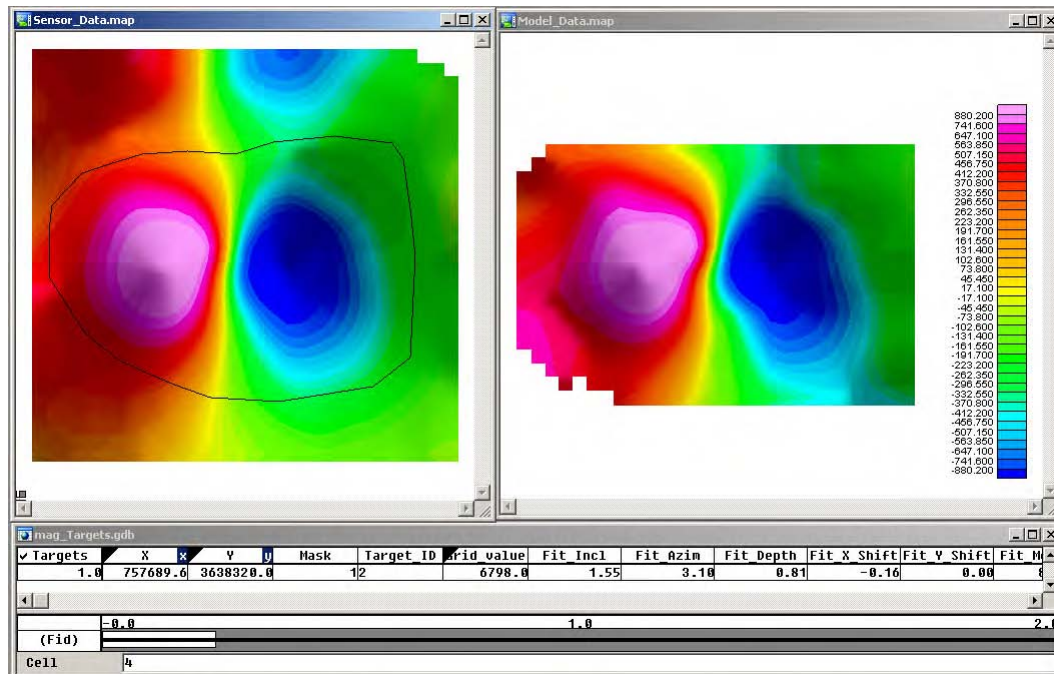


Figure 43. Measured (left) and modeled (right) magnetometer data after re-inversion with polygon mask (units = nT).

EM-61 model and inversion methods. EM-61 model and inversion methodologies have been developed and implemented in MATLAB®. Figure 44 shows a measured anomaly and the model fit to the data by the MATLAB® inversion code. EM-61 inversion is included as part of UX-Analyze.

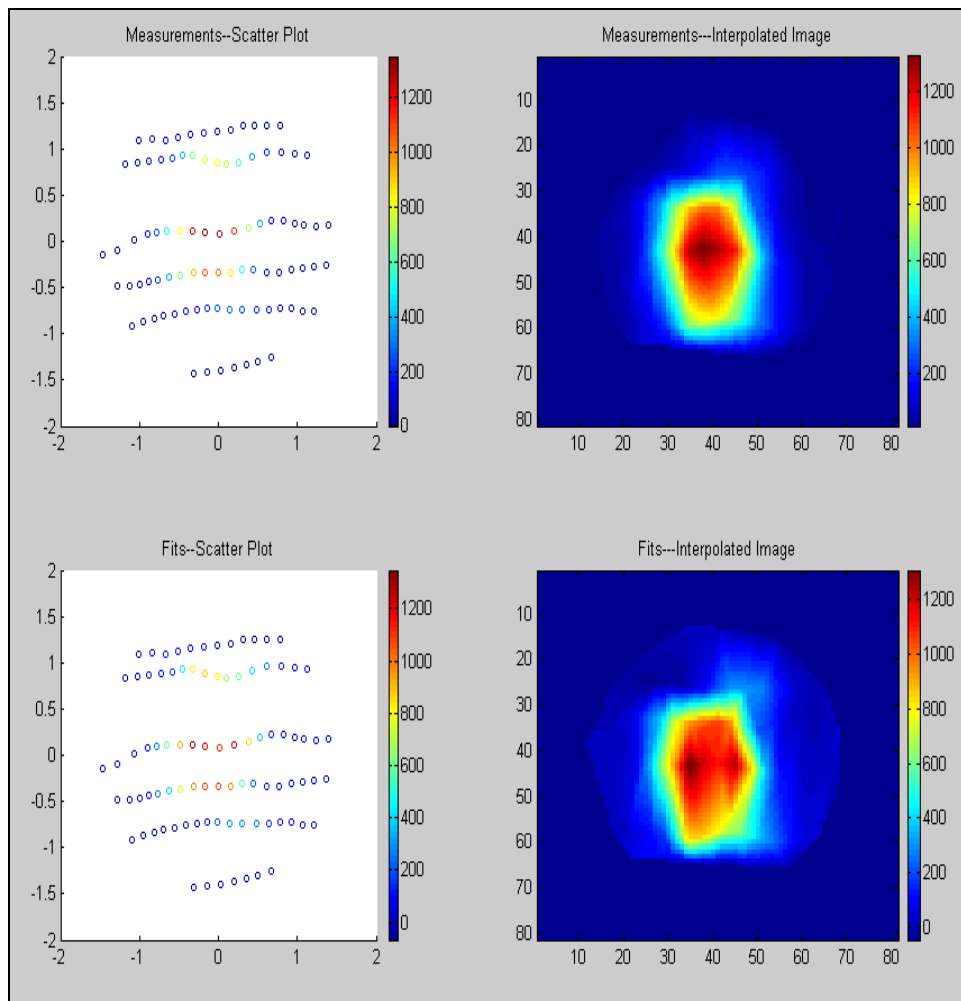


Figure 44. MATLAB® inversion of EM-61 data. Top shows a scatter plot and gridded plot of measured data. Bottom shows corresponding plots of model data (Units = mV).

GEM-3

The GEM-3 FDEM model represents the EMI response as a frequency-dependent magnetic dipole. It was implemented in MATLAB® and then translated to C code for integration with Oasis Montaj. The Geosoft-compatible version uses the Levenberg-Marquadt optimization algorithm to perform the inversion. Figure 45 shows a gridded map of an anomaly and its model fit for a single frequency. The complete frequency curve for the anomaly and the model fit for a single spatial point are shown in Figure 46.

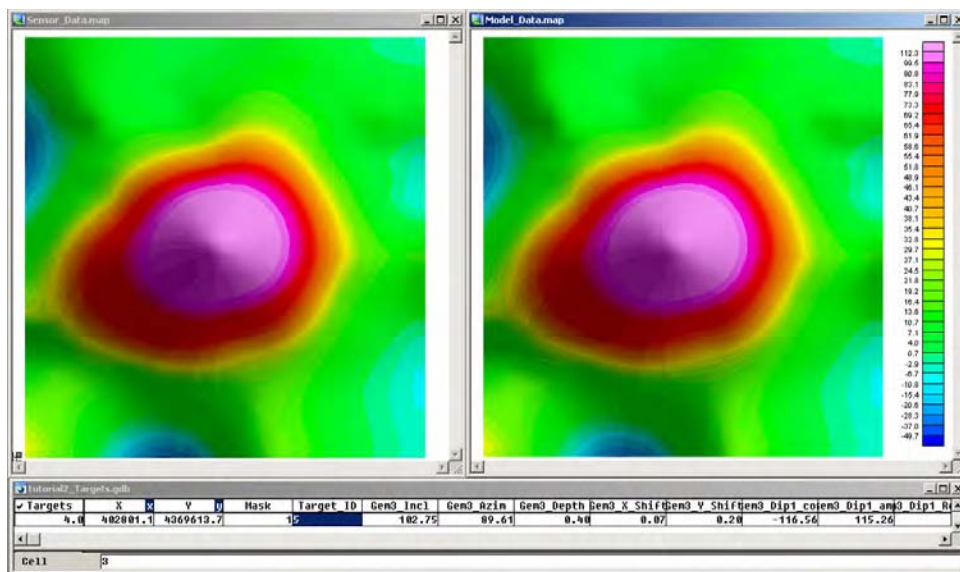


Figure 45. Gridded map of measured anomaly and model fit for GEM-3 (units = PPM).

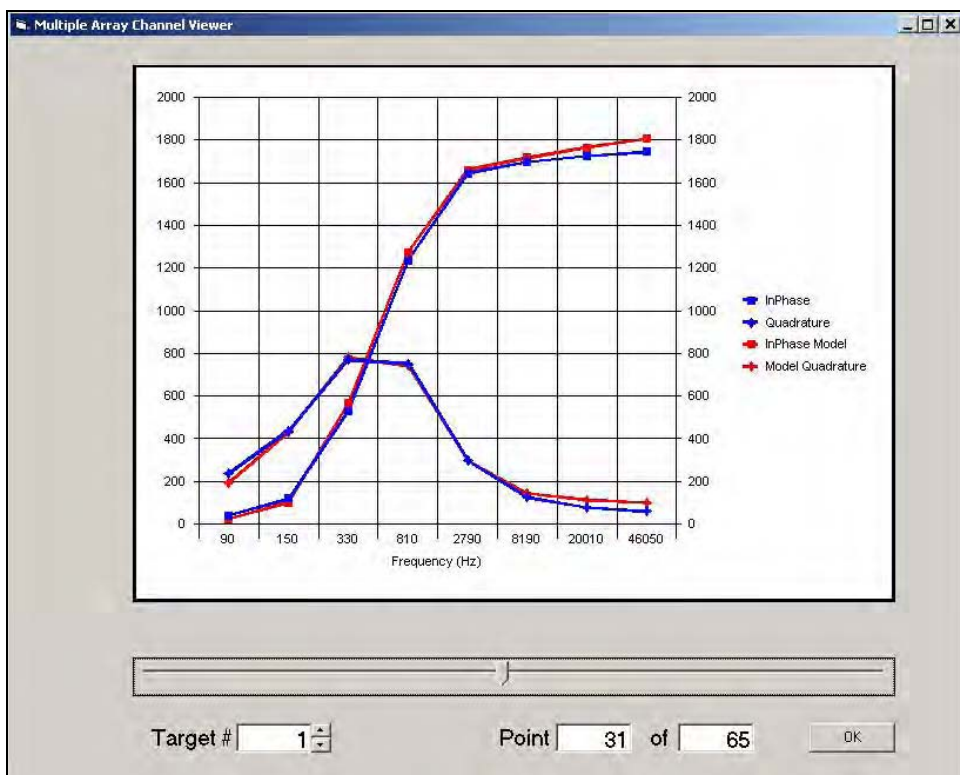


Figure 46. Measured and model frequency curves.

EM-63

The Pasion-Oldenborg EM-63 forward-modeling algorithm is a 13-parameter model (Pasion and Oldenborg 2001). This algorithm and inversion code were initially implemented in MATLAB® and later included in the MATLAB®-based UXOLAB. Figure 47 shows the output of the MATLAB® inversion of a target.

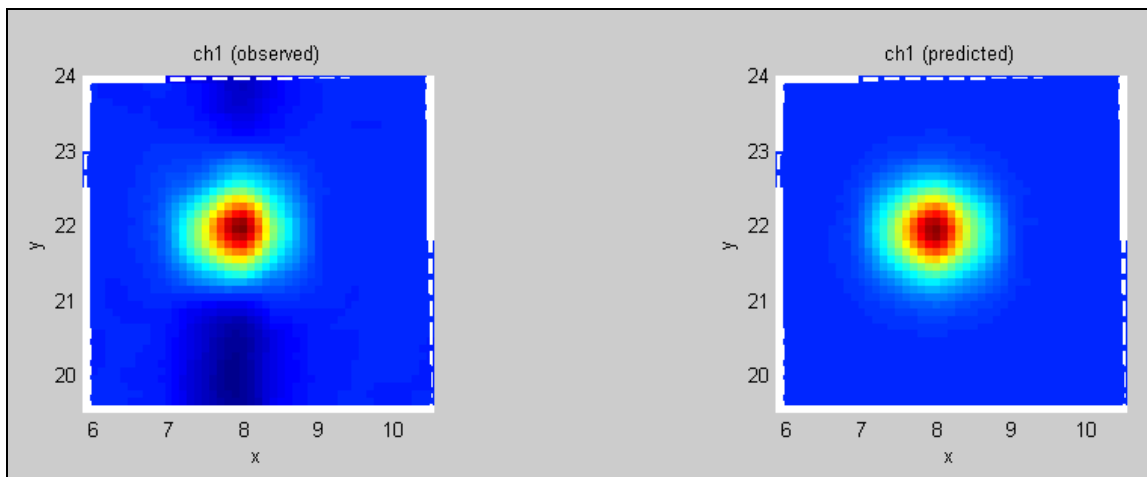


Figure 47. Gridded map of measured anomaly and model fit produced by MATLAB® inversion code for EM-63 data (units = mV).

The EM-63 model, combined with a constrained least-squares optimization algorithm, was packaged into a Geosoft-compatible DLL and a Geosoft GX was developed to execute it. This DLL was later integrated into the UX-Analyze environment. The images in this section of the report were created using a Beta release of Oasis Montaj Version 6.3.

UX-Analyze allows batch fitting of all anomalies in a target list as well as an Add/Review module that lets the user work with individual anomalies. Whichever mode is selected, the dialog shown in Figure 48 lets the user specify the database to process, the sensor type, and other basic parameters.

Once the required data are entered here, with EM-63 as the selected sensor type, clicking the <Next> button will bring up the EM-63 inversion parameters dialog shown in Figure 49. Parameters are described in Table 7.

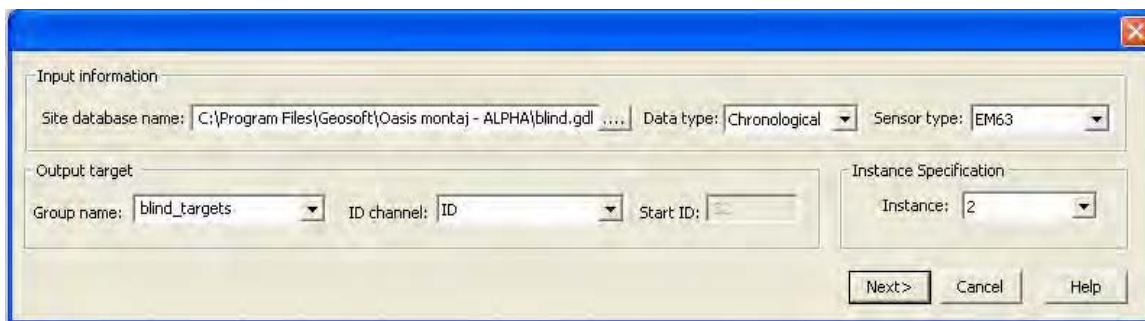


Figure 48. UX-Analyze target-fitting dialog box.

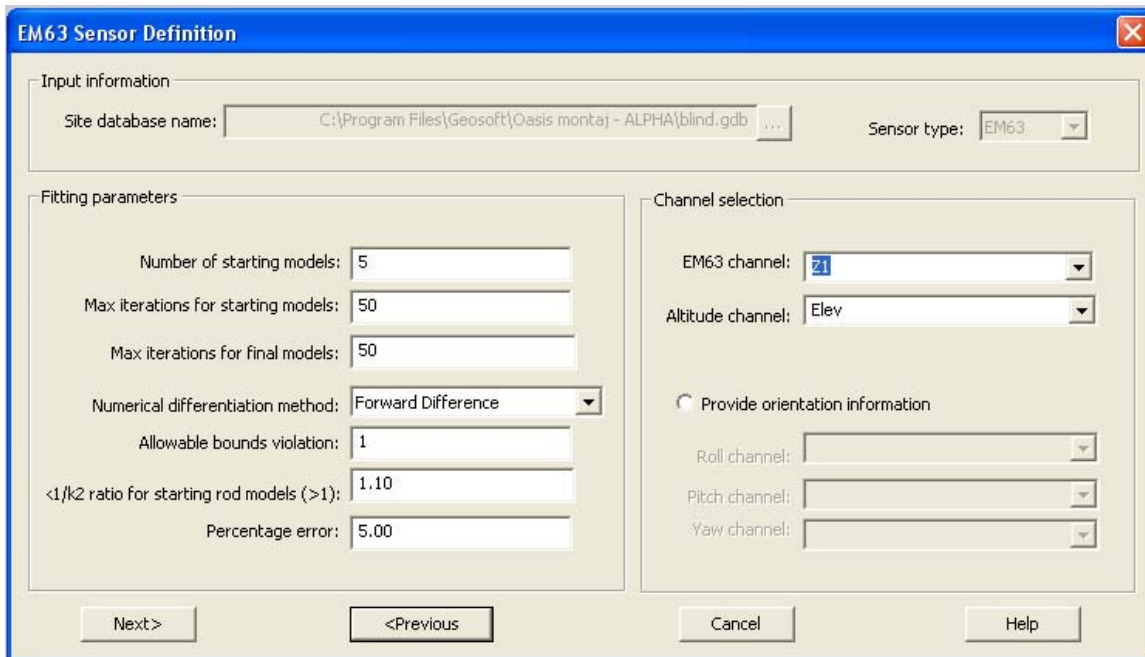


Figure 49. EM-63 inversion parameters dialog box.

Table 7. Advanced parameters that control the EM-63 inversion

Parameter	Description
Number of starting models	Number of different starting rod-like models
Max. iterations for starting models	Maximum number of iterations for determining the rod-like model
Max. iterations for final models	Maximum number of iterations for the refinement of the best fit rod-like model, where the model is not constrained to be a rod
Numerical differentiation method	Differentiation method for numerical calculation of gradients
Allowable bounds violation	Amount of deviation from zero of the 11-norm of the constraint violation. See comments in DONLP documentation.
k1/k2 ratio for starting rod models (must be > 1)	The minimum k1/k2 ratio for the starting models
Percentage error (0 to 100%)	The percentage error (of the amplitude) to assign to each data-point

If batch fitting was selected when the <Next> button is clicked on this dialog, fits are calculated for all anomalies. If Add/Review was selected, the dialog shown in Figure 50 appears along with the complete anomaly map shown in Figure 51. The shaded area on the complete map corresponds to the section of the map displayed in the Add/Review window. It can be moved around to select any portion of the map for review. Inside the Add/Review window (Figure 50), the user can manually add additional targets and review or modify inversion parameters for individual targets. Selecting an anomaly to add or refit will cause the fit to be recalculated for that anomaly and the fit results dialog, shown in Figure 52, to be displayed. Gridded maps of the anomaly and the model fit are also displayed, as shown in Figure 53.

Cooperative inversion

Joint inversion refers to the process of recovering anomaly parameters by simultaneously inverting measured data from two different sensors, such as Magnetometer and TDEM or Magnetometer and FDEM. Joint inversion of Magnetometer and TDEM (EM-63) data, while possible, has not proven to be practical with non-co-located data sets and is generally not feasible with “real” datasets (Butler et al. 2003, Pasion et al. 2003). Cooperative, or constrained, inversion refers to using data from one type of sensor to constrain the inversion of data from another type. The advantage of cooperative inversion is that it reduces the number of local minima that may be selected by the parameter search. The general cooperative inversion concept is shown in the flowchart in Figure 54. When performing cooperative inversion, anomaly detection is first performed on the data from each sensor individually. This may result in some targets only being detected by one of the sensors or, if detected by both sensors, the location calculated for the target for each sensor will likely be slightly different due to different sensor characteristics and data collection parameters. The anomaly lists will need to be merged prior to performing cooperative inversion. UXO-DAS provides a utility to merge anomaly lists from two sensors. Anomalies that appear in the list for both sensors (within a user-specified tolerance) are placed in an output anomaly list, which is used in the cooperative inversion. Anomalies that were detected by only one of the sensors are placed in separate output anomaly lists corresponding to the sensor that detected them. Cooperative inversion is implemented in UXOLAB using the location and depth from magnetic inversion to constrain the inversion of EM-63 data. Magnetic parameters can also be used to constrain inversion of data from FDEM sensors such as the GEM-3.

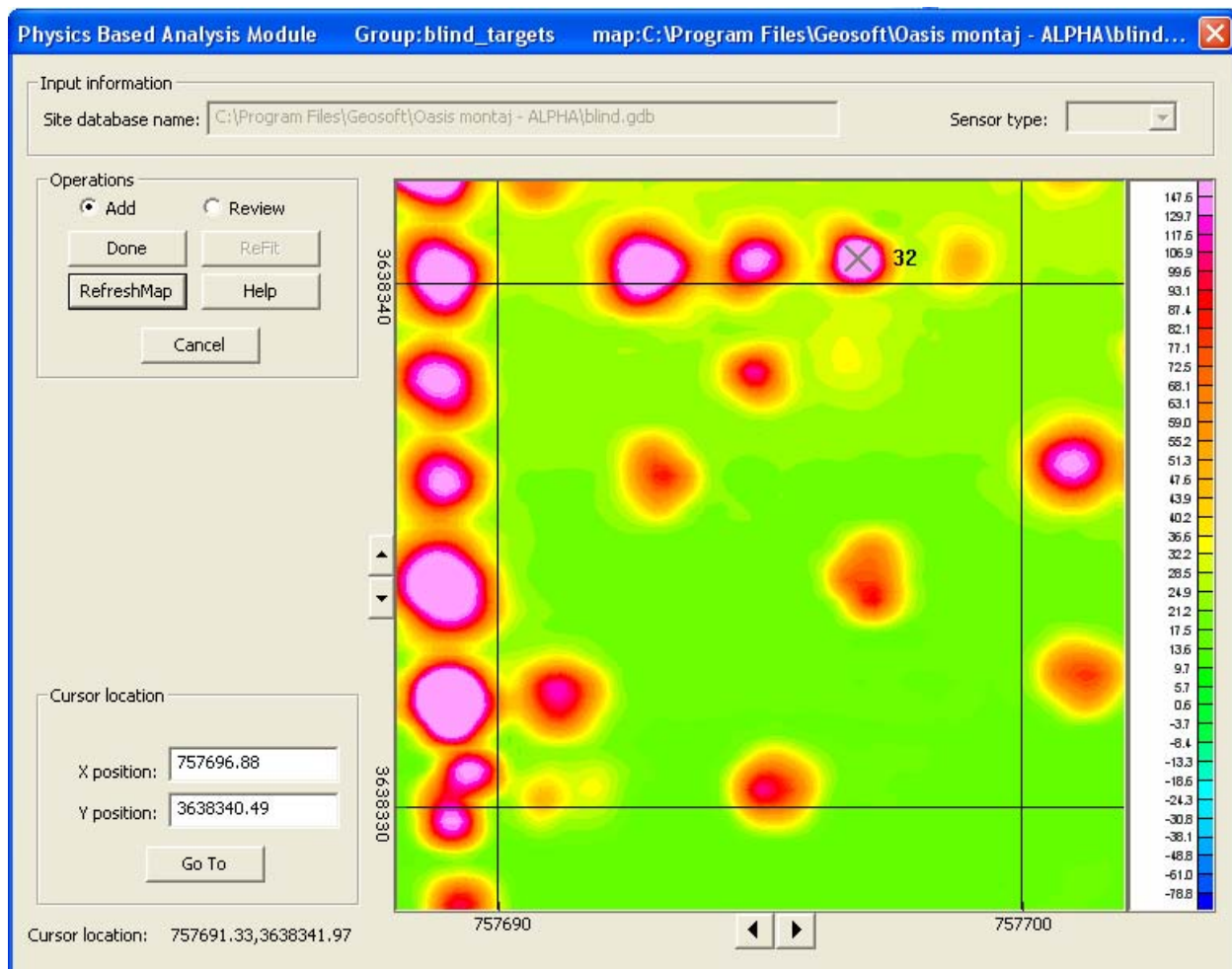


Figure 50. UX-Analyze Add/Review window. This dialog can be used to add new targets and review/modify inversion parameters.

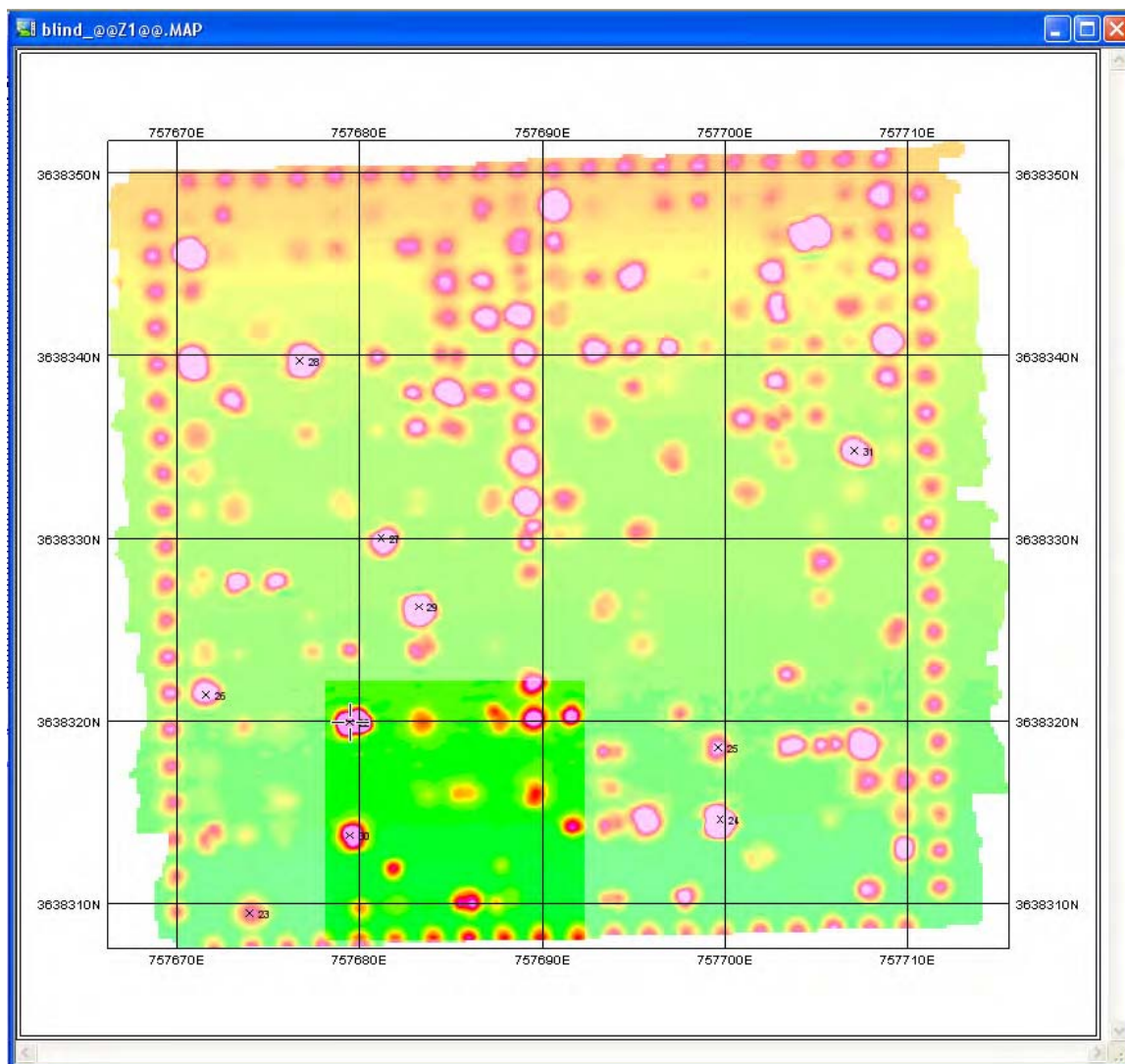


Figure 51. UX-Analyze complete anomaly map. Shaded region shows area currently displayed in Add/Review window.

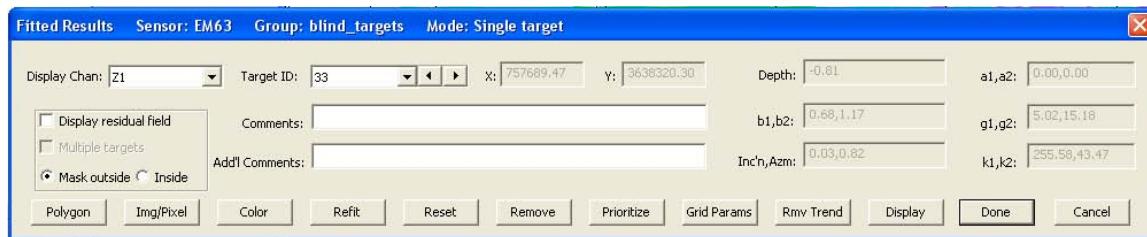


Figure 52. Fitted results dialog.

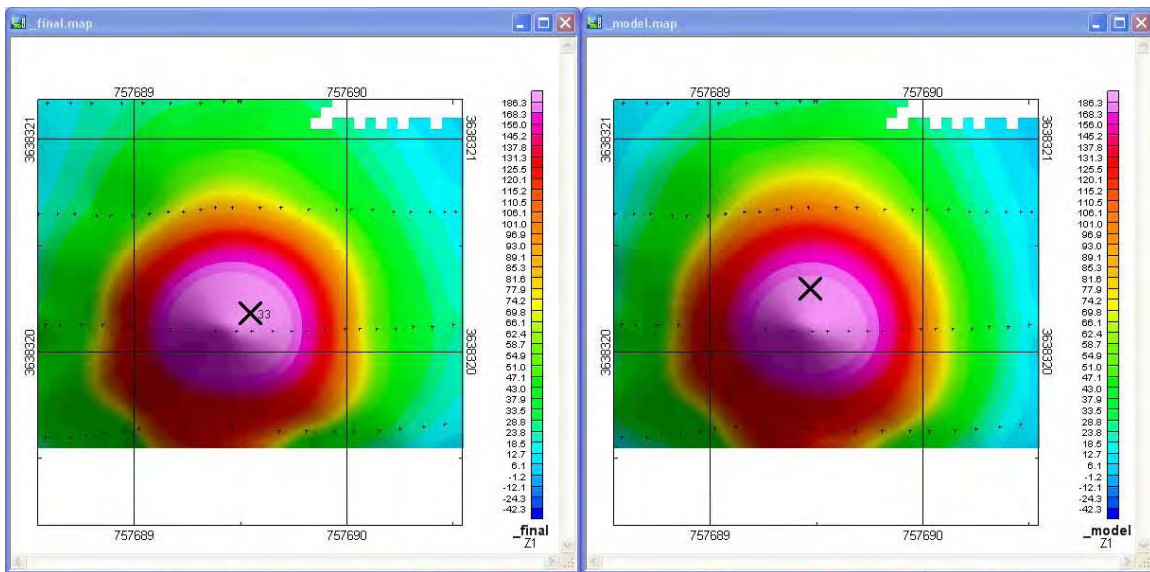


Figure 53. Gridded map of measured anomaly and model fit for EM-63.

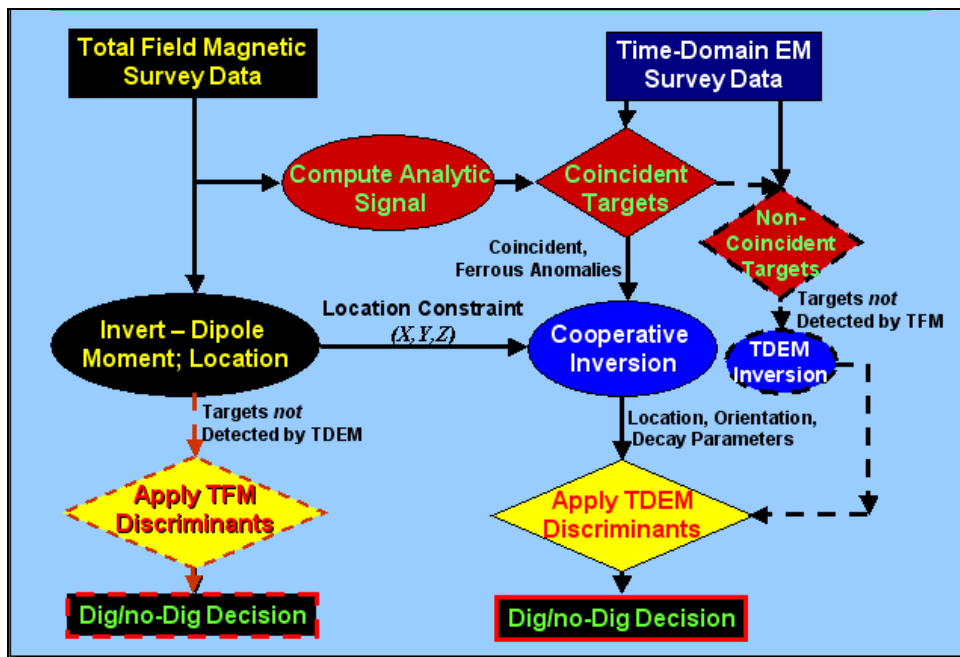


Figure 54. Cooperative inversion flowchart.

Parameter classification

After model parameters are recovered by inversion of measured data, the next step in the process is to classify the anomaly as UXO/non-UXO based on its parameters. The support vector machine algorithm (SVM) has been used in a wide variety of classification applications with success. The algorithm must be trained to classify data by supplying it with the model parameters for known UXO and known non-UXO. From the training data, the

algorithm constructs a decision boundary in parameter space that is applied to model parameters from anomalies of unknown type. The concept of SVM is illustrated in Figure 55, where a decision boundary has been calculated between two classes. In this simple example only two parameters represent the items being classified. In the case of UXO discrimination, there are often many more parameters involved. The SVM concept works in multi-dimensional space, although graphically displaying the results becomes impossible with more than three dimensions. The SVM algorithm was implemented in MATLAB® and is being included in UX-Analyze.

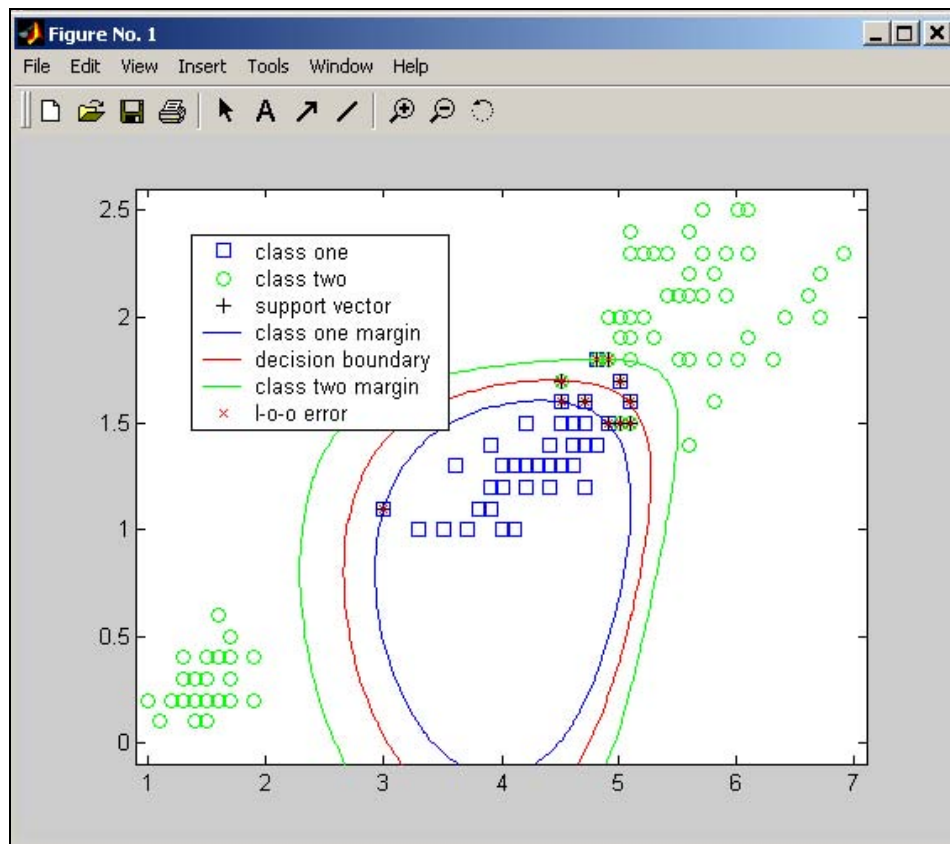


Figure 55. SVM concept in MATLAB®. Two classes of objects are separated using two parameters. The SVM algorithm can be used to separate multiple target classes defined by many parameters.

One major difficulty with classification algorithms is getting adequate training data to allow them to work properly. While obtaining training data for UXO is often possible, it can be particularly difficult to get data for representative non-UXO items at a site.

Signature matching

Another method for discrimination is comparing the sensor response to an anomaly with a library of target signatures. A signature-matching algorithm similar to the one in Goodson et al. (2002) for the GEM-3 is included in UXO-DAS. When this item is selected from the menu, as shown in Figure 56, the data for the anomalies that have been previously extracted are passed to the signature-matching module, where the user can interactively view the error in fit for each measurement point with its closest matching library signature. The user interface for this module is shown in Figure 56.

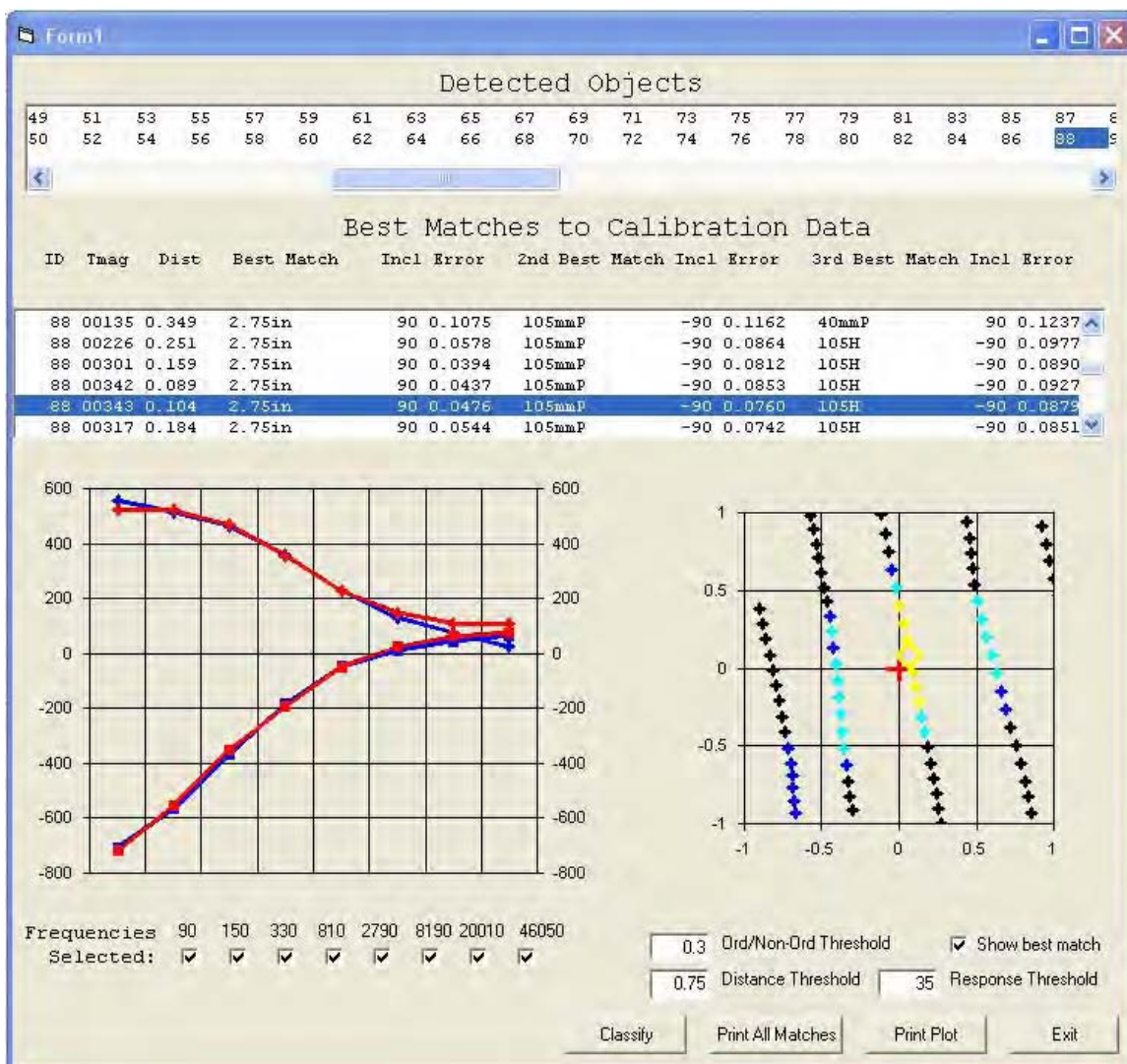


Figure 56. Signature-matching module. The measured signature curve (in blue) of a target is compared with a library signature curve (in red) of a 2.75-in rocket.

When comparing a data point to a calibration signature, the frequency measurements for the data point are normalized to make the total in-phase and quadrature responses for the data point equal to the total in-phase and quadrature responses, respectively, of the calibration signature. Once the magnitudes were equalized, the error in fit E was calculated by:

$$E = \frac{\sqrt{\sum_{k=1}^{k=7} (CI_k - PI_k)^2}}{\sum_{k=1}^{k=7} |CI_k|} + \frac{\sqrt{\sum_{k=1}^{k=7} (CQ_k - PQ_k)^2}}{\sum_{k=1}^{k=7} |CQ_k|} \quad (1)$$

where:

CI_k = the calibration in-phase response

PI_k = the data point in-phase response at frequency k.

CQ_k and PQ_k are the calibration and data point quadrature responses, respectively, at frequency k.

The text box at the top of the screen shown in Figure 56 displays the target IDs of the anomalies. When an item is selected in this box, it makes that item the active anomaly and will cause the other text boxes and graphics windows to be updated, reflecting the selection. The center textbox, labeled “Best Matches to Calibration Data,” consists of one line for each data point near the selected object that lists the ID, the total magnitude, the distance from the center of the anomaly, and information about the three closest matches of the point with calibration data. The information for each match consists of the ordnance type and inclination and the error between the data point and the calibration signature. The left graphics window shows the in-phase and quadrature data for the selected data point and for the calibration data. The right graphics box shows the positions of the data points around the center of the anomaly, shown at the origin in red. Points with match errors greater than the current ordnance/non-ordnance threshold are shown in black. Points with errors less than the threshold, but greater than two-thirds of the threshold, are shown in dark blue. Points with errors between one-third and two-thirds of the threshold are shown in cyan. Points with errors below one-third of the threshold are displayed in yellow. The currently displayed data point is shown as a diamond rather than a plus. Clicking on a point in this graphics box will display the signature comparison for the selected point in the left

graphics box. A row of check boxes at the bottom of the screen allows individual frequencies to be excluded from calculations. Clicking the Classify button will result in all the anomalies being classified using the current settings for the following parameters: Frequencies Selected, Response Threshold, Ordnance/Non-Ordnance Threshold, and Distance Threshold.

6 Results/Performance

Test site description

This chapter presents the results from two test sites: Aberdeen Proving Ground (APG) Standardized UXO Technology Demonstration Site and the Yuma Proving Ground (YPG) Standardized UXO Technology Demonstration Site. APG is located within a secured range area of the U.S. Army Aberdeen Proving Ground, Aberdeen, MD. The APG is located approximately 30 miles northeast of Baltimore, Maryland, at the northern end of the Chesapeake Bay. The Standardized UXO Demonstration Site encompasses 17 acres and is comprised of upland and lowland flats, woods, and wetlands (see Figure 57). The layout descriptions are as follows:

1. Calibration Lanes (<http://aec.army.mil/usaec/technology/uxo03c01b.html>) 0.30 acre
2. Blind Test Grid (<http://aec.army.mil/usaec/technology/uxo03c01a.html>) 0.48 acre
3. Open Field (<http://aec.army.mil/usaec/technology/uxo03c01c.html>) 13.68 acres
4. Scenario 1. Moguls (<http://aec.army.mil/usaec/technology/uxo03c01d.html>) 1.30 acres
5. Scenario 2. Wooded Area (<http://aec.army.mil/usaec/technology/uxo03c01e.html>)
1.35 acres

YPG is located within a secured range area of the U.S. Army Yuma Proving Grounds (see Figure 58). The YPG is located adjacent to the Colorado River in the Sonoran Desert. The UXO Standardized Technology Demonstration Site is located south of Pole Line Road, and east of the Counter-mine Testing and Training Range. The open field range, calibration grid, blind test grid, mogul area, and desert extreme area comprise the 350-m by 500-m general test site area. The open field site is the largest of the test sites and measures approximately 200 m by 350 m. To the east of the open field range are the Calibration Lanes and Blind Test Grids (BTG) that measure 30 m by 40 m and 40 m by 40 m, respectively. South of the open field is the 135-m by 80-m mogul area consisting of a sequence of man-made depressions. The desert extreme area is located southeast of the open field site and has dimensions of 50 m by 100 m. The desert extreme area, covered with desert-type vegetation, is used to test the performance of various sensor platforms in more severe desert conditions/environment.

The Layout description includes:

1. Blind Test Grid (<http://www.aec.army.mil/usaec/technology/uxo03c02a.html>)
0.17 ha (0.43 acre)
2. Calibration Lanes (<http://www.aec.army.mil/usaec/technology/uxo03c02b.html>)
0.11 ha (0.27 acre)
3. Open Field (<http://www.aec.army.mil/usaec/technology/uxo03c02c.html>)
6.22 ha (15.38 acres)
4. Scenario 1. Moguls (<http://www.aec.army.mil/usaec/technology/uxo03c02d.html>)
1.07 ha (2.64 acres)
5. Scenario 2. Desert Extreme (<http://www.aec.army.mil/usaec/technology/uxo03c02e.html>)
0.50 ha (1.23 acres).

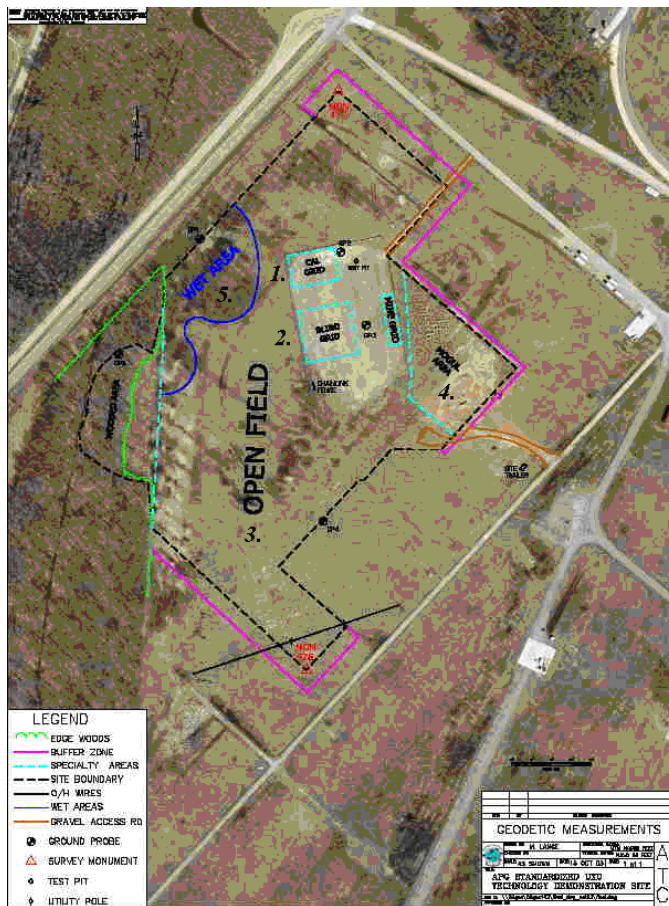


Figure 57. Aerial views with layout of the APG Standardized UXO Technology Demonstration Site.

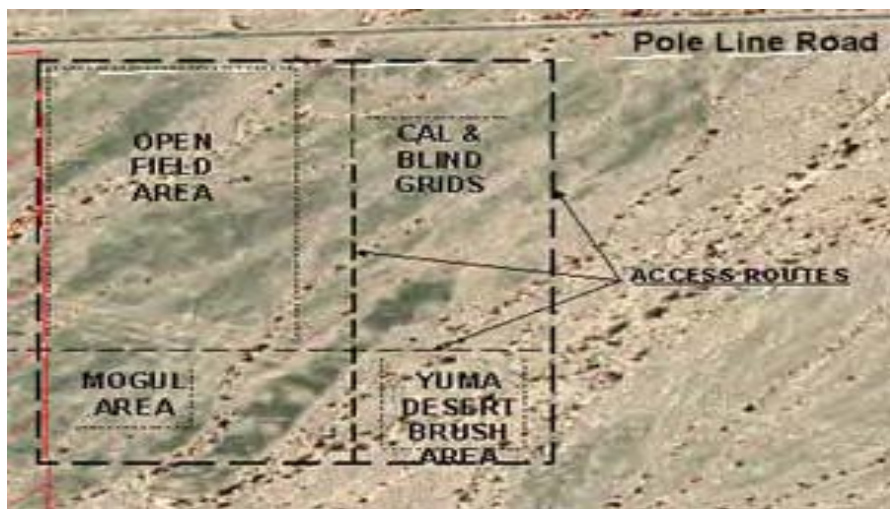


Figure 58. Overlay map of Standardized UXO Technology Demonstration Site.

Standardized test site scoring procedure

The algorithms and procedures developed as part of the EQT program were tested on data acquired at the Standardized UXO Test Sites at Aberdeen Proving Ground and Yuma Proving Ground. The following variable definitions were obtained from the Aberdeen Test Center (ATC) website (see Appendix A):

P_{det}^{dsc}	(# of discrimination-stage detections)/(# of emplaced ordnance in the test site).
P_{det}^{res}	(# of response-stage detections)/(# of emplaced ordnance in the test site).
P_{fp}^{res}	(# of response-stage false positives)/(# of emplace clutter items).
Emplaced Ordnance	An inert ordnance item buried by the government at a specified location in the test site.
Emplaced Clutter	A clutter item (i.e., nonordnance item) buried by the government at a specified location in the test site.
Discrimination Stage	The ability to correctly identify ordnance as such, and to reject clutter. For the same locations as in the RESPONSE STAGE anomaly column, the DISCRIMINATION STAGE column contains the output of the algorithms applied in the discrimination-stage processing. This column is prioritized based on the confidence that an ordnance item is present at the specified location. For electronic signal processing, priority ranking is based on algorithm output. For other systems, priority ranking is based on human judgment. The demonstrator also selects the threshold that provides optimum system performance (i.e., that retains all the detected ordnance and rejects the maximum amount of clutter).

Response Stage The ability of the demonstrator's system to detect emplaced targets without regard to ability to discriminate ordnance from other anomalies. The RESPONSE STAGE provides the location and signal strength of all anomalies deemed sufficient to warrant further investigation and /or processing as potential emplaced ordnance items. This list is generated with minimal processing (e.g., this list will include all signals above the system noise threshold). As such, it represents the most inclusive list of anomalies.

Results for the Blind Grid test, broken out by size, depth, and standard and nonstandard ordnance are presented in Tables 8-13. The "Standard" column of Tables 8-13 represents the following ordnances: 20mm, 40mm, M42, BLU-26, BDU-28, 57mm, MK118, 60mm, 81mm, M230, 105mm, and 155mm. The "Nonstandard" column represents other ordnances buried at the APG test site. Results by size and depth include both standard and nonstandard ordnance. The results by size show how well the demonstrator did at detecting/discriminating ordnance of a certain caliber range. Size categories are as follows:

Small Ordnance	Caliber of ordnance less than or equal to 40mm (includes 20mm projectile, 40mm projectile, submunitions BLU-26, BLU-63, and M42);
Medium Ordnance	Caliber of ordnance greater than 40mm and less than or equal to 81mm (includes 57mm projectile, 60mm mortar, 2.75-inch rocket, MK118 Rockeye, 81mm mortar);
Large Ordnance	Caliber of ordnance greater than 81mm (includes 105mm HEAT, 105mm projectile, 155mm projectile, 500-pound bomb).

The results are relative to the number of ordnances emplaced. Depth is measured from the closest point of anomaly to the ground surface.

RESPONSE STAGE results are derived from the list of anomalies above the demonstrator-provided noise level. Results for the DISCRIMINATION STAGE are derived from the demonstrator's recommended threshold for optimizing UXO field cleanup by minimizing false digs and maximizing ordnance recovery. The lower 90-percent confidence limit (CI) on probability of detection and probability of false positive was calculated assuming that the number of detections and false positives are binomially distributed random variables. All results in Tables 8-13 have been rounded

to protect the ground truth. However, lower confidence limits were calculated using actual results.

TM-4 magnetometer

Data were acquired with a TM-4 magnetometer at the Yuma Proving Ground test site in May 2003. Blind Grid scoring results from ATC are shown in Tables 8 and 9 (Standardized UXO Technology Demonstration Site (SUTDS) 2004). Because magnetometers cannot detect non-ferrous materials, the results are tabulated for all items (Table 8) and ferrous-only items (Table 9). Response Stage and Discrimination Stage results are identical because no discrimination processing was performed.

Table 8. Summary of YPG Blind Grid Results (Full Ground Truth)

Metric	Overall	Standard	Non-standard	By Size			By Depth, m		
				Small	Medium	Large	<0.3	0.3-<1	>=1
RESPONSE STAGE									
P _d	0.65	0.60	0.70	0.50	0.80	0.80	0.60	0.75	0.45
P _d L90%CI	0.55	0.49	0.55	0.37	0.63	0.58	0.50	0.60	0.17
P _{fp}	0.85						0.85	0.90	
P _{fp} L90%CI	0.82						0.80	0.78	
P _{ba}	0.00								
DISCRIMINATION STAGE									
P _d	0.65	0.60	0.70	0.50	0.80	0.80	0.60	0.75	0.45
P _d L90%CI	0.55	0.49	0.55	0.37	0.63	0.58	0.50	0.60	0.17
P _{fp}	0.85						0.85	0.90	
P _{fp} L90%CI	0.82						0.80	0.78	
P _{ba}	0.00								

EM-63 EMI system

Data were acquired with an EM-63 at the Yuma Proving Ground test site in May 2003. Blind Grid scoring results from ATC are shown in Table 10 (SUTDS 2005). Response Stage and Discrimination Stage results are identical because no discrimination processing was performed.

Table 9. Summary of YPG Blind Grid Results (Ferrous Only)

Metric	Overall	Standard	Non-standard	By Size			By Depth, m		
				Small	Medium	Large	<0.3	0.3-<1	>=1
RESPONSE STAGE									
P _d	0.70	0.70	0.70	0.60	0.80	0.80	0.70	0.80	0.45
P _d L90%CI	0.62	0.60	0.56	0.47	0.63	0.58	0.58	0.67	0.17
P _{fp}	0.85						0.85	0.90	
P _{fp} L90%CI	0.82						0.80	0.78	
P _{ba}	0.00								
DISCRIMINATION STAGE									
P _d	0.70	0.70	0.70	0.60	0.80	0.80	0.70	0.80	0.45
P _d L90%CI	0.62	0.60	0.56	0.47	0.63	0.58	0.58	0.67	0.17
P _{fp}	0.85						0.85	0.90	
P _{fp} L90%CI	0.82						0.80	0.78	
P _{ba}	0.00								

Table 10. Summary of YPG Blind Grid Results (for EM63)

Metric	Overall	Standard	Non-standard	By Size			By Depth, m		
				Small	Medium	Large	<0.3	0.3-<1	>=1
RESPONSE STAGE									
P _d	0.80	0.80	0.80	0.80	0.75	0.95	0.90	0.80	0.30
P _d L90%CI	0.74	0.73	0.67	0.70	0.59	0.75	0.82	0.65	0.08
P _{fp}	0.95						0.95	0.95	0.00
P _{fp} L90%CI	0.90						0.89	0.82	
P _{ba}	0.00								
DISCRIMINATION STAGE									
P _d	0.80	0.80	0.80	0.80	0.75	0.95	0.90	0.80	0.30
P _d L90%CI	0.74	0.73	0.67	0.70	0.59	0.75	0.82	0.65	0.08
P _{fp}	0.95						0.95	0.95	0.00
P _{fp} L90%CI	0.90						0.89	0.82	
P _{ba}	0.00								

GEM-3-E EMI system

Data were acquired with the GEM-3-E over the Calibration Lanes and Blind Grid at the Aberdeen Proving Ground Test Site in September 2003. Scoring results obtained from the ATC for the GEM-3-E on the Blind Grid at Aberdeen Proving Ground are provided in Tables 11-13 (unpublished). Table 11 shows the results using all eight frequencies acquired with the sensor. Discrimination was performed using signature matching to a

library consisting of signatures of the standard ordnances acquired in a test pit on-site. The discrimination processing removed virtually all background alarms, but resulted in the P_d being reduced from 0.85 to 0.60.

The reduction in P_d is probably the result of two main factors. The first one is the lack of signature data for non-standard ordnance items. The P_d for standard items did not drop as much as the P_d for non-standard items. The second major factor is depth of ordnance. The table shows that the deepest ordnance did not pass the discrimination process. Most likely, the deeper items of any given type were the ones not determined to be ordnance by the discrimination process. Discrimination requires a much higher signal-to-noise ratio than detection. Reporting results by the product of depth and size would have been very helpful in analyzing results.

Signature matching was also applied to the data excluding frequencies that have higher noise levels than the others. Table 12 shows the results of signature matching, excluding the 90-Hz data. The results obtained when excluding both the 90-Hz and 150-Hz data are shown in Table 13. Overall, the results are very similar regardless of the frequencies used. Excluding the lowest frequencies results in detecting fewer of the deepest targets, but has little effect on the overall detection rate.

UXO-DAS and UXO lab workshops

Two UXO software training/demonstration workshops were conducted in the summer of 2006. The first, on UXOLAB, was held June 27-29 at UBC in Vancouver, Canada. The second, on UXO-DAS, was held July 25-26 at the ERDC in Vicksburg, Mississippi. Attendees included ERDC personnel and representatives from AEC and private industry. The tutorials that were demonstrated at the UXO-DAS workshop are included in Appendix B.

Table 11. Summary of APG Blind Grid Results Using Signature Matching (All Frequencies)

Metric	Overall	Standard	Non-standard	By Size			By Depth, m		
				Small	Medium	Large	<0.3	0.3-<1	>=1
RESPONSE STAGE									
P _d	0.85	0.95	0.75	0.90	0.80	0.90	1.00	0.85	0.55
P _d L90%CI	0.81	0.87	0.63	0.82	0.68	0.66	0.94	0.70	0.37
P _{fp}	0.85						0.85	0.90	1.00
P _{fp} L90%CI	0.82						0.76	0.79	0.63
P _{ba}	0.55								
DISCRIMINATION STAGE									
P _d	0.60	0.75	0.40	0.65	0.50	0.70	0.80	0.65	0.05
P _d L90%CI	0.54	0.65	0.29	0.56	0.39	0.45	0.67	0.52	0.01
P _{fp}	0.65						0.65	0.65	1.00
P _{fp} L90%CI	0.59						0.53	0.53	0.63
P _{ba}	0.05								

Response Stage Noise Level: 37.00

Recommended Discrimination Stage Threshold: 0.00

Table 12. Summary of APG Blind Grid Results Using Signature Matching (Excluding 90-Hz Data)

Metric	Overall	Standard	Non-standard	By Size			By Depth, m		
				Small	Medium	Large	<0.3	0.3-<1	>=1
RESPONSE STAGE									
P _d	0.85	0.90	0.75	0.95	0.70	0.80	1.00	0.90	0.30
P _d L90%CI	0.77	0.80	0.63	0.85	0.58	0.55	0.91	0.78	0.13
P _{fp}	0.85						0.85	0.96	0.80
P _{fp} L90%CI	0.79						0.76	0.76	0.42
P _{ba}	0.50								
DISCRIMINATION STAGE									
P _d	0.65	0.75	0.45	0.70	0.50	0.70	0.80	0.70	0.05
P _d L90%CI	0.56	0.65	0.34	0.61	0.39	0.45	0.70	0.55	0.01
P _{fp}	0.71						0.88	0.80	0.80
P _{fp} L90%CI	0.57						0.53	0.51	0.42
P _{ba}	0.05								

Response Stage Noise Level: 32.00

Recommended Discrimination Stage Threshold: 0.00

**Table 13. Summary of APG Blind Grid Results Using Signature Matching
(Excluding 90-Hz and 150-Hz Data)**

Metric	Overall	Standard	Non-standard	By Size			By Depth, m		
				Small	Medium	Large	<0.3	0.3-<1	>=1
RESPONSE STAGE									
P _d	0.80	0.85	0.70	0.90	0.70	0.80	1.00	0.85	0.15
P _d L90%CI	0.73	0.76	0.59	0.79	0.55	0.55	0.91	0.74	0.04
P _{fp}	0.85						0.80	0.80	0.80
P _{fp} L90%CI	0.75						0.71	0.71	0.42
P _{ba}	0.40								
DISCRIMINATION STAGE									
P _d	0.60	0.70	0.45	0.65	0.50	0.70	0.75	0.65	0.05
P _d L90%CI	0.53	0.61	0.32	0.53	0.39	0.45	0.64	0.52	0.01
P _{fp}	0.65						0.65	0.60	0.60
P _{fp} L90%CI	0.57						0.56	0.51	0.25
P _{ba}	0.05								

Response Stage Noise Level: 27.00

Recommended Discrimination Stage Threshold: 0.00

7 Conclusions & Recommendations

Conclusions

The objective of this work was to develop software tools to allow importation, processing, visualization, and execution of advanced discrimination algorithms for data from magnetometer, time domain, and frequency domain electromagnetic geophysical sensors. Geosoft Oasis Montaj, a commercial mapping software package, was chosen as the base platform because of its rich set of available mapping tools, its extensibility, and its acceptance in the geophysical community. Oasis Montaj also serves as the target platform for UXO software development in several SERDP/ESTCP projects including the development of a QA/QC-tools module and the UX-Analyze module for UXO discrimination. These efforts have been coordinated and leveraged with the EQT work.

At this time, the interface for the importation of data from the current standard and significant next generation devices is mature and in place. In addition, the current interface is flexible enough with a wizard type interface to allow for the creation of import templates for virtually any multi-dimensional sequential data.

Significant effort has been spent to develop the tools necessary for addressing quality assurance and control procedures in a standardized manner. Automated procedures have been implemented to perform a variety of data corrections for systematic sensor problems such as time lag between sensor measurement and positioning data and instrument drift. The performance of these routines has been proven and the implementation is intuitive and user friendly.

Existing automated anomaly-picking algorithms in Geosoft UX-Detect were tested with data from a variety of sensor types. A new anomaly-picking algorithm based on histogram analysis was developed for multi-channel data and initial testing was performed. This routine is currently a stand-alone program, but its results can be imported into Oasis Montaj. Routines were developed and tested to extract data around each selected anomaly to use for further analysis.

Advanced modeling and inversion methodologies for Magnetic and TDEM data were developed and packaged into a MATLAB®-based program called UXOLAB. Data can be pre-processed in Oasis Montaj and then exported to UXOLAB to use its inversion and discrimination routines. The procedure for inversion of EM-63 data using the Pasion-Oldenburg algorithm has been implemented in C/Fortran code that can be executed directly from the UXO-DAS menu within Oasis Montaj. This code has also been integrated into UX-Analyze.

Advanced modeling and inversion methodologies for Magnetic and FDEM data, as well as classification algorithms, were developed in MATLAB®. Procedures were developed to execute the MATLAB® versions of the algorithms from Oasis Montaj, allowing the more extensive database and visualization tools available in Oasis Montaj to be used in conjunction with the advanced algorithms. The FDEM inversion algorithm was implemented in C code and integrated into UXO-DAS. Magnetometer and EM-61 inversion capabilities are included in UX-Analyze.

A signature-matching algorithm for classification of FDEM data was developed and integrated into UXO-DAS. This algorithm has proven successful in classifying ordnance when the signal-to-noise ratio is high.

Recommendations

The signature-matching algorithm should be modified to operate on TDEM data in addition to FDEM. In addition, it needs to be extended to perform signature matching in three dimensions. To support this approach, it is recommended that test stand data be collected for sensors of interest.

Procedures to effectively discriminate UXO from non-UXO items using the recovered model parameters from inversion are still being developed. Determining the combination of parameters and classification algorithms that will work best under the specific circumstances at a given site is a complex issue that needs further study. One major issue is that the fundamental question of the uniqueness of the measured signal from ordnance types has not been completely defined. The question of the orthogonality of the experimental signatures for even the ATC test set for a limited number of orientations and depths has not been analyzed and the variation quantified. Analysis of complete experimental datasets for orthogonality should be performed and documented to determine the

degree of identification that is possible. Models that transform data into other parameter spaces for comparison should be similarly investigated for orthogonality to determine uniqueness for solutions. In addition, methods that perform transformations into other spaces for comparison should be analyzed for error propagation by the transform method.

References

- Billings, S. D., J. M. Stanley, and C. Youmans. 2002a. Magnetic discrimination that will satisfy regulators. *UXO/Countermine Forum 2002, Orlando, FL.*
- Billings, S. D., L. R. Pasion, and D. W. Oldenburg. 2002b. *Discrimination and identification of UXO by geophysical inversion of total-field magnetic data.* ERDC/GSL TR-02-16. Vicksburg, MS: U.S. Army Engineer Research and Development Center.
- Butler, D. K., E. R. Cespedes, C. B. Cox, and P. J. Wolfe. 1998. *Multisensor methods for buried unexploded ordnance detection, discrimination and identification.* Technical Report SERDP-98-10, Vicksburg, MS: U.S. Army Engineer Waterways Experiment Station.
- Butler, D. K., L. R. Pasion, S. Billings, D. Oldenburg, and D. Yule. 2003. Model-based Inversion for Enhanced UXO Detection and Discrimination. *In Detection and Remediation Technologies for Mines and Mine-like Targets VII*, ed. R. S. Harmon, J. H. Holloway, Jr., and J.T. Broach, *Proceedings of SPIE* 5089:958-969.
- George, V., T. W. Altshuler, and E. M. Rosen. 1998. DARPA background clutter data collection experiment: Excavation results. *In Society of Professional Optical Engineers (SPIE) Proceedings*, 3392 (3392-106):1000-1011.
- Goodson, R. A., H. H. Bennett, T. A. DeMoss, D. M. Cargile, J. C. Morgan, and M. P. Fields. 2002. *Analysis of GEM-3 Data from the Advanced UXO Detection/Discrimination Technology Demonstration—U.S. Army Jefferson Proving Ground, Madison, Indiana.* Technical Report ERDC/EL TR-02-25. Vicksburg, MS: U.S. Army Engineer Research and Development Center.
- Miller, J., T. Bell, D. Keiswetter, and D. Wright. 2001. Feature-based characterization of UXO-like targets using broadband electromagnetic induction. *In UXO Forum 2001 Proceedings.* UXO Forum 2001, New Orleans, LA.
- Office of the Under Secretary of Defense (Acquisition and Technology). 1997. *Annual Report to Congress—Unexploded Ordnance Clearance, A Coordinated Approach to Requirements and Technology Development.* Joint UXO Coordinating Office (JUXOCO), Office of the Under Secretary of Defense (Acquisition and Technology) 25 March 1997.
- Pasion, L. R., and D. W. Oldenburg. 2001. *Locating and characterizing unexploded ordnance using time domain electromagnetic induction.* ERDC/GSL TR-01-10. Vicksburg, MS: U.S. Army Engineer Research and Development Center.
- Pasion L. R., S. D. Billings, and D. W. Oldenburg. 2003. Joint and cooperative inversion of magnetic and time domain electromagnetic data for the characterization of UXO. *Proceedings of the Symposium on Application of Geophysics to Environmental and Engineering Problems 2003 (CD), Environmental and Engineering Geophysical Society, San Antonio, TX 2003.*

- Simms, J. E., R. J. Larson, W. L. Murphy, and D. K. Butler. 2004. *Guidelines for planning unexploded ordnance (UXO) detection surveys*. Technical Report ERDC/GSL TR-04-8. Vicksburg, MS: U.S. Army Engineer Research and Development Center.
- Standardized UXO Technology Demonstration Site (SUTDS)*. 2004. *Blind Grid Scoring Record No. 362*. (U.S. Army Engineer Research and Development Center), Commander, U.S. Army Environmental Center ATTN: SFIM-AEC-PCT Aberdeen Proving Ground, MD 21005-5059, July 2004.
- Standardized UXO Technology Demonstration Site (SUTDS)*. 2005. *Blind Grid Scoring Record No. 216*. (U.S. Army Engineer Research and Development Center), Commander, U.S. Army Environmental Center ATTN: SFIM-AEC-PCT Aberdeen Proving Ground, MD 21005-5059, March 2005.
- Valentine, J. D., and A. E. Rana. 1996. Centroid and full-width at half maximum uncertainties of histogrammed data with an underlying Gaussian distribution-The Moments Method. *IEEE Transactions on Nuclear Science*, 43(5):2501-2508.
- Zhang, Y., L. Collins, Y. Haitao; C. E. Baum; and L. Carin. 2003. Sensing of unexploded ordnance magnetometer and induction data: Theory and signal processing. *Geoscience and Remote Sensing*. 41(5):1005–1015. Digital Object Identifier 10.1109/TGRS.2003.810922.

Appendix A

Definitions from ATC website

Anomaly	Location of a system response deemed to warrant further investigation by the demonstrator for consideration as an emplaced ordnance item.
Detection	An anomaly location that is within Rhalo of an emplaced ordnance item.
Emplaced Ordnance	An ordnance item buried by the government at a specified location in the test site.
Emplaced Clutter	A clutter item (i.e., non-ordnance item) buried by the government at a specified location in the test site.
Rhalo	A pre-determined radius about the periphery of an emplaced item (clutter or ordnance) within which a location identified by the demonstrator as being of interest is considered to be a response from that item. If multiple declarations lie within Rhalo of any item (clutter or ordnance), the declaration with the highest signal output within the Rhalo will be utilized. For the purpose of this program, a circular halo 0.5 m in radius will be placed around the center of the object for all clutter and ordnance items less than 0.6 m in length. When ordnance items are longer than 0.6 m, the halo becomes an ellipse where the minor axis remains 0.5 m and the major axis is equal to the half length of the ordnance plus 0.5 m.
Small Ordnance	Caliber of ordnance less than or equal to 40 mm (includes 20-mm projectile, 40-mm projectile, submunitions BLU-26, BLU-63, and M42).
Medium Ordnance	Caliber of ordnance greater than 40 mm and less than or equal to 81 mm (includes 57-mm projectile, 60-mm mortar, 2.75-in. rocket, MK118 Rockeye, 81-mm mortar).
Large Ordnance	Caliber of ordnance greater than 81 mm (includes 105-mm HEAT, 105-mm projectile, 155-mm projectile, 500-lb bomb).
Shallow	Items buried less than 0.3 m below ground surface.
Medium	Items buried greater than or equal to 0.3 m and less than 1 m below ground surface.
Deep	Items buried greater than or equal to 1 m below ground surface.
Response Stage Noise Level	The level that represents the point below which anomalies are not considered detectable. Demonstrators are required to provide the recommended noise level for the Blind Grid Test Area.

Discrimination Stage Threshold	The demonstrator-selected threshold level believed to provide optimum performance of the system by retaining all detectable ordnance and rejecting the maximum amount of clutter. This level defines the subset of anomalies the demonstrator would recommend digging based on discrimination.
Binomially Distributed Random Variable	A random variable of the type which has only two possible outcomes, say success and failure, is repeated for n independent trials with the probability p of success and the probability 1-p of failure being the same for each trial. The number of successes x observed in the n trials is an estimate of p and is considered to be a binomially distributed random variable.

Response and discrimination stage data

The scoring of the demonstrator's performance is conducted in two stages. These two stages are termed the RESPONSE STAGE and DISCRIMINATION STAGE. For both stages, the probability of detection (P_d) and the false alarms are reported as receiver operating characteristic (ROC) curves. False alarms are divided into those anomalies that correspond to emplaced clutter items, measuring the probability of false positive (P_{fp}) and those that do not correspond to any known item, termed background alarms.

The RESPONSE STAGE scoring evaluates the ability of the system to detect emplaced targets without regard to ability to discriminate ordnance from other anomalies. For the RESPONSE STAGE, the demonstrator provides the scoring committee with the location and signal strength of all anomalies that the demonstrator has deemed sufficient to warrant further investigation and/or processing as potential emplaced ordnance items. This list is generated with minimal processing (e.g., this list will include all signals above the system noise threshold). As such, it represents the most inclusive list of anomalies.

The DISCRIMINATION STAGE evaluates the demonstrator's ability to correctly identify ordnance as such and to reject clutter. For the same locations as in the RESPONSE STAGE anomaly list, the DISCRIMINATION STAGE list contains the output of the algorithms applied in the discrimination-stage processing. This list is prioritized based on the demonstrator's determination that an anomaly location is likely to contain ordnance. Thus, higher output values are indicative of higher confidence that an ordnance item is present at the specified location. For electronic signal processing, priority ranking is based on algorithm output. For other systems, priority ranking is based on human judgment. The demonstrator

also selects the threshold that the demonstrator believes will provide “optimum” system performance (i.e., that retains all the detected ordnance and rejects the maximum amount of clutter).

Note: The two lists provided by the demonstrator contain identical numbers of potential target locations. They differ only in the priority ranking of the declarations.

Response Stage Definitions	
Response Stage Probability of Detection (Pd^{res})	$Pd^{res} = (\text{No. of response-stage detections})/(\text{No. of emplaced ordnance in the test site}).$
Response Stage False Positive (fp^{res})	An anomaly location that is within Rhalo of an emplaced clutter item.
Response Stage Probability of False Positive (Pfp^{res})	$Pfp^{res} = (\text{No. of response-stage false positives})/(\text{No. of emplaced clutter items}).$
Response Stage Background Alarm ($bare$)	An anomaly in a blind grid cell that contains neither emplaced ordnance nor an emplaced clutter item. An anomaly location in the open field or scenarios that is outside Rhalo of any emplaced ordnance or emplaced clutter item.
Response Stage Probability of Background Alarm ($Pbare$)	Blind Grid only: $Pbare = (\text{No. of response-stage background alarms})/(\text{No. of empty grid locations}).$
Response Stage Background Alarm Rate (BAR^{res})	Open Field only: $BAR^{res} = (\text{No. of response-stage background alarms})/(\text{arbitrary constant}).$

Note that the quantities Pd^{res} , Pfp^{res} , $Pbare$, and BAR^{res} are functions of t^{res} , the threshold applied to the response-stage signal strength. These quantities can therefore be written as $Pd^{res}(t^{res})$, $Pfp^{res}(t^{res})$, $Pbare(t^{res})$, and $BAR^{res}(t^{res})$.

Discrimination Stage Definitions	
Discrimination	The application of a signal processing algorithm or human judgment to response-stage data that discriminates ordnance from clutter. Discrimination should identify anomalies that the demonstrator has high confidence correspond to ordnance, as well as those that the demonstrator has high confidence correspond to nonordnance or background returns. The former should be ranked with highest priority and the latter with lowest.
Discrimination Stage Probability of Detection (Pd^{disc})	$Pd^{disc} = (\text{No. of discrimination-stage detections})/(\text{No. of emplaced ordnance in the test site}).$
Discrimination Stage False Positive (fp^{disc})	An anomaly location that is within Rhalo of an emplaced clutter item.

Discrimination Stage Definitions	
Discrimination Stage Probability of False Positive (Pfp^{disc})	$Pfp^{disc} = (\text{No. of discrimination stage false positives})/(\text{No. of emplaced clutter items}).$
Discrimination Stage Background Alarm (ba^{disc})	An anomaly in a blind grid cell that contains neither emplaced ordnance nor an emplaced clutter item. An anomaly location in the open field or scenario that is outside Rhalo of any emplaced ordnance or emplaced clutter item.
Discrimination Stage Probability of Background Alarm (Pba^{disc})	$Pba^{disc} = (\text{No. of discrimination stage background alarms})/(\text{No. of empty grid locations}).$
Discrimination Stage Background Alarm Rate (BAR^{disc})	$BAR^{disc} = (\text{No. of discrimination-stage background alarms})/(\text{arbitrary constant}).$

Note that the quantities Pd^{disc} , Pfp^{disc} , Pba^{disc} , and BAR^{disc} are functions of t^{disc} , the threshold applied to the discrimination-stage signal strength. These quantities can therefore be written as $Pd^{disc}(t^{disc})$, $Pfp^{disc}(t^{disc})$, $Pba^{disc}(t^{disc})$, and $BAR^{disc}(t^{disc})$.

Metrics to characterize the discrimination stage

The demonstrator is also scored on efficiency and rejection ratio, which measure the effectiveness of the discrimination stage processing. The goal of discrimination is to retain the greatest number of ordnance detections from the anomaly list, while rejecting the maximum number of anomalies arising from non-ordnance items. Efficiency measures the amount of detected ordnance retained by the discrimination, while the rejection ratio measures the fraction of false alarms rejected. Both measures are defined relative to the entire response list, i.e., the maximum ordnance detectable by the sensor and its accompanying false positive rate or background alarm rate.

Efficiency (E)

$E = Pd^{disc}(t^{disc})/Pd^{res}(t_{min}^{res})$; Measures (at a threshold of interest) the degree to which the maximum theoretical detection performance of the sensor system (as determined by the response stage t_{min}) is preserved after application of discrimination techniques. Efficiency is a number between 0 and 1. An efficiency of 1 implies that all of the ordnance initially detected in the response stage was retained at the specified threshold in the discrimination stage, t^{disc} .

False Positive Rejection Rate (R_{fp})

$R_{fp} = 1 - [P_{fp}^{disc}(t^{disc}) / P_{fp}^{res}(t^{min^{res}})]$; Measures (at a threshold of interest) the degree to which the sensor system's false positive performance is improved over the maximum false positive performance (as determined by the response stage t^{min}). The rejection rate is a number between 0 and 1. A rejection rate of 1 implies that all emplaced clutter initially detected in the response stage were correctly rejected at the specified threshold in the discrimination stage.

Background Alarm Rejection Rate (R_{ba})

BLIND GRID	$R_{ba} = 1 - [P_{ba}^{disc}(t^{disc}) / P_{ba}^{res}(t^{min^{res}})]$
OPEN FIELD	$R_{ba} = 1 - [\text{BAR}^{disc}(t^{disc}) / \text{BAR}^{res}(t^{min^{res}})]$.

Measures the degree to which the discrimination stage correctly rejects background alarms initially detected in the response stage. The rejection rate is a number between 0 and 1. A rejection rate of 1 implies that all background alarms initially detected in the response stage were rejected at the specified threshold in the discrimination stage.

Appendix B

Tutorial 1

This tutorial was distributed during the Workshop held at ERDC on July 25 – 26, 2006. It is a PowerPoint display illustrating the use of UXO-DAS within the Oasis Martaj software, which is a part of Geosoft software.

Tutorial 1 UXO-DAS Mag data

Start Oasis Martaj

If you haven't started GEOSOFT yet, do so by selecting

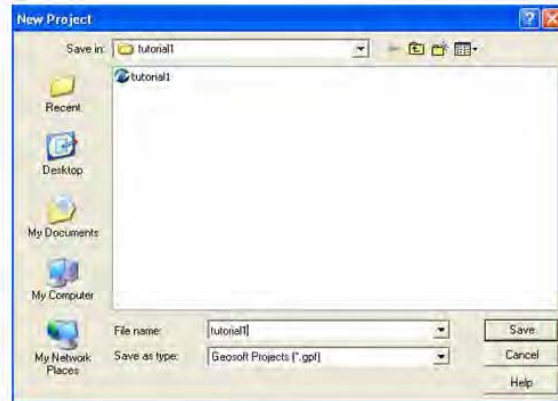
START => All Programs

Geosoft => Oasis Martaj => Oasis Martaj



Start a new Project

- Select File => Project => New
Save in C:Tutorial Directory



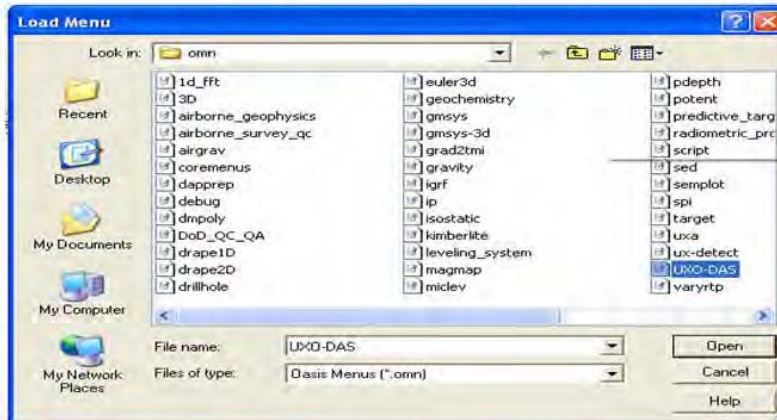
Open Existing Project

- If you want to work on an existing Project click yes.
- Otherwise click no and start a new project



Load UXO-DAS Menu

- From the menu bar: GX => Load Menu
- Choose UXO-DAS from the list of files:



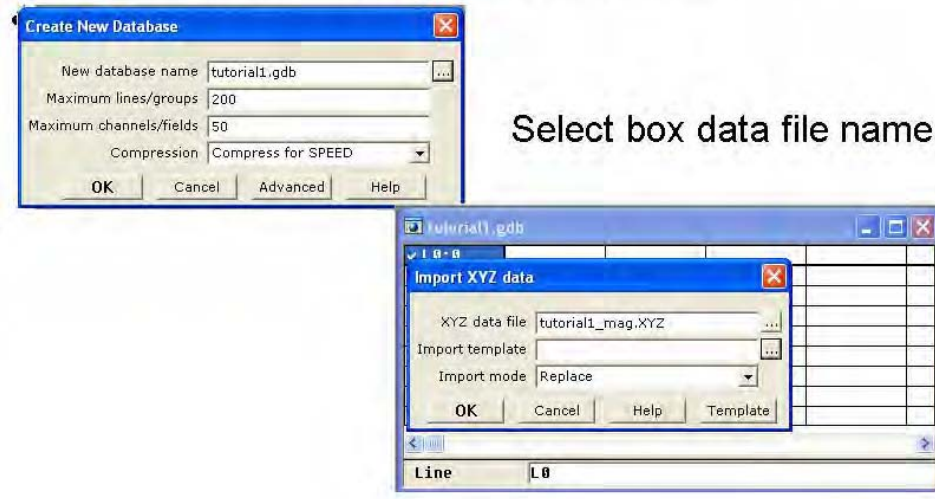
Load UX-Detect Menu

- From the menu bar: GX => Load Menu
- Choose UX-Detect from the list of files:
- The menu bar will now have two additional options and you can start working on the new project



Importing Mag Data

- UXO-DAS => Import sensor data => Geosoft X,Y
- Type in New database name as Tutorial1



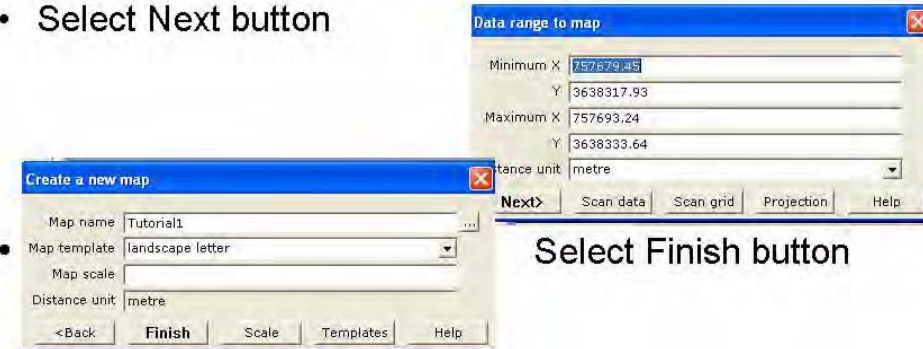
Mag Data

- The final window will show the database.

L141:B	X	Y	Z	Z1
0.0	757693.24	3638333.35	-6.82	
1.0	757693.09	3638333.34	-7.61	
2.0	757692.95	3638333.34	-8.39	
3.0	757692.80	3638333.34	-9.24	
4.0	757692.65	3638333.34	-9.79	
5.0	757692.50	3638333.34	-10.59	
6.0	757692.35	3638333.34	-11.17	
7.0	757692.21	3638333.33	-11.73	

Mapping

- Select: Mapping => New Map => New Map from XYZ
- Type: Tutorial1 for Map Name
- Select Next button

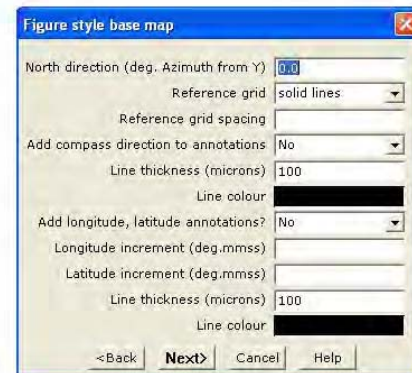
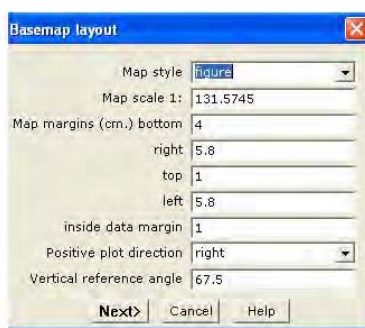


Select Finish button

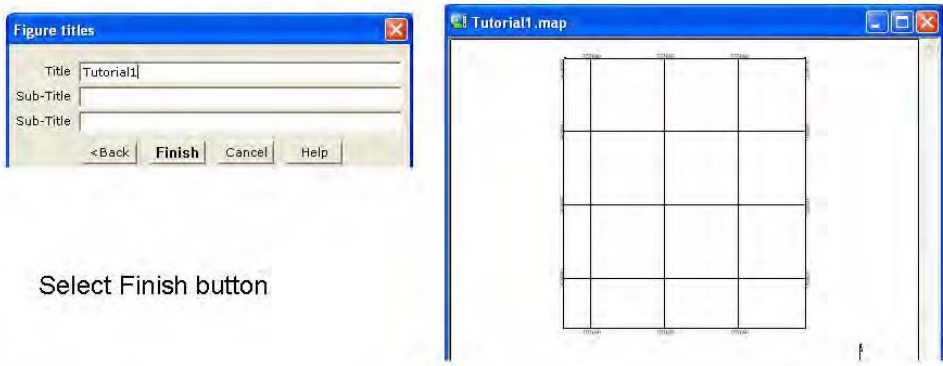
A blank screen will appear

Basemap

- Mapping => Basemap => Draw basemap
- Select Next key for each window

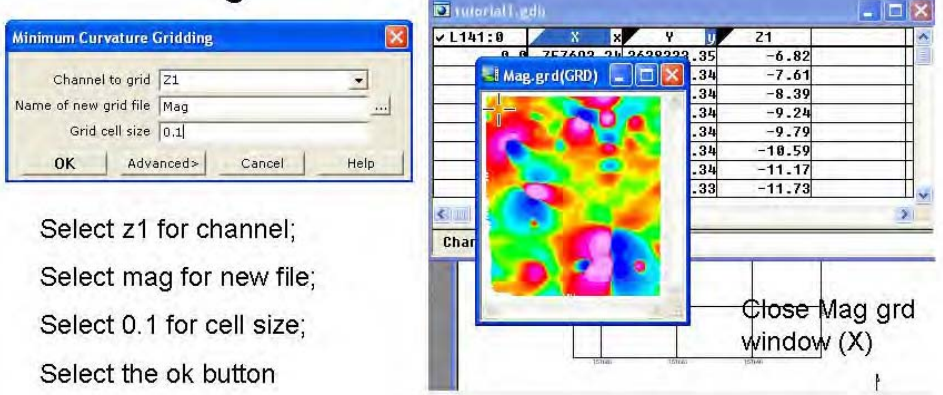


- Type Tutorial1 for the Title
- Select the Finish key to produce this map



Gridding

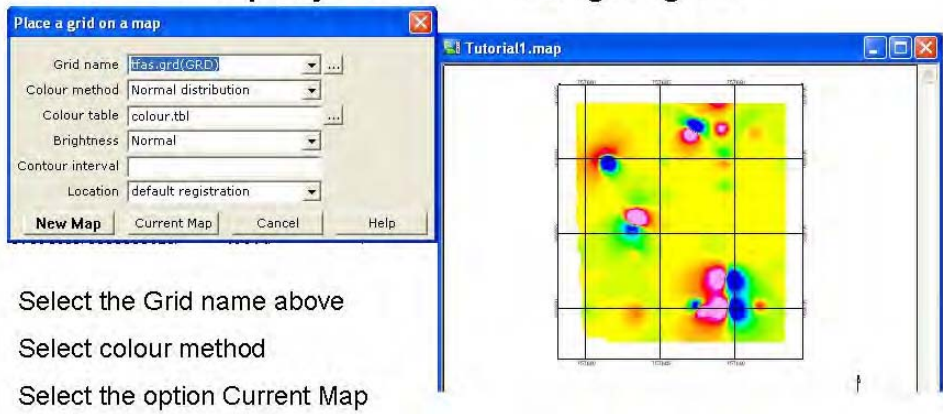
- Select:
- Grid => Gridding => Minimum Curvature => Dialog Controls



Display Grid

- Select:

Grid => Display Grid => Single grid



Create Analytic Signal Grid

- Ux-Detect => Total field magnetic data => Calculate and display analytic signal grid

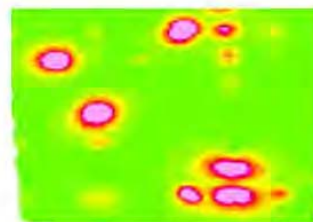


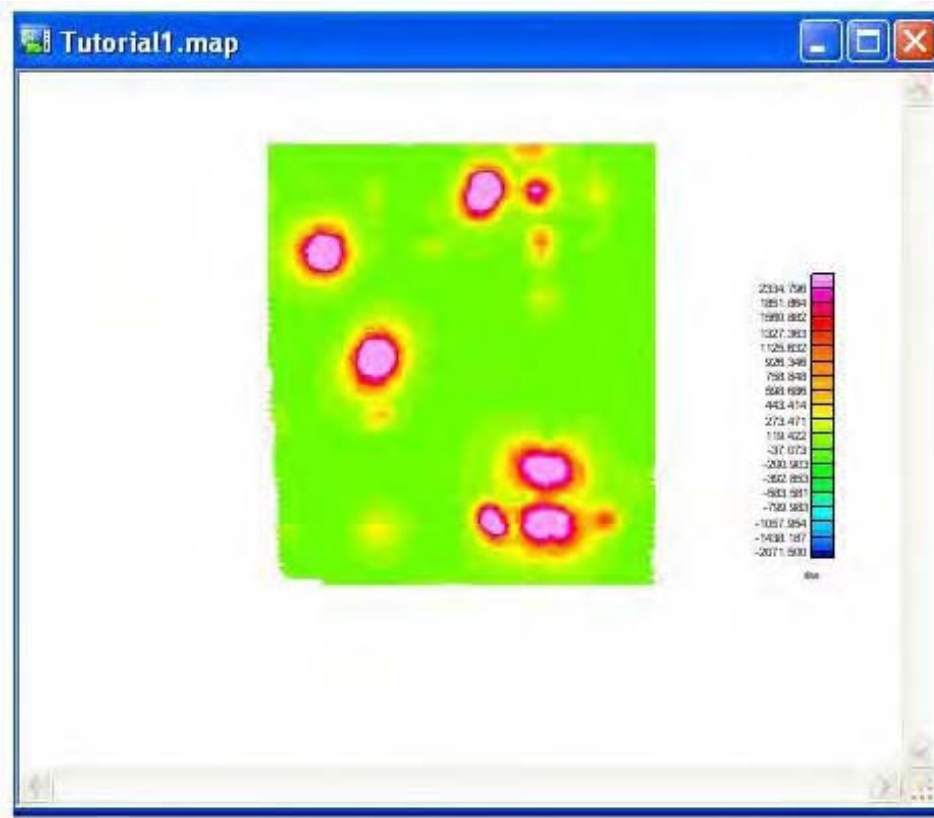
Select channel z1

Select current map for display grids

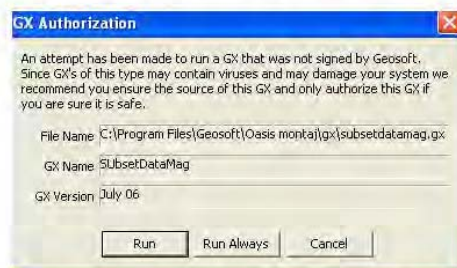
Select ok button

Next screen will be this map



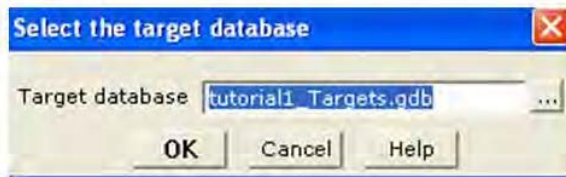


- UXO-DAS => Model inversion => Mag



- (If the program is not Geosoft this box will appear) Enter Run Always

- UX-Detect => Total Field magnetic data => Locate targets => Peakedness

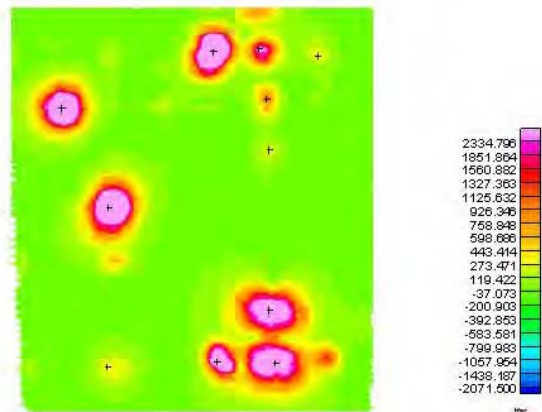


- Select Grid down arrow
- Select window size=20
- Select cutoff rate = 20
- Name grid to be "peak"
- Select ok button

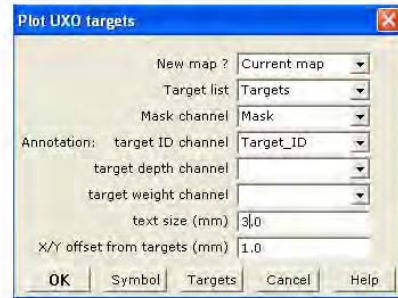
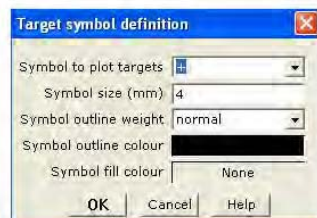


Ux-Detect

- Result of Peakedness Grid and locate targets



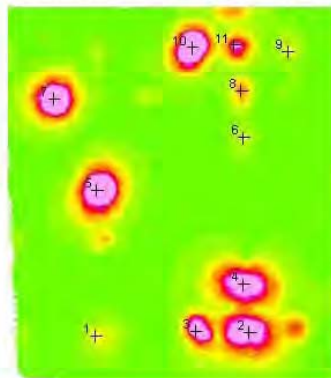
- Ux-Detect => Target map => Create target map
- Blank out the target depth and weight options
- Change text size = 3
- Select Symbol button



Select size=4 (Ok twice)

- Select ok button
- Click outside of grid
- The grid is now

numbered with database legend with + symbol



Minimize this map and
click on the original
database to make it the
active database.

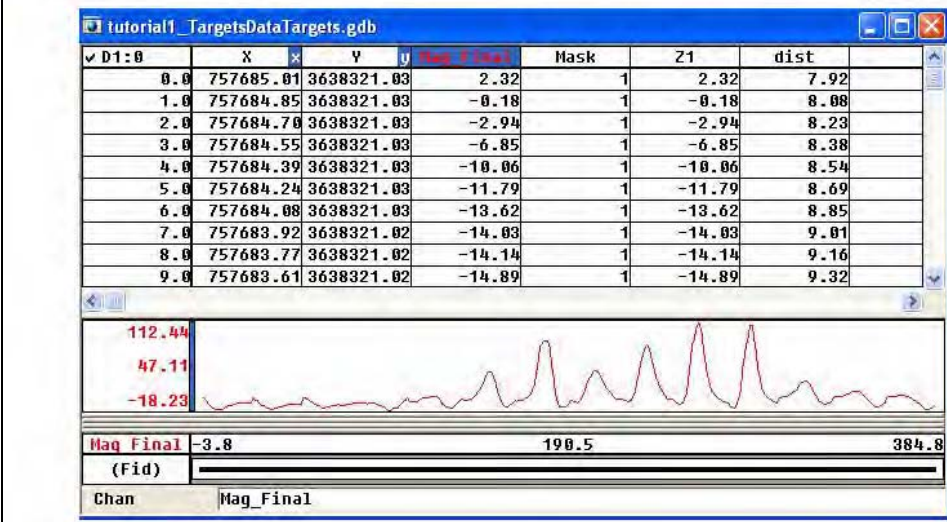
SAVE Changes



- UXO-DAS => Extracted Anomalies => Mag
- Select by down arrow:
- Type Size =4 and Name =dist



- Click Mag Final => Show Profile



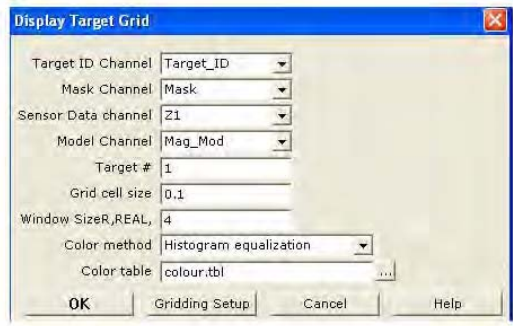
- Min Anomaly database
- Make the target database active
- UXO-DAS => Model Inversion => Mag



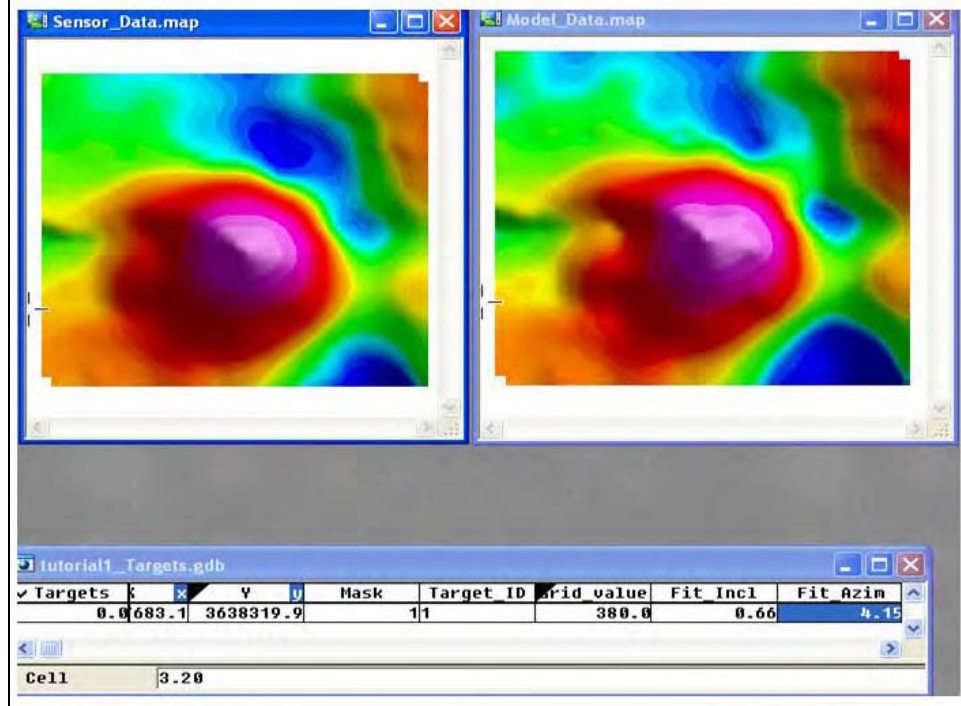
- Right click on any block => display all
- To show additional variables

Targets	x	y	Mask	Target ID	Grid value	Fit Incl	Fit Azim
0.089.1	3638319.9		11		388.0	0.66	4.15
1.089.0	3638320.0		12		6798.0	1.55	3.10
2.087.3	3638320.1		13		6543.0	1.45	3.05
3.089.4	3638322.1		14		6972.0	1.50	3.20
4.083.2	3638326.0		15		30834.0	0.62	1.17
5.089.4	3638328.2		16		394.0	1.95	1.76
6.081.4	3638329.9		17		27810.0	2.69	2.27
7.089.3	3638330.2		18		1341.0	1.86	4.62
8.091.2	3638331.9		19		400.0	1.38	5.10
9.087.2	3638332.0		110		31913.0	0.00	0.00
10.089.0	3638332.1		111		3999.0	0.00	0.00

- UXO-DAS => display target grid
- Select by arrow key
- Grid cell=0.1
- Select ok button



[Arrange two maps and database In this format]



Tutorial 2

Tutorial 2

UXO-DAS GEM-3 data

Start a new Project

- Select File => Project => New
Save in C:Tutorial2 Directory



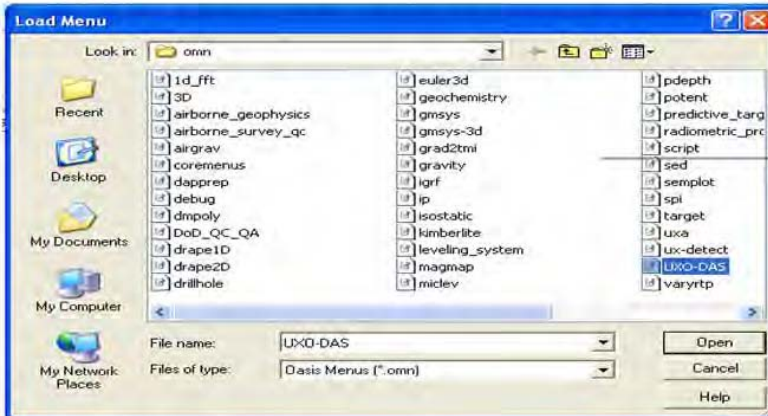
Open Existing Project

- If you want to work on an existing project click yes.
- Otherwise click no and start a new project



Load UXO-DAS Menu

- From the menu bar: GX => Load Menu
- Choose UXO-DAS from the list of files:



Load other Menus

- From the menu bar: GX => Load Menu
- Choose UX-Detect from the list of files:
- From the menu bar: GX => Load Menu
- Choose Dod_QC_QA from the list of files:
- The menu bar will now have three additional options. The last option will appear as UX-Process on the menu bar.

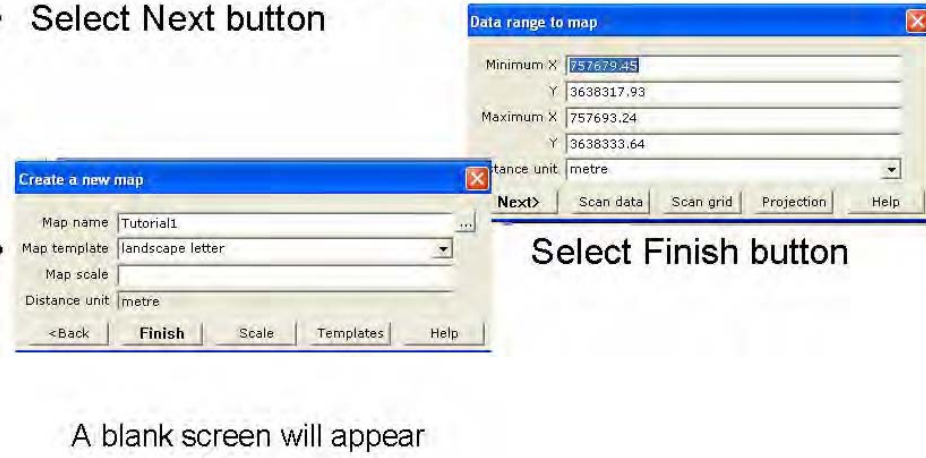


Importing GEM-3 Data

- UXO-DAS => Import sensor data => GEM-3
- Type in New database name as Tutorial2
- The final window will show the database.

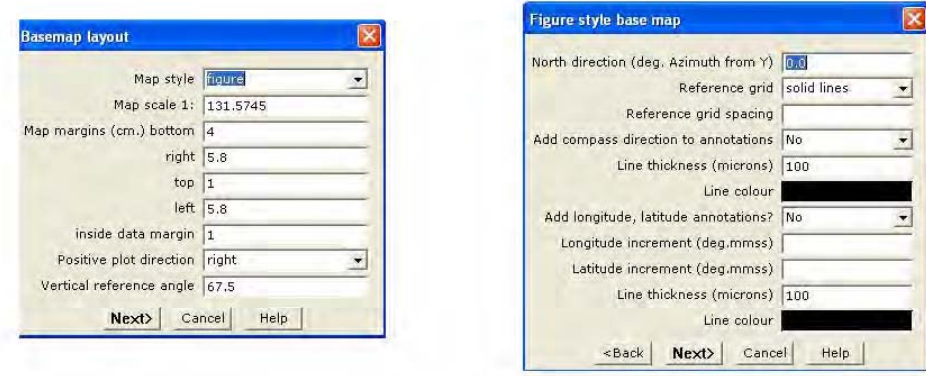
Mapping

- Select: Mapping => New Map => New Map from XYZ
- Type: Tutorial2 for Map Name
- Select Next button

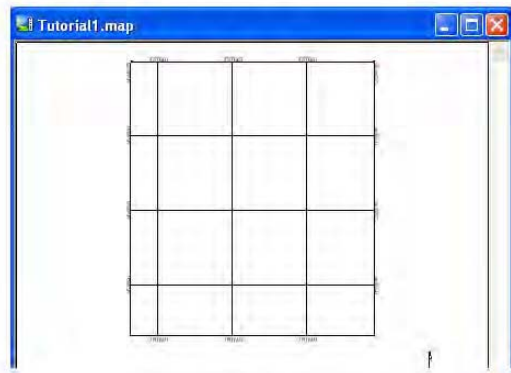


Basemap

- Mapping => Basemap => Draw basemap
- Select Next key for each window



- Type Tutorial2 for the Title
- Select the Finish key to produce this map

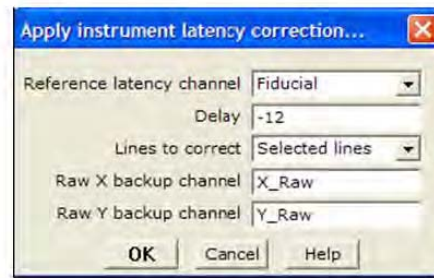


Gridding

- Select: Grid => Gridding => Minimum Curvature => Dialog Controls
- Grid => Display Grid => Color Shaded
- Select: Normal
 - Select qsum for channel;
 - Select qsum for new file;
 - Select 0.1 for cell size;
 - Select the ok button

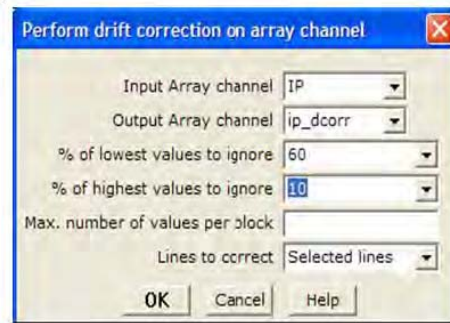
Lag Correction

- UX-PROCESS => Grid => Gridding
- Select Display Grid => Colorshade
- Select down arrow ref channel
- Change delay = -12
- Select ok button

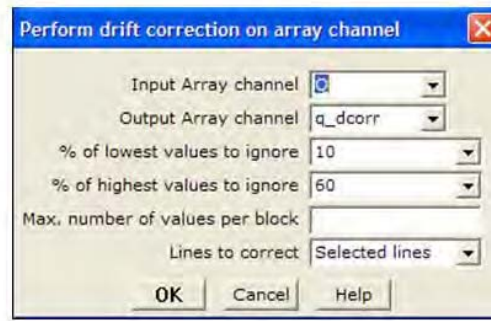


Remove Background

- UXO-DAS => Drift Correction
- Inphase and quadrature channels
- Select by down arrow
- Change lowest values to 60
- Blank the max. number
- Select ok button

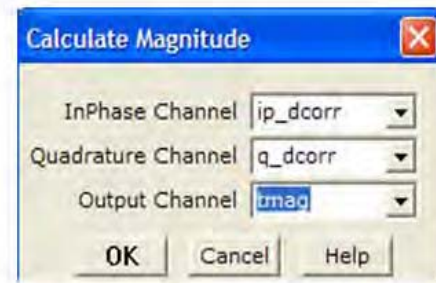


- The drift correction is next done to quadrature
- The lowest and highest values are reversed
- Select ok button



Calculate Magnitude

- UXO-DAS => Calculate Magnitude
- Name inphase, quad and output channel
- Select ok button



Grid Tmag Channel

- Select:
- Grid => Gridding => Minimum Curvature => Dialog Controls
- Grid => Grid Display => Color Shaded

Select Tmag for channel;

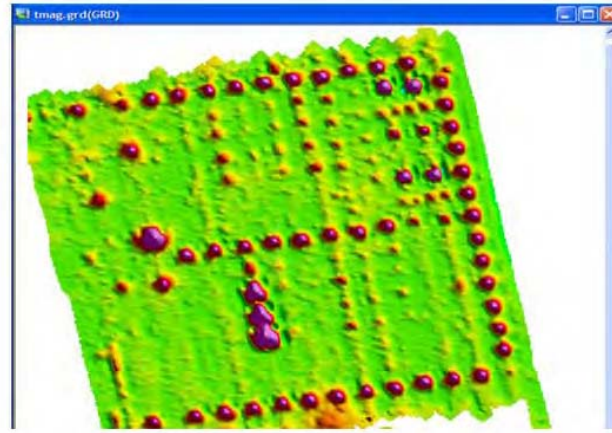
Select Tmag for new file;

Select 0.1 for cell size;

Select the ok button

Map Display

- Grid => Grid Display => Color Shaded



Pick Targets

- UX-Detect => EM data => digitize additional targets
- This will produce a target list of discrete locations.
- UX-Detect => Target map => Create target map
- Blank out two variable and change symbol as done in Tutorial 1.

Extract Anomalies

- UXO-DAS => Extract Anomalies => GEM-3
- Use active original database
- Select all drop arrows as shown.
- Select ok button
- Close original database

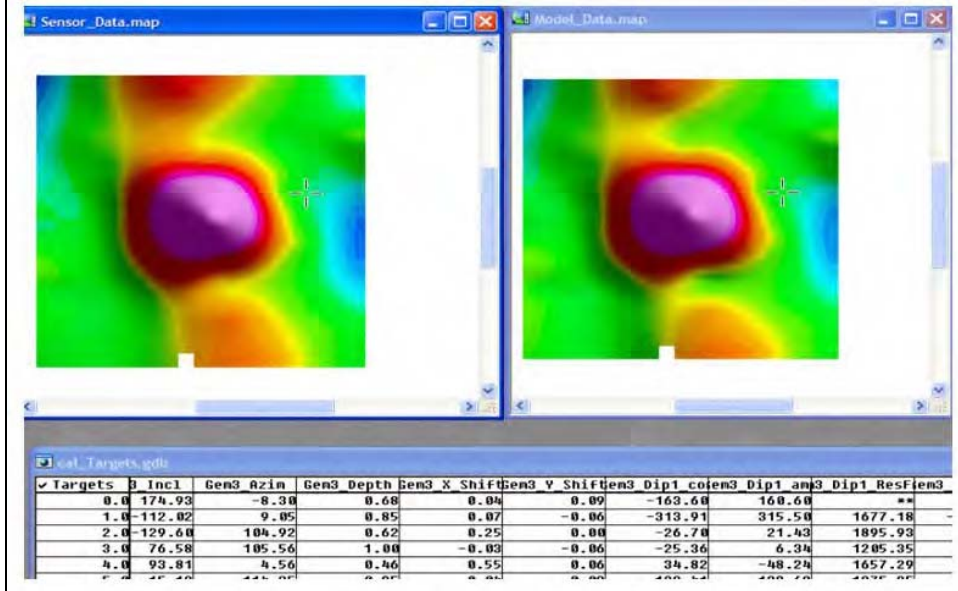


Inversion

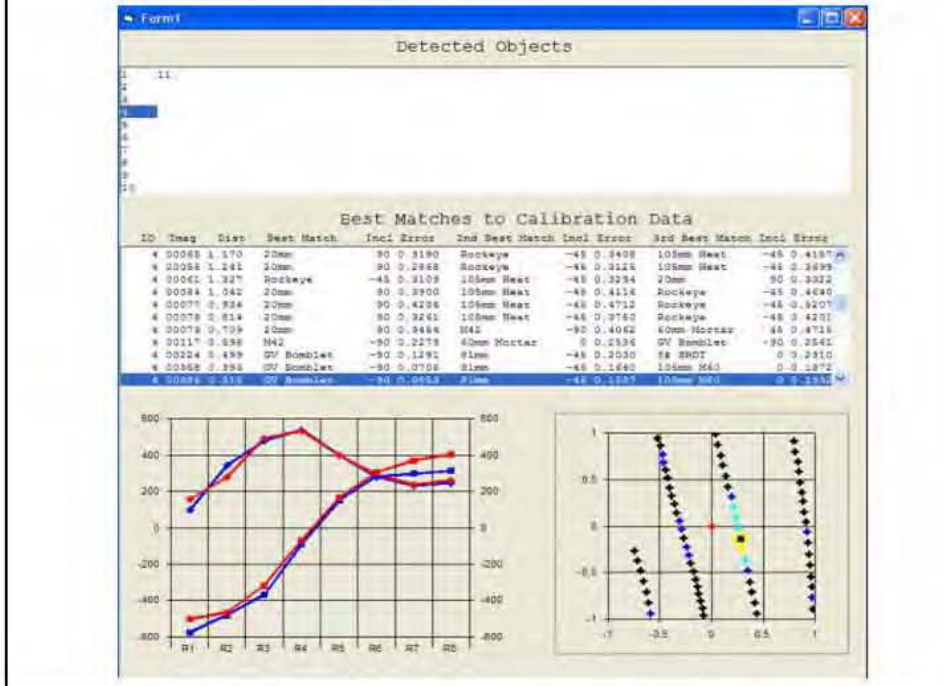
- UXO-DAS => Model Inversion => GEM-3
- Use target list made in Anomaly.
- Select all drop arrows as shown.
- Select ok button



UXO-DAS => display target grid



UXO-DAS => classification => GEM-3 library matching



Tutorial 3

Tutorial 3

UX-ANALYZE

Start a new Project

- Select File => Project => New
Save in C:\Tutorial3 Directory



Load UXA Menu

- From the menu bar: GX => Load Menu
- Choose UXA from the list of files
- Data => Open database
Select tutorial3.gdb

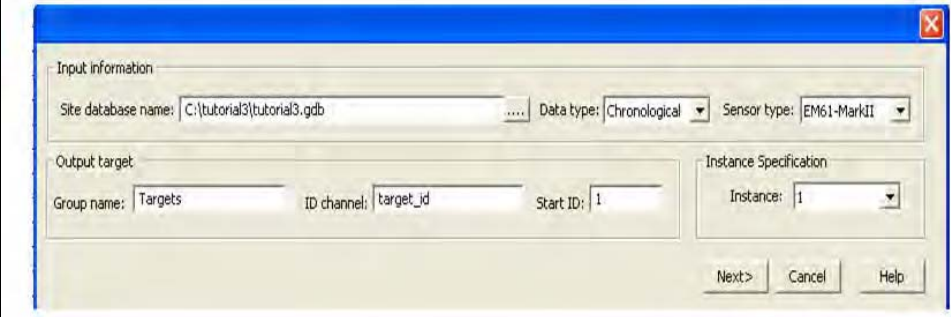
UX-Analyze

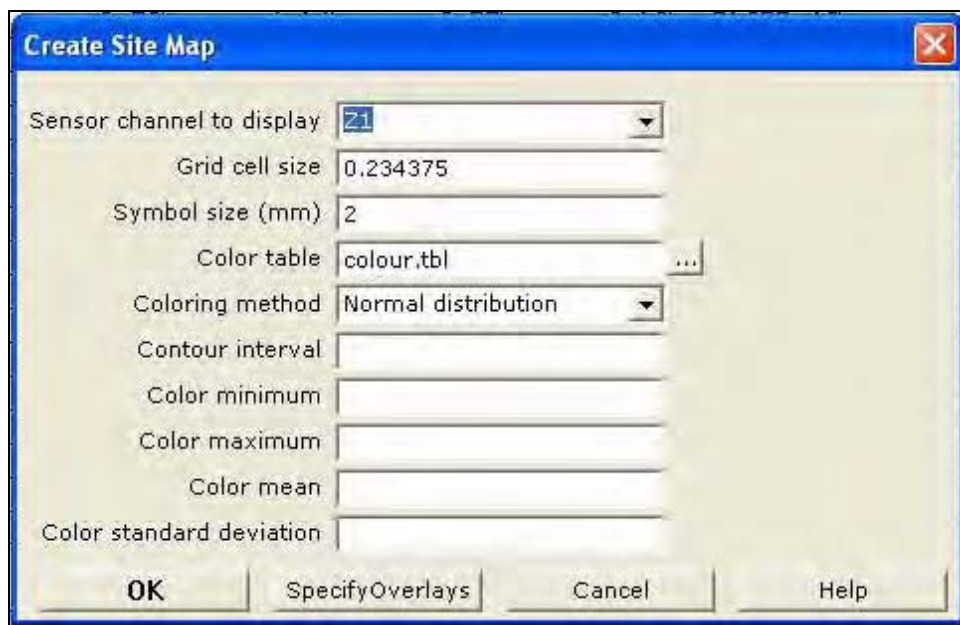
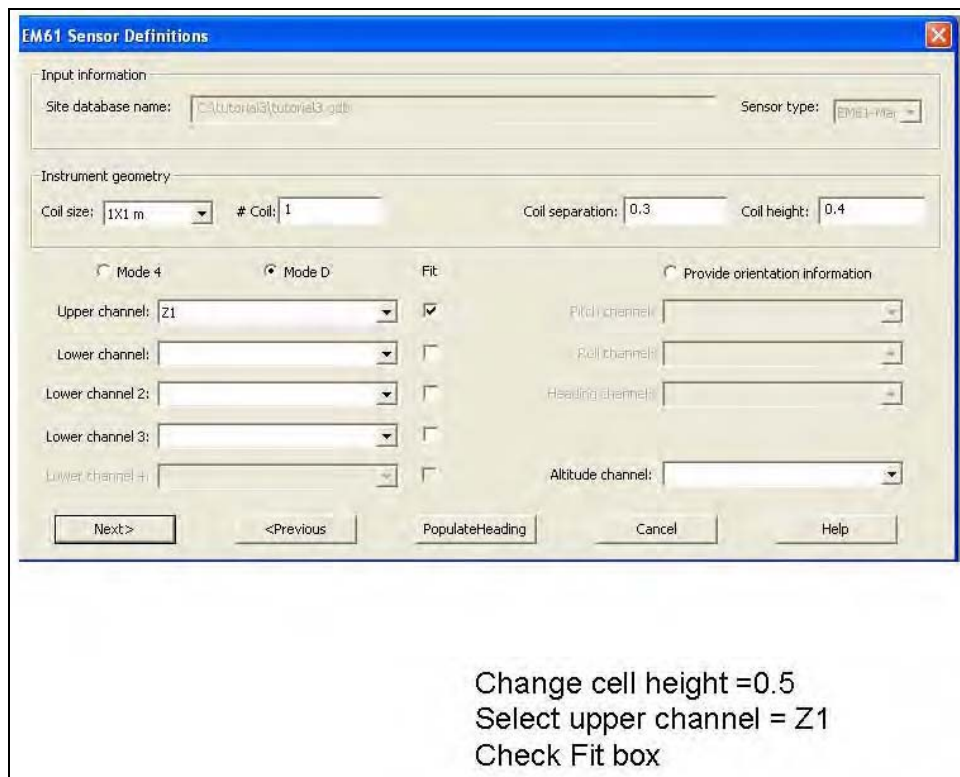
- UX-Analyze => Settings

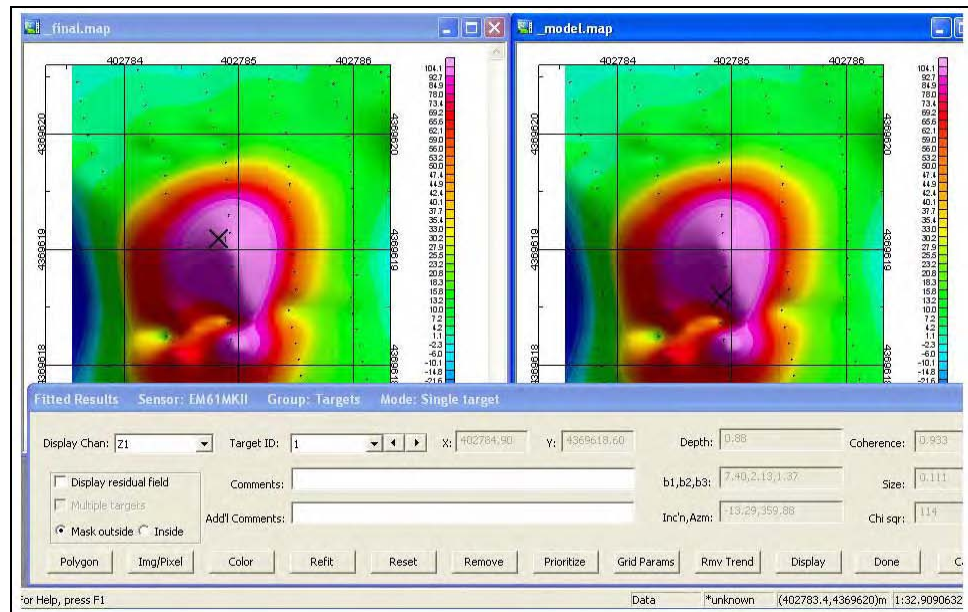
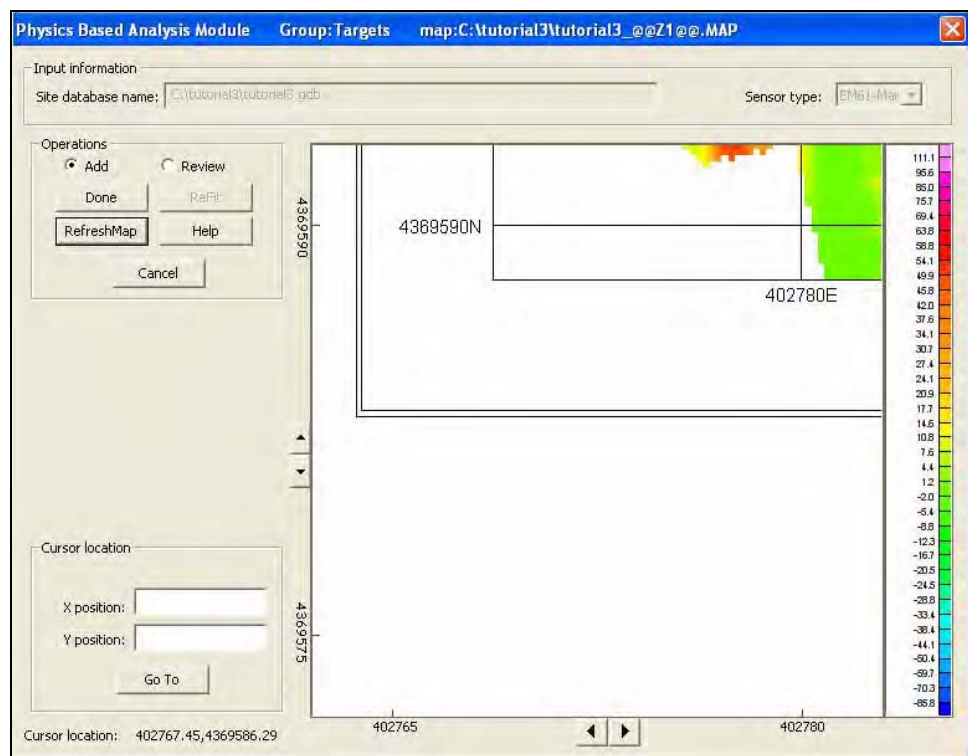


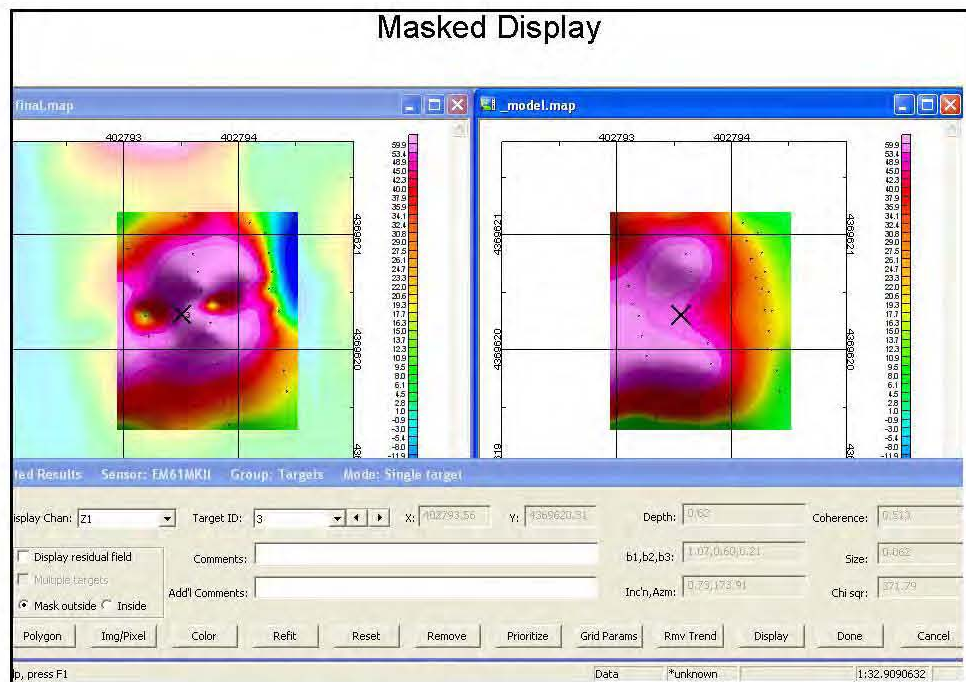
Change window size=15 and anomaly=3; arbitrary to area of map highlighted

- UX-Analyze = Add/Review targets









REPORT DOCUMENTATION PAGE

*Form Approved
OMB No. 0704-0188*

Public reporting burden for this collection of information is estimated to average 1 hour per response, including the time for reviewing instructions, searching existing data sources, gathering and maintaining the data needed, and completing and reviewing this collection of information. Send comments regarding this burden estimate or any other aspect of this collection of information, including suggestions for reducing this burden to Department of Defense, Washington Headquarters Services, Directorate for Information Operations and Reports (0704-0188), 1215 Jefferson Davis Highway, Suite 1204, Arlington, VA 22202-4302. Respondents should be aware that notwithstanding any other provision of law, no person shall be subject to any penalty for failing to comply with a collection of information if it does not display a currently valid OMB control number. **PLEASE DO NOT RETURN YOUR FORM TO THE ABOVE ADDRESS.**

1. REPORT DATE (DD-MM-YYYY) September 2009		2. REPORT TYPE Final report		3. DATES COVERED (From - To)	
4. TITLE AND SUBTITLE Unexploded Ordnance (UXO) Data Analysis System (DAS)				5a. CONTRACT NUMBER	
				5b. GRANT NUMBER	
				5c. PROGRAM ELEMENT NUMBER	
6. AUTHOR(S) Ricky A. Goodson, John Cliff Morgan, Dwain K. Butler, Morris P. Fields, Hollis H. Bennett, Jr., and Tere A. DeMoss				5d. PROJECT NUMBER	
				5e. TASK NUMBER	
				5f. WORK UNIT NUMBER	
7. PERFORMING ORGANIZATION NAME(S) AND ADDRESS(ES) U.S. Army Engineer Research and Development Center Environmental Laboratory 3909 Halls Ferry Road Vicksburg, MS 39180-6199				8. PERFORMING ORGANIZATION REPORT NUMBER ERDC/CHL TR-09-16	
9. SPONSORING / MONITORING AGENCY NAME(S) AND ADDRESS(ES) U.S. Army Engineer District, Jacksonville 701 San Marco Boulevard Jacksonville, FL 32207-0019				10. SPONSOR/MONITOR'S ACRONYM(S)	
				11. SPONSOR/MONITOR'S REPORT NUMBER(S)	
12. DISTRIBUTION / AVAILABILITY STATEMENT Approved for public release; distribution is unlimited.					
13. SUPPLEMENTARY NOTES					
14. ABSTRACT This report documents efforts to develop a common processing and interpretation platform for UXO survey data, hereinafter referred to as the UXODAS. Development of the common software platform assumes (1) that the data will be accessible in readable formats, and (2) that the data result from the most commonly used geophysical sensor types, specifically total field magnetometers (TFM), frequency-domain electromagnetic induction (FDEM) systems, and time-domain electromagnetic induction (TDEM) systems. The common platform will enable interoperability and incorporate in a readily available software package the capability and tools to import, process, interpret and visualize the results of UXO geophysical surveys. The software platform will be a continuing work in progress, with the capability to easily incorporate new processing and interpretation tools (modules) as they become available. The immediate goal is to make available to the user community the processing and interpretation tools developed under the Army Environmental Quality Technology UXO Research and Development Program by the US Army Engineer Research and Development Center (ERDC).					
15. SUBJECT TERMS Frequency-domain electromagnetic induction (FDEM) systems		Time-domain electromagnetic induction (TDEM) systems Total field magnetometers		Unexploded ordnance (UXO)	
16. SECURITY CLASSIFICATION OF:			17. LIMITATION OF ABSTRACT	18. NUMBER OF PAGES	19a. NAME OF RESPONSIBLE PERSON
a. REPORT UNCLASSIFIED	b. ABSTRACT UNCLASSIFIED	c. THIS PAGE UNCLASSIFIED			19b. TELEPHONE NUMBER (include area code)
Standard Form 298 (Rev. 8-98) Prescribed by ANSI Std. Z39-18					